AERIAL RADIOMETRIC AND MAGNETIC SURVEY

HOUSTON NATIONAL TOPOGRAPHIC MAP

TEXAS GULF COAST

PREPARED FOR THE U.S. DEPARTMENT OF ENERGY
GRAND JUNCTION OFFICE
GRAND JUNCTION, COLORADO
UNDER BENDIX FIELD ENGINEERING CORPORATION SUBCONTRACT NO. 77-036-S

Geodata International, Inc.
7035 JOHN W. CARPENTER FRWY.
DALLAS, TEXAS 75247

VOL. 1

Grand Junction Office
P.O. Box 2567, Grand Junction, CO 81501

FOR IMMEDIATE RELEASE
September 14, 1978

DOE ISSUES REPORT ON AERIAL GAMMA RAY AND MAGNETIC SURVEY OF HOUSTON QUADRANGLE, TEXAS

The Grand Junction, Colorado, Office, U.S. Department of Energy (DOE), will place on open file on September 28, 1978, a report covering 2,222 line miles of fixed wing aerial geophysical survey covering the Houston National Topographic Map Series 1:250,000 quadrangle, Texas.

The survey was flown in April 1977 by Geodata International, Inc., Dallas, Texas. This survey was flown as part of the National Uranium Resource Evaluation (NURE) program of the DOE's Grand Junction Office to acquire and compile geologic and other information with which to assess the magnitude and distribution of uranium resources and to determine areas favorable for the occurrence of uranium in the United States.

Traverse lines were flown east-west at a spacing of 3-1/8 miles (5 kilometers) and tie lines were flown north-south at a spacing of 18-3/4 miles (30 kilometers). Ground clearance was a nominal 400 feet. Sampling intervals were one second.

Volume 1 of the final report includes sections on instrumentation, data reduction, geology, and data analysis, as well as appendices which contain statistical data, single and average record listings and a production summary.

Volume II of the final report contains record location and geology maps, radiometric profiles for potassium, uranium, thorium, and their ratios, and anomaly maps for potassium, uranium, thorium, and their ratios. All maps and profiles are at a scale of 1:500,000.

Simultaneously with open filing at 11:00 a.m. MDT on September 28, 1978, copies of Volumes 1 and/or 2 of this report and copies of all maps and profiles in Volume 2 at full scale (1:250,000) will be available for purchase from Geodata Inc., 7035 John W. Carpenter Freeway, Dallas, Texas 75247; phone (214) 630-1600. Geodata will provide two purchase options for the open file material.

No. 78-101
News Media Contact: Peter Mygatt, 303/242-8621, Ext. 293
To order microfiche: Contact Library, Ext. 278

Option 1 - $125.00 consists of the complete Volume 1 and Volume 2 reports.

Option 2 - $150.00 consists of 1:250,000 maps and profiles for one quadrangle.

Computer readable magnetic tapes containing measurement and location information will be available 21 days after open filing for sale for the cost of copying, on a per quadrangle basis, at $80.00 per data tape; i.e., statistical analysis data, single record reduced data, raw spectral data, magnetic data. Inquiries and orders should be addressed to:

Frank D. Hammerling
UCC-ND Computer Applications Dept.
4500 North Building
Oak Ridge National Laboratory
P. O. Box X
Oak Ridge, Tennessee 37380
Phone (615) 438-8611, extension 36113

These reports are also available on microfiche from the Grand Junction Office of DOE. The total price of Volume 1 and 2 on microfiche is $10.00. Prepaid orders should be sent to: Bendix Field Engineering Corporation, Technical Library, P.O. Box 1569, Grand Junction, Colorado, 81501. Checks or money orders should be made out to Bendix Field Engineering Corporation, the operating contractor for DOE's Grand Junction Office.

The report, GJBX-102(78), entitled "Aerial Radiometric and Magnetic Survey, Houston National Topographic Map, Texas Gulf Coast," will be placed on open file on September 28, 1978, at the following places and times:

GRAND JUNCTION, CO: Technical Library, Grand Junction Office, Department of Energy, 11 a.m. MDT

ALBUQUERQUE, NM: Government Publications Section, Zimmerman Library, University of New Mexico, 11 a.m. MDT

ANCHORAGE, AK: Division of Geological & Geophysical Surveys, 323 E. 4th Avenue, 8 a.m. ADT

ATLANTA, GA: Department of Energy, Suite 438, 1365 Peachtree Street, 1 p.m. EDT

AUSTIN, TX: Bureau of Economic Geology, Geology Building, University of Texas, 12 noon CDT

CAMBRIDGE, MA: Massachusetts Institute of Technology, Lindgren Library, 14E-210, 1 p.m. EDT

CASPER, WY: Natrona County Public Library, 11 a.m. MDT

DENVER, CO: Colorado Geological Survey, Department of Natural Resources, State Centennial Bldg., 1313 Sherman St., Rm. 715, 11 a.m. MDT

GOLDEN, CO: U.S. Geological Survey Library, 1526 Cole Blvd., (West Colfax and Hawthorne), 11 a.m., MDT

LARAMIE, WY: Wyoming Geologicl Survey, P.O. Box 3008, University Station, 11 a.m. MDT

LAWRENCE, KS: Kansas Geological Survey, 1930 Avenue "A", Campus West, The University of Kansas, 12 noon CDT

CORPUS CHRISTI, TX: Corpus Christi State University, 6300 Ocean Drive 12 noon CDT

LUBBOCK, TX: Documents Library, Texas Tech University, 12 noon CDT

MENLO PARK, CA: U.S. Geological Survey, Library, 345 Middlefield Road, 10 a.m. PDT

NORMAN, OK: Oklahoma Geological Survey, The University of Oklahoma, 830 Van Vleet Oval, Rm. 163, 12 noon CDT

PITTSBURGH, PA: Department of Energy, Suite 221, 9 Parkway Center, 875 Greentree Road 1 p.m. EDT

RESTON, VA: U.S. Geological Survey Library, Gifts & Exchange Unit, National Center, 1 p.m. EDT

SALT LAKE CITY, UT: Documents Division, Marriott Library, University of Utah, 11 a.m. MDT

SOCORRO, NM: New Mexico Bureau of Mines, Campus Station, 11 a.m. MDT

SPOKANE, WA: U.S. Geological Survey Library, U.S. Court House, Rm. 678, 10 a.m. PDT

SALT LAKE CITY, UT: Utah Geological Survey, 606 Black Hawk Way, 11 a.m. MDT

AERIAL RADIOMETRIC AND MAGNETIC SURVEY
HOUSTON NATIONAL TOPOGRAPHIC MAP
TEXAS GULF COAST

PREPARED FOR THE U.S. DEPARTMENT OF ENERGY
GRAND JUNCTION OFFICE
GRAND JUNCTION, COLORADO

UNDER BENDIX FIELD ENGINEERING CORPORATION SUBCONTRACT NO. 77-036-S

JUNE 28, 1978

GEODATA INTERNATIONAL, INC.
7035 JOHN W. CARPENTER FREEWAY
DALLAS, TEXAS 75247

TABLE OF CONTENTS

TABLE OF CONTENTS (Continued)

LIST OF ILLUSTRATIONS

LIST OF ILLUSTRATIONS (Continued)

SECTION I

INTRODUCTION

A. AREA SURVEYED

Geodata International, Inc., Dallas, Texas, conducted an airborne gamma ray and total magnetic field survey of the Texas Gulf Coast area during the period from March 20, 1977 to May 4, 1977. This survey covered all or parts of the following National Topographic Maps:

- o Houston
- o Seguin
- o Austin
- o Crystal City
- o Beeville and Bay City
- o Laredo and Corpus Christi
- o McAllen and Brownsville

Geodata International had previously surveyed portions of the total area in May and June of 1974 under AEC Contract AT(05-1)-1632. The results of this earlier work are given in a report entitled "Gamma Radiation Spectral Survey of the Jackson/Goliad Formations in Texas".

The more recent survey was flown under a flight plan which would permit coalescing the old data with the new to produce combined results for each of the NTM series given above. This report is concerned with the Houston quadrangle which was flown in its entirety under the new survey. Subsequent reports will cover the other quadrangles flown and will include both the older and newer survey results.

The specific area of this report is outlined in Figure 1. Each map line was flown in an east-west direction with a maximum length of 120 miles, and each tie line was flown in a north-south direction with a maximum length of 69 miles. Map lines were surveyed at a spacing of 3-1/8 miles (5 km.) and tie lines were surveyed at a spacing of 18-3/4 miles (30 km.) as indicated in Figure 2.

The Houston NTMS report consists of two volumes with Volume 1 giving the description of the program and results. Volume 2 presents the flight line profile data and statistical analysis results.

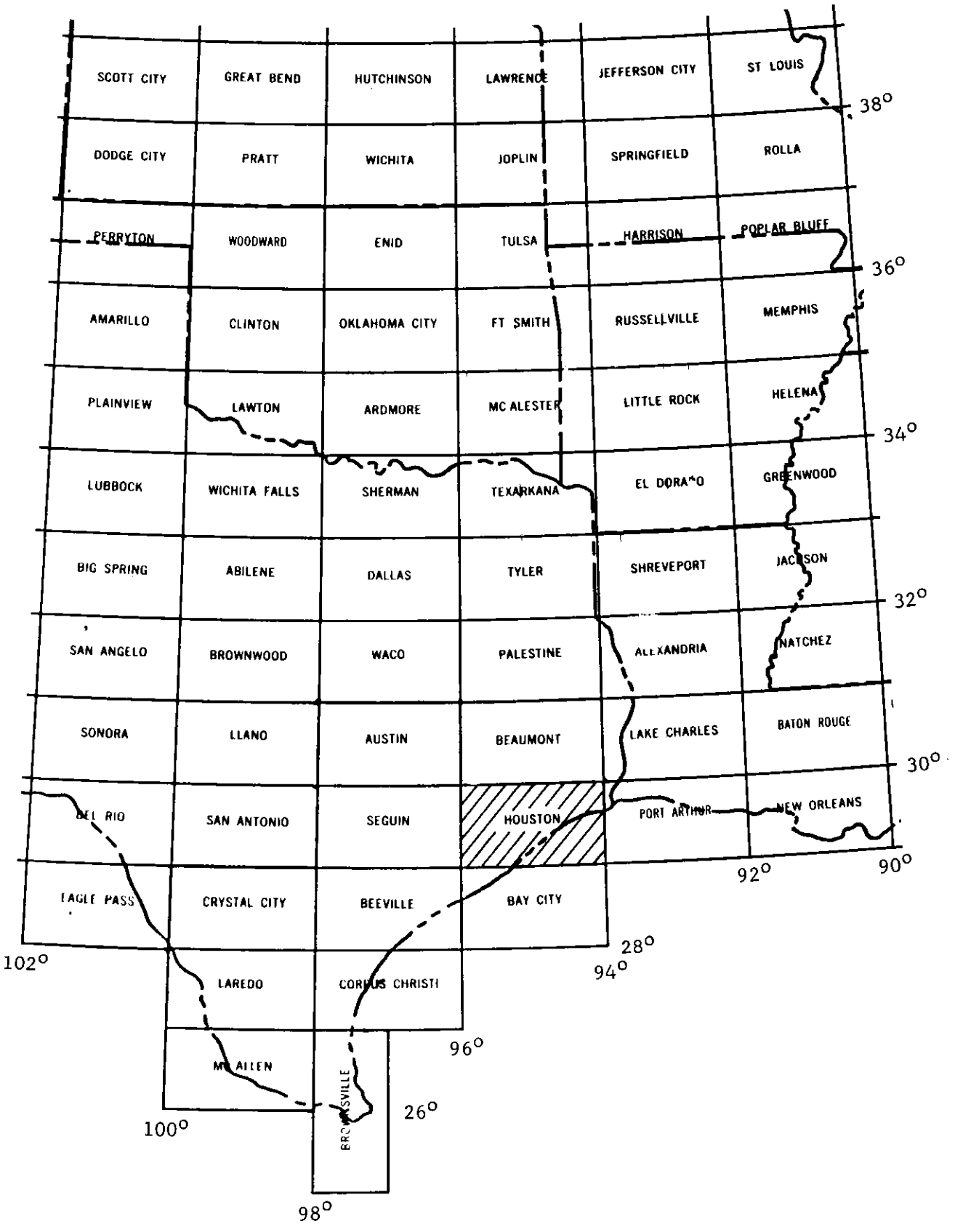

Figure 1. Index Map Showing Area Surveyed

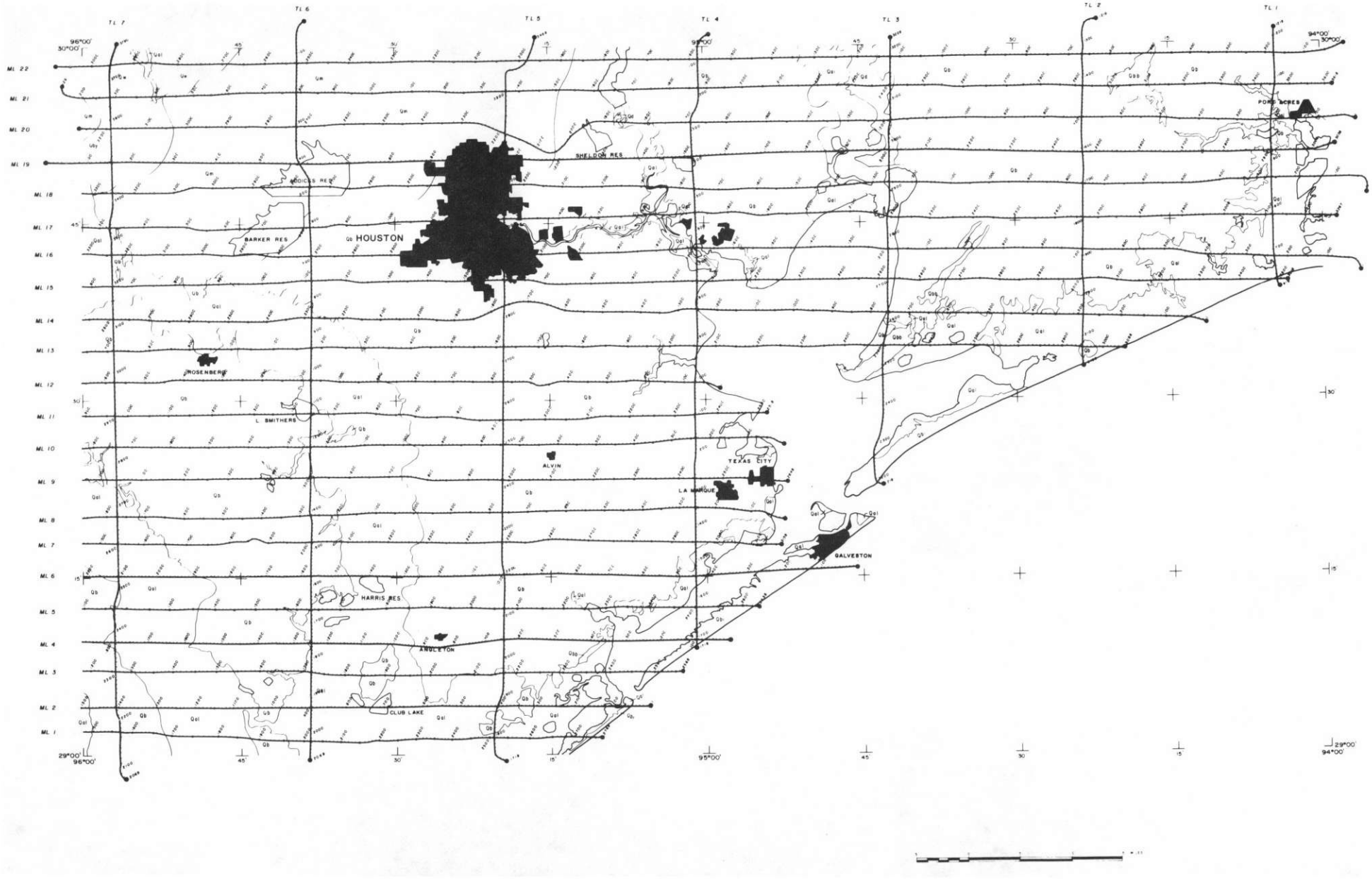

Figure 2. HOUSTON NTMS Indicating Flight Line Location

B. SUMMARY OF THE GEOLOGY AND PHYSIOGRAPHY OF THE HOUSTON SHEET

The Quaternary aged unconsolidated deposits of the Houston Map Sheet form part of the Coastal Plain of Texas. The most extensive geological unit is the Beaumont Formation which is composed of fluviatile, non-marine deposits. Similar deposits of Pleistocene age are mapped in the Deweyville, Montgomery, Bentley and Willis formations. The only non-Quaternary rocks crop out in the vicinity of the Hockley Salt Dome and may belong to the Catahoula Formation which is thought to have potential as a locus for uranium mineralization. No known occurrences of uranium ore occur in the surveyed area.

Major gulfward flowing rivers cross the coastal plain and the submerged mouths of the Trinity and San Jacinto rivers form the Galveston/Trinity Bay area. Sabine Lake in the northeast of the map sheet is a second major area of inland saline water, and occurs at the confluence of the Neches and Sabine river/valleys.

Soils which overlie the geological formations are classified into seven associations. Major variations in water content of these soils may have a significant effect on the radioactivity measurements of a particular area. Certain soils are of very recent development and have very similar characteristics to the underlying geology. In other areas the soils are more maturely developed and changes in texture,chemistry and mineralogy have occurred post-deposition of the parent geologic material.

SECTION II

THE GEODATA AIRBORNE SYSTEM

A. SYSTEM DESCRIPTION

For this survey the Geodata Phase I Airborne System was installed in the DC-3 aircraft number N1010S. The gamma ray detectors on board the aircraft consisted of nine (9) NaI(Tl) crystals. Each crystal is 11½" in diameter by 4" thick, giving a volume of 415.5 cubic inches per crystal. Eight of these crystals are positioned to measure the total radiation environment composed of atmospheric, surface, cosmic and background gamma radioactivity. These are denoted the 4π crystals or 4π detectors since their solid angle view is 4π steradians. The ninth crystal is shielded with 3½" of lead below and with 2" of lead around the vertical surface, which effectively shields the crystal from direct gamma radiation from the earth's surface. This is denoted the 2π detector or 2π crystal. The 2π detector is used to determine the atmospheric contribution of ^{214}Bi to the detected gamma ray events produced in the unshielded crystals.

Each crystal with its preamplifier and six photomultiplier tubes is housed in a thin wall stainless steel cylinder. A thermostatted heater strip is placed on the inside wall of this housing to maintain temperature control. The stainless steel housing is in turn encased in a fibre glass re-enforced polyurethane case to protect the crystals against thermal shock and to maintain better temperature control.

A block diagram of the complete system is shown in Figure 3. The model numbers refer to Canberra equipment unless otherwise indicated. Every one second during a survey flight line data are accumulated from the eight unshielded crystals and the single shielded crystal. The resulting one second spectra are stored in the Canberra Model 7000 Pulse Height Analyzer (PHA) with the 8-crystal spectrum contained in one-half of a 512 location memory and the single crystal spectrum contained in the other half. At the end of one second, the PHA switches to another 512 location memory and continues accumulating data without interruption. The first 512 location memory then reads out onto the magnetic tape. This "flip-flop" operation continues throughout the flight line permitting data accumulation continuously without loss of time for read-out. Each of the two spectra consists then of 256 channels. The first channel contains the live time in milliseconds for each spectrum and the last channel contains the cosmic count from 3.0 to 6.0 MeV for each spectrum.

To insure spectral calibration integrity during the survey, digital stabilizers are used which provide automatic digital gain calibration. This equipment maintains the correct channel location of the natural ^{40}K peak. Since no calibration source is present during the survey, no additional dead time is introduced into the system.

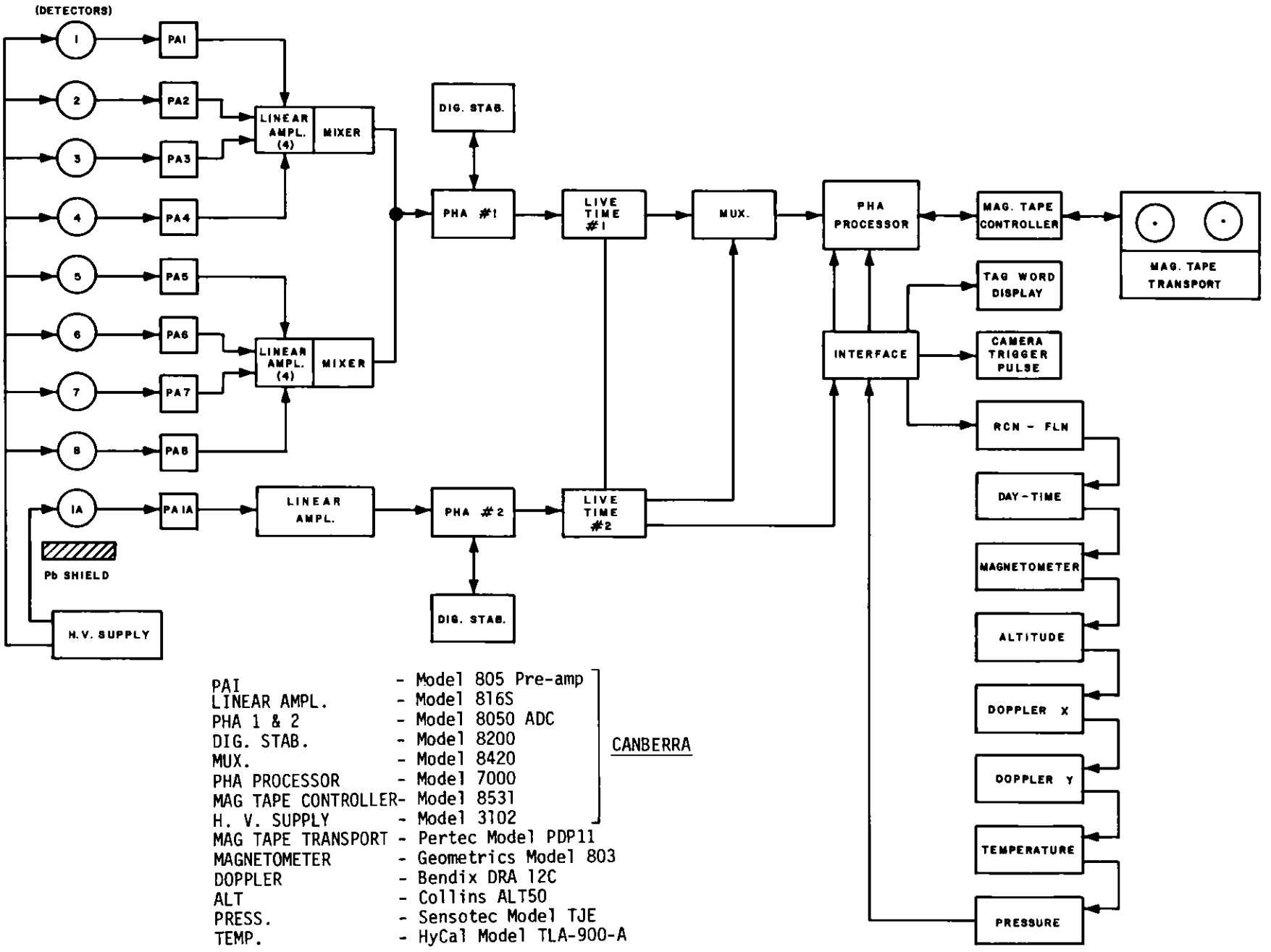

PAI	- Model 805 Pre-amp	CANBERRA
LINEAR AMPL.	- Model 816S	
PHA 1 & 2	- Model 8050 ADC	
DIG. STAB.	- Model 8200	
MUX.	- Model 8420	
PHA PROCESSOR	- Model 7000	
MAG TAPE CONTROLLER	- Model 8531	
H. V. SUPPLY	- Model 3102	
MAG TAPE TRANSPORT	- Pertec Model PDP11	
MAGNETOMETER	- Geometrics Model 803	
DOPPLER	- Bendix DRA 12C	
ALT	- Collins ALT50	
PRESS.	- Sensotec Model TJE	
TEMP.	- HyCal Model TLA-900-A	

Figure 3. Functional Block Diagram

In addition to the two spectra, other information pertaining to the survey operation is read out each second. These "tag words" precede the spectra on the tape and consist of:

- o Record number
- o Flight line number
- o Day, month, year, hour, minute, second
- o Doppler location information
- o Magnetometer data
- o Barometric pressure
- o Air temperature
- o Altimeter data

Three dimensional position information is provided continuously by the combination of the radar altimeter and doppler navigation systems. The altimeter is a highly accurate Collins ALT-50 system, and the voltage output of this system is recorded.

The Doppler System provides along-track and across-track position information with respect to a base point and a heading. In addition to the Doppler system, a 35 mm camera photographs the earth beneath the aircraft every three seconds. At a 400 foot altitude and normal survey speed, this frame rate produces a 20% overlap from frame to frame. The navigator provides another check on position as discussed in Part B below.

The device used to measure the earth's total magnetic field is a 0.25 gamma proton precession magnetometer. The sensor is towed as a "bird" on a 100 foot cable to minimize the magnetic effects of the aircraft. North-South, and East-West tests are flown to determine the small heading corrections to be made to the magnetometer data. These heading corrections are applied during processing.

The Phase I equipment has three basic operating modes: (1) CALIBRATE, which allows the proper gain calibration of the radiation detectors to be set; (2) OPERATE, which allows data to be received, reduced and recorded, and (3) PLAYBACK, which allows the operator to examine recently acquired data.

B. SURVEY PROCEDURES

At the start of the survey, ^{137}Cs resolution checks were made on all crystals individually. In this process each of the six photomultipliers on a crystal were gain-aligned, and then the resolution of that crystal was determined. The resolution of the eight 4π crystals functioning together was then determined from the equivalent ^{137}Cs resolution as calculated from the 2.615 MeV photopeak of ^{208}Tl. During the survey, daily checks of gain

and resolution were made at the Dallas office using flight data from the previous day. This is accomplished by computer summing all one-second data records for each flight line to produce an end of flight line spectrum (EOFL). Figure 4 is an example of such a spectrum. Both the 4π (PHA-1) and the 2π (PHA-2) spectra were plotted for each flight line. In order to have this information before the beginning of the following survey day, the field data tapes are air freighted to Dallas counter-to-counter at the end of each day's flying. Call-in to the Dallas office by the flight crew was required before survey operations for that day could commence.

In addition to the EOFL spectra, the re-formatted field tapes are dumped to permit observation of the live-time, raw data spectral sums, altimeter signal, magnetometer signal, etc. for each second along the line. Normally, only the first and last flight lines of any one day are checked in this manner on an immediate basis.

Prior to running a given day's survey, the flight crew performs preflight operations. These consist of servicing and power-up of the ground station magnetometer, normal aircraft preflight procedures, electronic systems check-out and weather forecasts for the area. The co-pilot/navigator briefs the crew on the planned survey area, sequence of flight lines, hazards and restricted areas, and emergency airfields within or adjacent to the survey area. The flight technician then contacts the Dallas office for information on possible equipment problems not evident in equipment check-out procedures. If problems exist, the survey is delayed until they are corrected. If the previous day's data are good, the aircraft proceeds to the test line selected for the area.

During the ferry to the test line, the flight technician tunes the magnetometer and runs a short equipment test which is equivalent to flying a survey line. The test line is then flown, and the total count over the test line compared to the average of the previous flights. If the total count value is within 20% of the mean value for that line, the aircraft proceeds to the start of the first line of the survey schedule for that day.

The co-pilot/navigator is responsible for the doppler navigation and makes updates as required based on visual check points. The record numbers associated with each one second data are displayed to the navigator, and he writes these record numbers on his flight map at various visual check points along the line such as cross-roads, rivers, etc. He is also responsible for monitoring the camera operation and signals the flight technician when to start and terminate each line.

Survey operations are terminated when any of the following occur: the job is complete; fuel runs low; darkness approaches; bad weather is encountered; the equipment malfunctions; aircraft trouble develops. After survey operations, the aircraft is returned to the test line and reflys

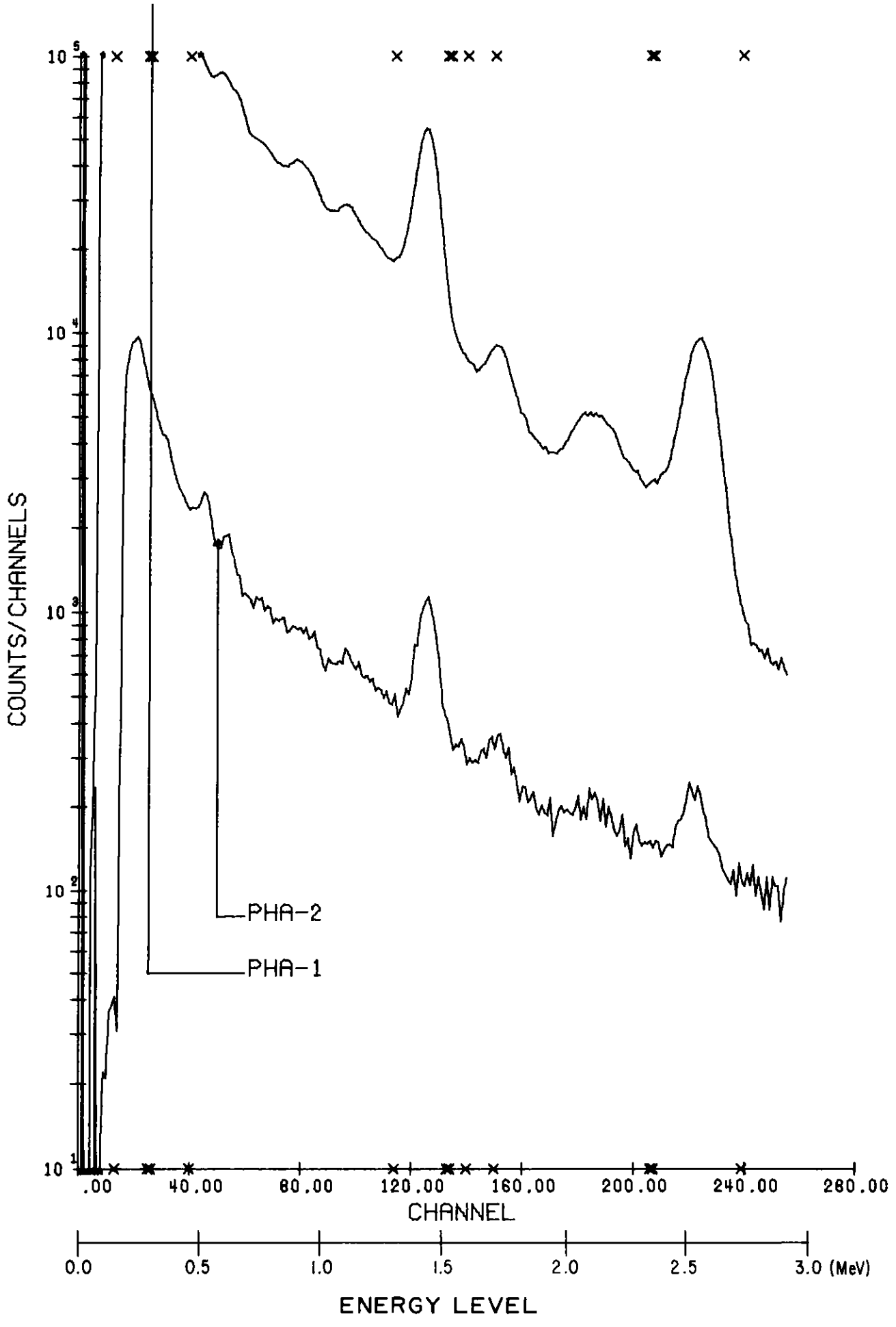

Figure 4. Typical End-of-Flight Line Spectral Plot

the line. This is not done if the system is down or return was forced by severe weather or aircraft malfunction affecting safety of flight. After the test line is flown the aircraft is returned to base.

Postflight operations consist of aircraft inspection, required service or maintenance ordered, data tapes packaged and shipped to the home office.

SECTION III

DATA REDUCTION AND ANALYSIS

A. COMPUTER PROCESSING FLOW

The processing flow chart representative of the work performed for this survey is shown in Figure 5. The original field data tapes contain the various tag words, 4π spectrum and 2π spectrum for each one second along the flight line. The REFORM program sums the proper energy bins of the spectra for each second and produces a trailer record for each line which contains the accumulated 4π and 2π spectra for the line. The CDTCRT is a data certification program which is run immediately upon receipt of the field data tapes and produces the EOFL spectral plots, Figure 4. The tapes indicated as customer tapes in Figure 5 are reformatted in the manner specified in the General Specifications prior to release. The program identification and function is given below:

PROGRAM	FUNCTION
REFORM	Produce energy group sums and EOFL spectra.
FIXMOD	Primary processing for matrix reduction, BIAIR computation, live times, background and altitude correction.
STACK	Flight path recovery to produce plots of actual paths at a scale of 1:250,000.
DOPTAP	Single record processing with latitude/ longitude, IGRF and single point statistical adequacy computation. Produces microfiche.
MMPLT	Averaged record processing with averaged statistical adequacy computation. Produces radiometric stacked profiles plot tapes.
GNDMRG	Merges aircraft magnetometer and ground magnetometer in proper time sequence and transfers temperature, pressure and altitude information.
RMPLT	Produces tapes for magnetometer stacked profile plots.
GEOLOG	Produces averaged value microfiche with geology and plot tape for standard deviation "dot plots" related to geologic type.
HISTO, MERGE and SRT1	Programs preliminary to obtaining the histograms as a function of geologic type for the entire area.
DMPLOT	Produces plot tape for the area histograms.

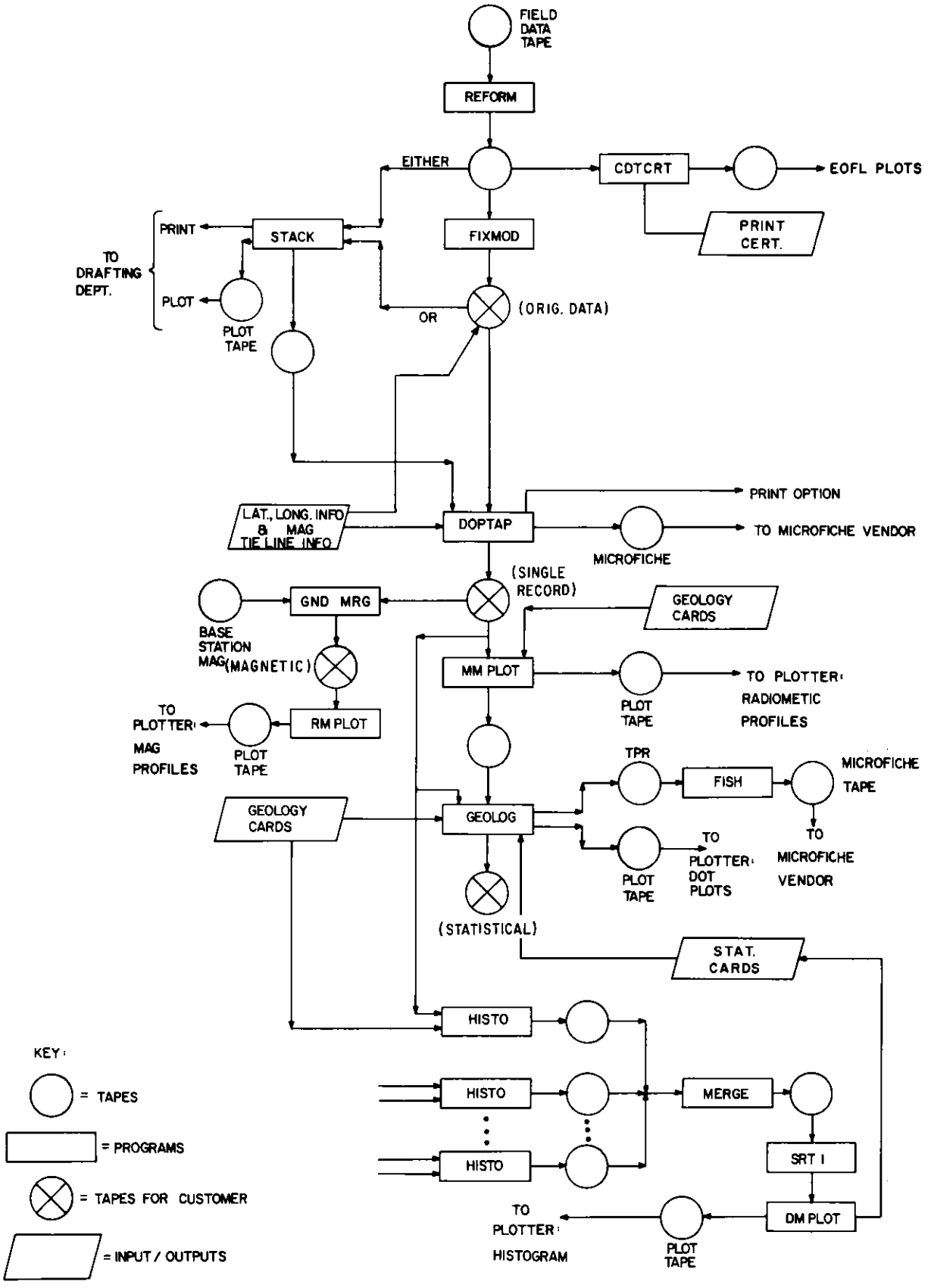

FIGURE 5 DATA FLOW DIAGRAM

As stated in the above list of program functions, the FIXMOD program performs the primary processes for determining the reported eTh, eU and K counting rate associated with the earth's surface as measured at 400 feet above the surface. For this reason the analytical work of this program is described in more detail below.

Each one second of 4π spectral data is summed by the REFORM program according to the following energy intervals (bins).

Cosmic:	3.0 to 6.0	MeV
^{208}Tl photopeak:	2.410 to 2.796	MeV
^{214}Bi photopeak:	1.05 to 1.322 plus 1.638 to 2.410	MeV
^{40}K photopeak:	1.322 to 1.638	MeV

In general these raw sums contain counts not only from ground sources but from aircraft background and atmospheric radioactivity as well. To determine the counts in the energy bins which are caused only by the isotope associated with the bin a 4 x 4 matrix method is used. This matrix may be formed through the use of a standard cosmic spectrum plus the Walker Field Pad determinations of α, β and γ or from four standard spectra representing respectively cosmic, thorium, uranium and potassium pure spectra at a 400 foot altitude.

This matrix multiplication is represented by:

$$\begin{bmatrix} A_{11} & A_{12} & A_{13} & A_{14} \\ A_{21} & A_{22} & A_{23} & A_{24} \\ A_{31} & A_{32} & A_{33} & A_{34} \\ A_{41} & A_{42} & A_{43} & A_{44} \end{bmatrix} \bullet \begin{bmatrix} COS \\ TL \\ BI \\ K \end{bmatrix} = \begin{bmatrix} MCOS \\ MTL \\ MBI \\ MK \end{bmatrix}$$

where the A_{ij} are the elements of the 4 x 4 matrix; the column matrix on the left represents the four raw data sums and the column matrix on the right is the counts in each energy bin caused only by the indicated isotope. These matrix result counts are for the measured live time. To obtain the counts per second it is necessary to divide by the live time, LTC1, thus:

$$MCOS/LTC1 = COS1$$
$$MTL/LTC1 = TL1$$
$$MBI/LTC1 = BI1$$
$$MK/LTC1 = K1$$

The Tl1, BI1 and K1 counts per second contain the aircraft associated backgrounds caused by thorium, uranium and ^{40}K. Geodata has determined these backgrounds for this installation to be 8.5 counts per second in the ^{208}Tl energy interval due to background ^{208}Tl, 17.3 counts per second in the ^{214}Bi energy intervals due to background ^{214}Bi and 20.3 counts per second in the ^{40}K interval due to background ^{40}K. For this work the background counting rates were determined by over water flights at the Lake Mead Dynamic Test Range and confirmed by flights over the Gulf of Mexico during the survey period. The backgrounds are checked during the survey by observing counting rates over large water bodies under the flight path.

These backgrounds are subtracted from the above determined count rate values

$$\overline{Tl1} = Tl1 - 8.5$$

$$\overline{BI1} = BI1 - 17.3$$

$$\overline{K1} = K1 - 20.3$$

The $\overline{BI1}$ value contains counts caused by atmospheric ^{214}Bi which must be subtracted before altitude correction is applied. The 2π crystal data is used to determine the magnitude of the count to be subtracted. Since the predominant variable source affecting the 2π crystal is the atmospheric ^{214}Bi, it is possible to utilize most of the spectrum in the BIAIR determination and thereby produce some improvement in the statistical error. The energy range used for the 2π crystal is from 1.05 to 2.41 MeV. Within this range the aircraft background has been determined as 9.2 counts per second and the 2π cosmic count from 3.0 to 6.0 MeV must be multiplied by 1.4899 to determine the cosmic count in the 1.05 to 2.41 MeV range.

It was determined through the test flights at the Dynamic Test Range that the 2π counting rate increased significantly as the aircraft flew from water to land at a given altitude. The effect increased at lower altitudes. Conversation with Mr. Ralph Falconer and Mr. Dave Purvance of Bendix Field Engineering office in Grand Junction, Colorado, indicated that this may be caused by the scattering of ^{208}Tl gammas into the shielded crystal. Experimentation with the data obtained at the Test Range confirmed the cause, and it was necessary to subtract counts from the 2π total sum based on the $\overline{Tl1}$ value determined from the 4π data. The correction factor is .06 $\overline{Tl1}$. This correction was checked on data obtained during the survey by using lines that passed over large water bodies and observing the BiAIR value over water and over land. The correction appears to work exceptionally well. Thus, the 2π counting rate caused by atmospheric ^{214}Bi is given by

$$\overline{BI2} = \frac{BI2 - 1.4899\ COS2}{LTC2} - 9.2 - .06\ \overline{Tl1}$$

where

BI2 = the raw 2π sum from 1.05 to 2.41 MeV

COS2 = the raw 2π sum from 3.0 to 6.0 MeV

LTC2 = Live time associated with the 2π data.

$\overline{T11}$ = Average of the 4π corrected ^{208}Tl counting rate over 19 records

For this survey five 19-second groups of 2π data are averaged in the determination of BIAIR on a sliding basis. The averaged counting rate so determined must be related to an equivalent counting rate in the 4π crystals for the two energy intervals used. This conversion is accomplished by a so called geometric factor which is a multiplier to the averaged 2π counting rate after all corrections. Thus,

$$BIAIR = \overline{\overline{BI2}} * G(x)$$

where

BIAIR = the expected 4π counting rate caused by atmospheric ^{214}Bi in the two energy intervals

$\overline{\overline{BI2}}$ = the five 19 second group average of BI2

G(x) = the geometric factor.

For the DC-3, N1010S installation the value of the geometric factor at 400 feet is 6.22.

The final ^{214}Bi counting rate caused by surface sources is then

$$BISUR = \overline{BI1} - BIAIR$$

The quantities $\overline{T11}$, BISUR and $\overline{K1}$ are then corrected to an equivalent counting rate at 400 feet through the equations indicated below:

$$TLS = \overline{T11}\, e^{-\mu_1(400-x)}$$

$$BIS = BISUR\, e^{-\mu_2(400-x)}$$

$$KS = \overline{K1}\, e^{-\mu_3(400-x)}$$

where

TLS, BIS, KS = respective counting rates at 400 feet caused by surface sources

μ_1, μ_2, μ_3 = respective linear total attenuation coefficients

x = aircraft height above the surface in feet.

The correctness of the altitude factors is evidenced in the data presented in Figure 6. These data are the counting rates produced by the survey aircraft and system over the same ground path at the Lake Mead Dynamic Test Range corrected to 400 feet according to the above equations.

B. FLIGHT PATH RECOVERY

Processing beyond the FIXMOD program is not pursued until the flight paths have been determined to scale, laid down on the base maps, and pick-points confirmed. The program utilized to produce the flight paths to a scale of 1:250,000 is the STACK. This program may be run using as input either the REFORM or FIXMOD output tapes. Pick-point record numbers and the distance in inches to scale between these record numbers as determined on the base map, are used as other input to this program. A plot is produced which has the appearance indicated in Figure 7. The full plot of this flight path is laid on the base map and the map locations of various pick-point record numbers are checked. Discrepancies require correction and re-running of the STACK program until all record numbers occur on the base map in their proper location.

C. DATA PRESENTATION

For the Houston Quadrangle, the surveyed area was positioned geographically to completely cover the National Topographic Map. The topographic map has been used as the flight base and sufficient geographical and 15' location information have been shown. The flight line pattern has been superpositioned onto these base maps, and the standard deviation levels for each independent variable and each ratio of these variables have been plotted (NGRMS) based on the data contained within the total map area. Every fifth data point along each map line has its standard deviation value shown at the location of that value. Therefore, there are six NGRMS sheets which indicate the location and magnitude of anomalous data, Figure 8.

The multivariable map line profile, which represents all variables as a function of their location for each line, is presented at a scale of 1:500,000 in Volume II. Each profile presents:

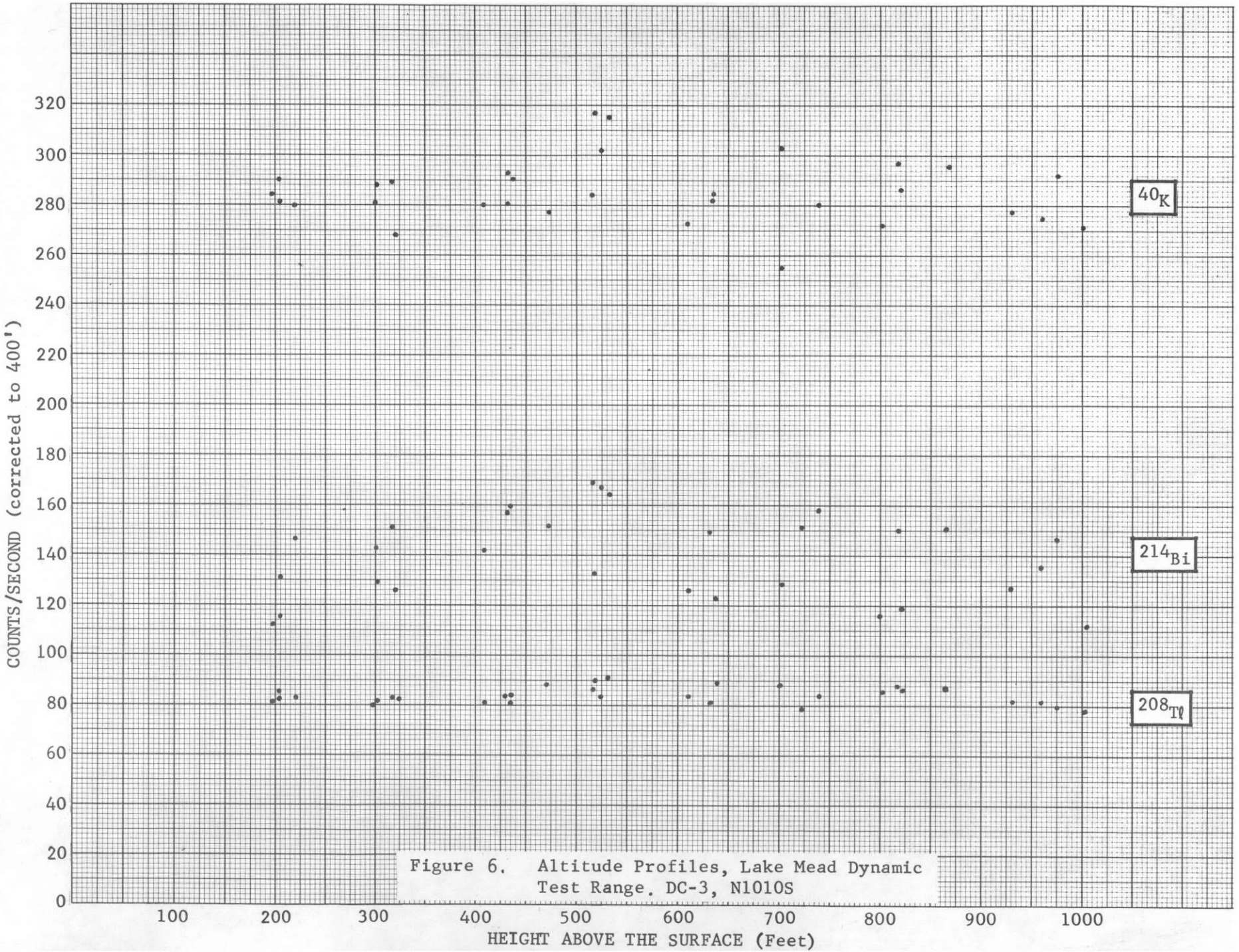

Figure 6. Altitude Profiles, Lake Mead Dynamic Test Range, DC-3, N1010S

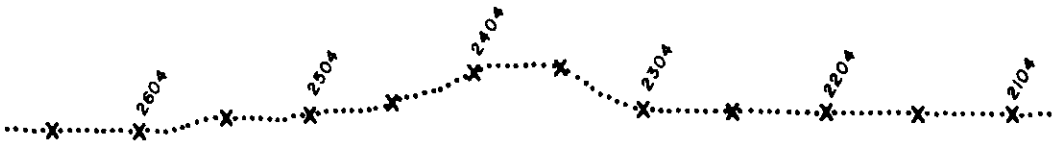

Figure 7. Computer Presentation of Typical Map Line

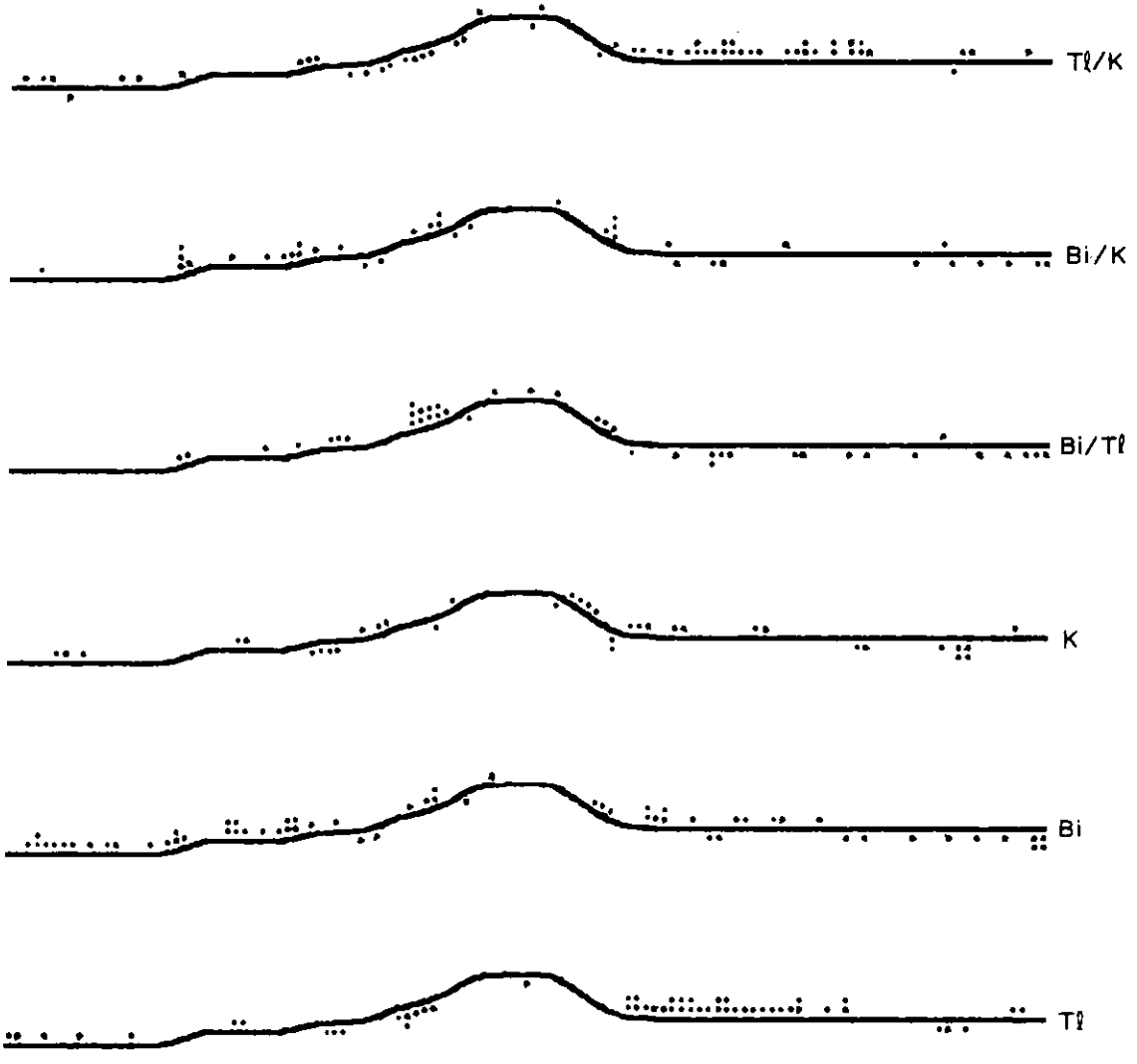

Figure 8. Typical Map Line Showing Statistical Deviations

1. Aircraft altitude above the surface
2. eTh (^{208}Tl from ^{232}Th decay series)
3. eU (^{214}Bi from ^{238}U decay series)
4. K (^{40}K from natural potassium)
5. BiAir (atmospheric ^{214}Bi)
6. Gross count (greater than 400 keV)
7. Residual magnetic field
8. eU/eTh (^{214}Bi/^{208}Tl) ratio
9. eU/K (^{214}Bi/^{40}K) ratio
10. eTh/K (^{208}Tl/^{40}K) ratio
11. Geologic data with flight path superimposed
12. Statistical adequacy and altitude flags

The residual magnetic field map line profile, which represents five variables as a function of their latitude and longitude location for each line, plus geologic data at a scale of 1:500,000 is presented in Volume II as:

1. Aircraft altitude
2. Atmospheric temperature
3. Atmospheric pressure
4. Residual magnetic field data
5. Magnetic field base line station data
6. Geological data with flight path superimposed

Microfiche for the single point unaveraged data are produced by the DOPTAP program. Microfiche for the 7-point linear average data, including mean values and standard deviations as a function of geologic type, are produced by the GEOLOG program. Both sets of microfiche are furnished with this report.

In addition to the above presentation items the following is supplied:

- Histograms of the radiation data distribution within each geologic unit.
- Histograms of the average velocity distribution for each one-second record for each map and tie line.
- Histograms of the average altitude distribution for each one-second record for each map and tie line
- Tables giving the average radiation concentration of each geologic unit for each line.
- A map containing the location of anomalous radiation data.
- Set of maps showing the standard deviation data as a function of location and radiation variable.

These types of presentation will be explained in Section V of this report.

D. STATISTICAL ANALYSIS PROCEDURES

It is necessary to exclude from the statistical analysis all variables which have too low a counting rate to be statistically valid and data which were obtained at altitudes above 1000 feet. To this end a statistical adequacy test was run on all data, for each data record. If a given value of Tl, Bi or K failed the test, that variable value and any ratio value associated with it were not used in the statistical determinations of mean and standard deviation values. In addition such values are indicated on the radiometric profiles by a vertical "tic" mark along the base line for the variable and are flagged in the single record and averaged record listings (microfiche). The ratio values are set to zero in the Radiometric Profile Plots. The flags in the listings appear under the heading AKUT for altitude, ^{40}K, ^{214}Bi and ^{208}Tl respectively. The flags are zero for statistically valid data and one for rejected data in the case of K, U and T. For altitude (A) a zero indicates altitudes to 700 feet; a one (1) indicates altitudes between 700 and 1000 feet, and a two (2) indicates altitudes above 1000 feet.

The tests used to reject data were as follows:

(1) $\overline{Tl1} < 1.5\sqrt{Tlw - \overline{Tl1}} = 1.5\sigma T$

(2) $BiSUR < 1.5\sqrt{Biw - BiSUR} = 1.5\sigma B$

(3) $\overline{K1} < 1.5\sqrt{Kw - \overline{K1}} = 1.5\sigma K$

where the "w" subscript refers to the respective window counting rates from the raw data and $\overline{Tl1}$, BISUR and $\overline{K1}$ have previously been defined. If any of the above inequalities were true, the associated variable was flagged and that value was rejected in all statistical determinations.

The values of the radicals in the above equations which are indicated as σT, σB, σK and the barred values were calculated on the basis of a single record value for determining flags in the single record listings and on the basis of the 7-point weighted values for determining flags in the averaged records listings.

The mean value and standard deviations were calculated assuming the data to have a normal distribution within a geologic type. The equation used in determining the variance is:

$$\sigma^2 = \frac{1}{N-1}\left(\sum_{i=1}^{N} X_i^2 - NX^2\right)$$

where N is the number of statistically valid samples for a given geologic type, X_i is the value of the variable for sample number i and X is the mean value of the variable for the geologic type. Values from the entire survey of the area are used in these computations.

E. OTHER CORRECTIONS

In addition to the above, corrections must be applied to the magnetic data which consist of diurnal corrections using the tie line data and heading corrections dependent on the heading of the aircraft.

The heading correction for the aircraft and equipment used in this survey were determined by flying a predetermined path at the survey altitude in first an east to west direction then in a west to east direction. The same procedure is used on a north-south path. Based on these data the heading corrections are:

West to East travel: +3.56 gammas
East to West travel: -3.56 gammas
North to South travel: -1.0 gammas
South to North travel: +1.0 gammas

The diurnal corrections applied to these data were as follows:

DATE FLOWN	ML	CORRECTION (GAMMAS)
4/4/77	1	5.39
4/4/77	2	0.88
4/4/77	3	5.27
4/4/77	4	-0.23
4/4/77	5	5.26
4/4/77	6	-4.10
4/5/77	7	15.80
4/5/77	8	13.58
4/5/77	9	24.76
4/5/77	10	20.87
4/5/77	11	19.49
4/5/77	12	27.03
4/5/77	13	3.57
4/5/77	14	1.93
4/6/77	15	42.32
4/6/77	16	53.16
4/6/77	17	39.98
4/6/77	18	44.05
4/6/77	19	60.47
4/6/77	20	34.46
4/12/77	21	-4.20
4/12/77	22	12.84

SECTION IV

GEOLOGY OF THE SURVEYED AREA

A. GENERAL

The airborne gamma ray survey was conducted over a sequence of Quaternary sedimentary deposits. The sediments are part of the coastal plain of the Gulf Coast Geosyncline and overlie Mesozoic, Paleozoic and Precambrian rocks. The Paleozoic and Precambrian units were deformed and metamorphosed during the Late Paleozoic and compressed into the largely subsurface Quachita and Marathon fold belts. The basement surface and overlying rocks have a relatively gentle homoclinal dip towards the south and are situated on the southern flank of the stable cratonic interior of the continent. Positive and negative warpings, faults, salt intrusions and igneous masses have modified the overall homoclinal dip and caused variations in the width of the plain and the character of the present day shoreline. Four major structural features are located in the Gulf Coast Geosyncline in Texas. They are:

(1) the Rio Grande Embayment
(2) the San Marcos Arch
(3) the Houston-East Texas Embayment
(4) the Sabine Arch.

Many of the Cenozoic strata outcrop in subparallel belts which are progressively younger seaward. Structurally these rocks are relatively undeformed, but where deformation occurs it is largely gravitational and tensional. The sedimentary mass is lithologically variable, lenticular in cross-section and achieves a maximum thickness of 50,000 feet or more in the Northern Gulf of Mexico. This three dimensional structural-stratigraphic unit is termed the "Coastal Province" (Murray, 1961). Much of the province is submerged beneath shallow continental shelf and deeper waters. In contrast, the coastal plain is a geomorphic-topographic feature of low relief with elevations generally below 1000 feet above sea level. Surface drainage within the coastal plain is entirely into the Gulf of Mexico.

East of the Brazos River the coastal plain is essentially coincidental with the inner margin of the Mesozoic sediments. West and south of the Brazos River the inner margin of the coastal plain follows the Balcones Escarpment to the vicinity of Del Rio and approximates the contact between the Cretaceous Gulf and the Cretaceous Comanche series.

A consensus of published geologic opinion is that during Cenozoic times the Rocky Mountains became the major source of sediments for the geosyncline. The Eocene aged Midway Group represents the most widespread Cenozoic marine unit. Following the deposition of the Midway Group the sedimentation rate increased rapidly. The major centers of clastic input became coincident with the locations of major deltaic complexes (Fisher and MacGowen, 1967). Deltaic and other nearshore marine and non-marine facies grade gulfward and down-dip into middle and outer marine facies. As the rates of sedimentation exceeded the rate of structural downwarping the depocenters migrated.

Between Eocene and Quaternary times the geosynclinal depocenter in the Northern Gulf of Mexico shifted gradually from the Rio Grande Embayment of south Texas northeastward to southern Lousisiana. The Eocene aged depocenter is in south Texas, whereas the Early Oligocene depocenter is in the Houston-East Texas Embayment. There was a gulfward migration of the geosynclinal axis and of the coastal plain strandline accompanying the change in depocenter location.

Many of the stratigraphic units increase in thickness towards the Gulf of Mexico. Importantly much of the gulfward thickening of the stratigraphic units takes place across growth faults. Growth faults are normal faults which have a substantial increase in throw with depth and thickening of sediments on the downthrown side. Throws of several thousand feet are common. Growth faults usually form arcuate patterns, downthrown and concave towards the gulf. Fault alignment is usually subparallel to the basin margins. The locus of maximum growth faulting accompanied both a shift in the depocenter and the gulfward migration of the geosynclinal axis.

Many salt domes are known to exist within the Gulf Coast Geosyncline. These salt diapirs are concentrated in areas of greater than normal sedimentary thickness; their growth appears genetically related to periods of abnormally great sedimentation.

B. LOCAL GEOLOGY

The Houston 1:250,000 sheet, of the Geologic Atlas of Texas, shows the surficial geology of an area bounded by latitudes 29°00' to 30°00' north and longitudes 93°45' to 96°00' west. The enclosed area includes all of Chambers County, most of Brazoria, Fort Bend, Harris and Jefferson counties and minor parts of Orange, Liberty, Waller and Matagorda counties.

The coastal plain has a major marine indentation in the Galveston/Trinity Bay area which represents the submerged mouths of the Trinity and San Jacinto river valleys. Sabine Lake in the northeastern corner of the sheet represents a second major area of inland saline water, at the submerged junction of the Neches and Sabine river valleys.

The geology of the Houston Sheet is Quaternary, with one minor exception. The most extensive surficial geological unit is the Beaumont Formation, composed of fluviatile, non-marine and unconsolidated sediments. Dividing the Beaumont Formation into geographically isolated sections are alluvial deposits of the Recent floodplains of the gulfward flowing rivers. Along the coast the alluvium was deposited in coastal mudflat or coastal backswamp environments. Barrier island deposits form a narrow slither of sand along the margin of the land-sea contact.

In the northwestern section of the sheet older fluvial formations, with similar characteristics to the Beaumont Formation,occur. Of the older deposits the Montgomery Formation (elsewhere referred to as the Upper Lissie Formation) has the greatest extent.

Salt domes are scattered throughout the area. In one instance Tertiary aged sandstone is exposed overlying a salt diapir. The sandstone is believed to be associated with the Miocene aged Catahoula Formation. The salt domes are often the locii of oil or gas fields and as such may be associated with escaping hydrogen sulfide and other gasses which aid in the formation of reducing environments suitable for uranium mineralization and deposition. However, neither published reports of uranium mineralization nor areas of high radioactivity have been found for the Quaternary sediments of the Houston Sheet.

C. DESCRIPTION OF THE GEOLOGY OF THE STRATIGRAPHIC UNITS OF THE HOUSTON 1:250,000 SHEET OF THE GEOLOGIC ATLAS OF TEXAS

Cenozoic

Quaternary

Fill and Spoil (FS)

Fill (F) is the material dredged for raising the land surface above the naturally occurring level of alluvium and barrier island deposit and for creating land. Spoil (S) is material dredged while deepening waterways which forms islands. Both deposits are variously comprised of mud, silt and sand with shells and organic debris.

Alluvium (Qal)

The alluvium is composed of clay, silt and/or sand. Organic matter is locally abundant. The sediment was deposited in a variety of environments including point bar, natural levee, stream channel, backswamp, coastal marsh, mudflat and narrow beach.

Barrier Island Deposits (Qbi)

These deposits are mainly well-sorted, fine grained sands with abundant shell and shell fragments. The sands interfinger with clay and silt in a landward direction. They include beachridge, spit, tidal channel, tidal delta and sand dune deposits.

Recent or Late Pleistocene

Deweyville Formation (Qd)

The Deweyville Formation includes sand, silt clay and gravels formed in a variety of depositional environments including point bar, natural levee, stream channel and backswamp.

Locally the thickness of the Deweyville Formation exceeds 50 feet. High level Deweyville Surfaces eat into the Beaumont Formation and high level Deweyville deposits along the Trinity River are intermediate in position between the Beaumont surface and the level of most Deweyville deposits.

Pleistocene

Beaumont Formation (Qb, Qbb)

The Beaumont Formation (Qb) is mainly clay, silt and sands, deposited in stream channels, point bar, natural levee, backswamp and to a lesser extent coastal marsh and mudflat environments. Concretions of calcium carbonate, iron and iron-manganese oxides have formed in the zone of weathering. The surface is almost featureless and is characterized by abandoned river channels. Pimple mounds occur on meanderbelt ridges and are separated by areas of low, relatively smooth, featureless backswamp deposits. The formation has a thickness of approximately 100 feet.

Montgomery Formation (Qm)

The Montgomery Formation consists of clay, silt, sand and very minor siliceous gravel of granule and small pebble size; gravel is more abundant to the northwest. Locally the Montgomery Formation is calcareous with concretions of calcium carbonate, iron oxide and iron manganese oxides common in the zone of weathering. The deposits are mainly fluviatile with a faily flat and featureless surface except for numerous shallow rounded depressions and pimple mounds; thickness of the formation is ca. 100 feet.

Bentley Formation (Qby)

The Bentley Formation is composed of clay, silt, and minor amounts of gravel. The gravel is slightly coarser than in the Montgomery Formation and is non-calcareous. Iron oxide concretions are more abundant than in the Montgomery Formation. The deposits are mainly fluviatile. The surface is gently undulating and the total vertical thickness is approximately 100 feet.

Willis Formation (Qw)

Clay, silt and sand, with siliceous gravels comprise the Willis Formation. The sand is usually coarser than in the younger units. The formation is deeply weathered and lateritic. It is indurated by clay and cemented by iron-oxides. The deposit is fluviatile, non-calcareous and has a maximum thickness of 75 feet.

Tertiary - Miocene

Tertiary Rocks of the Hockley Salt Dome (T)

Sandstone, thought to be of the Catahoula Formation occurs over the Hockley Salt Dome. The sandstone is very fine grained, hard with abundant porcellaneous to opaline cement. It is poorly bedded and jointed.

D. SOILS IN THE HOUSTON QUADRANGLE

The soils of the Houston Sheet have been grouped into seven soil associations (Godfrey, McKee and Oakes, 1971). The soils that comprise several of the associations are very similar. Variations in soils between associations can generally be attributed to the changes in underlying geology which is the parent material from which the soils have formed. The soil profiles owe their character to other environmental factors as well as geology. These factors are described as climatic,biologic, topographic and age of soil

The Beaumont Formation which is the most extensive geologic formation has been correlated with two soil associations: one east and the other west of the Trinity River Valley. Both associations have similar soils and one description applies to both. The soils are Pelluderts, Argiaquolls and Albaqualfs. The Pelluderts are poorly to moderately drained, clayey soils formed in river alluvium. The clay is partly montmorillonitic with a tendency to swell and crack with changes in moisture. Pedoturbation accompanies volume change and results in mixing of profile material. The Argiaquolls and Albaqualfs are poorly drained and formed on loamier or sandier textured alluvium. The profile remains saturated throughout much of the year. The Argiaquolls have clay enriched, subsurface horizons underlying a coarser textured, more siliceous, upper horizon. The Albaquolls have accumulated organic material in the upper mineral horizon. Leaching of the soil components is limited in the Albaquolls and base cation content is high throughout the profile.

The Willis Formation is geologically and topographically older than the Beaumont Formation and is correlated with a soil association comprised of Paleudalfs and Ochraqualfs. These soils are formed on loamy textured parent alluvium and lack the heavy clay texture of the Beaumont Pelluderts. The longer period of exposure to weathering and modification by percolating water has developed a mature, well segregated profile. Eluviation of clay to subsurface horizons is a dominant process in all three soils, leaving loamier surfaces over clay enriched subsoils. The Ochraqualfs occur on the poorer drained areas and retain high levels of moisture throughout the year.

The Montgomery and Bentley formations have similar soils to those of the Beaumont, however, a tongue of older and more maturely developed soils envelopes the Houston Metropolitan Area. The characteristics of these Paleudalfs, Fragiudalfs and Ochraqualfs are closer to those of the Willis Formation than that of the Beaumont.

The alluvial valleys of the Brazos, San Bernard and Colorado rivers are correlated with two soil associations. The upper parts of each valley are associated with Haplaquolls, Udifluvents and Haplustolls whereas the lower sections of the valley are mapped as predominantly Hapludolls and Udifluvents. These are loamy to clayey, immaturely developed soils of the Recent floodplains. The Udifluvents have undergone very little modification

of the original textural, mineralogical and sedimentary characteristics of the river alluvium. The Hapludolls and Haplustolls vary mainly in the degree and length of time that the soil profile is moist. Both soils have organically enriched surface horizons and little leaching of base cations has occurred.

The soil association of the Trinity River Valley is comprised of Haplaquolls and Haplaquepts. These are young soils on Recent alluvium. The soils are generally clayey and would be classified as vertisols if the profile were allowed to dry more frequently. The major difference between the two soils is that the Haplaquoll has more organic matter in its surface horizon than the Haplaqualf. Both soils are located on poorly drained bottomland and rarely dry out completely.

The beaches and coastal marshes of the coastal zone have their own soil association comprised of Haplaquolls, Fluvaquents and Udipsamments. The Udipsamments are very poorly developed, sandy textured soils of the beaches and barrier island dunes. Very little pedogenic alteration of parent texture or minerals has occurred. In the coastal marshes which are periodically covered by salt water the soils are saline, with clayey or loamy textures. Due to low lying relief, high water tables, and inundation by the sea, the profiles are usually saturated. The Haplaquolls have accumulated humus in their surface horizons; the Fluvaquents have only minor organic accumulation, and very minor alteration to texture, mineral or sedimentary characteristics of the original alluvium.

SECTION V

RESULTS OF DATA ANALYSIS

A. GEOLOGIC BASE MAP

The Houston geologic base map is produced to the scale of the NTMS with the geologic data obtained from the Houston 1:250,000 sheet, the Geologic Atlas of Texas. The base map is presented in Volume II of this report without the superpositioned flight lines at a scale of 1:500,000, and at a scale of 1:250,000 as a separate sheet.

B. NATIONAL GAMMA RAY MAP SERIES (NGRMS)

The geologic base has been photographically screened to allow emphasis of the flight line locations and of the information regarding data analysis. These maps are used as the base for presenting statistical information on the six variables:

- o ^{208}Tl
- o ^{214}Bi
- o ^{40}K
- o $^{214}Bi/^{208}Tl$ Ratio
- o $^{214}Bi/\ ^{40}K$ Ratio
- o $^{208}Tl/\ ^{40}K$ Ratio

The six NGRMS sheets are presented in Volume II of this report at a scale of 1:500,000 and as separate sheets at a scale of 1:250,000.

The statistical information is summarized on these maps through the utilization of one, two or three dots above or below the flight line at every fifth data point. One dot above the line indicates that the counting rate or ratio value at that point is between 1σ and 2σ greater than the mean value for that geologic type. The mean and σ values are determined for each geologic type based on all flight line data from the area, as is discussed further in Part F below. Two dots indicate values between 2σ and 3σ, and three dots show values greater than 3σ. Dots below the line indicate counting rate or ratio values which are less than the mean value by 1, 2 or 3σ in the same manner.

C. RADIOMETRIC STACKED PROFILE DATA

The profiles of Map Lines 1-22 and Tie Lines 1-7 are presented in Volume II of this report at a scale of 1:500,000 and at a scale of 1:250,000 as separate sheets. The same vertical scale is used for a given variable for all map lines, but the vertical scale changes to fit the specific variable plotted. The scales used for each variable are:

1. Altitude

   100 feet/division; aircraft altitude above the surface; no averaging.

2. Tl (^{208}Tl)

   10 counts/second/division (C/S/div). Seven seconds of data are averaged with weighting of 1:2:3:4:3:2:1 and the average value plotted at the center of the group of 7.

3. Bi (^{214}Bi)

   20 C/S/div; 7-second weighted average as for Tl.

4. K (^{40}K)

   15 C/S/div; 7-second weighted average as for Tl.

5. Bi Air

   20 C/S/div; 95-second non-weighted average.

6. Residual Magnetic Field (RMAG)

   20 gammas/division; the residual magnetic field is the total magnetic field as measured by a proton precession magnetometer from which has been subtracted the International Geomagnetic Reference Field (Stassinapoulous; NSSDC-72-12). Heading and diurnal corrections have been applied. (Section III,E.)

7. Total Count, 400 KeV to 2.80 MeV (GC)

   250 C/S/div; no averaging

8. ^{214}BI/^{208} Tl Ratio (Bi/Tl)

   0.4/division; 7-second weighted averaging as for Tl.

9. ^{214}Bi/^{40}K Ratio (Bi/K)

   0.5/division; 7-second weighted averaging as for Tl.

10. ^{208}Tl/^{40}K Ratio (Tl/K)

    0.2/division; 7-second weighted averaging as for Tl.

11. Geology

    The surface geology along the flight line, with a width of about six miles, is displayed above the profiles and the flight path is superimposed.

D. MAGNETIC STACKED PROFILE DATA

For each of the 22 Map Lines and 7 Tie Lines a magnetic multiple-parameter stacked profile is produced at a scale of 1:500,000 in Volume II of this report, and at a scale of 1:250,000 as separate sheets. The same vertical scale is used for a given variable for all map lines, but the vertical scale changes to fit the specific variable plotted. The scales used for each variable are:

1. Altitude

   100 feet/division; aircraft altitude above the surface; no averaging.

2. Temperature

   1 degree celsius/division; no averaging.

3. Barametric Pressure

   0.25 inches mercury/division; no averaging.

4. Base Station - Magnetic Field

   10 gammas/division; no averaging.

5. Residual Magnetic Field

   10 gammas/division; no averaging. Heading and diurnal corrections have been applied, (Section III, E.).

E. MAGNETIC TAPES AND LISTINGS

The description of the magnetic tapes and their listings is presented in Appendix II.

F. STATISTICAL PRESENTATION OF DATA BY GEOLOGIC TYPE

After the flight lines are superimposed on the geologic base, it is possible to select the record numbers associated with each geologic type existing below the aircraft as it travels along the flight path. This information is used as input to various programs to produce interpretation information based on the statistical variations within the geologic types existing in the area.

The first group of data in the averaged output microfiche listing gives the computed mean and standard deviation for all six radiometric variables for each geologic type. These values were computed on the basis of the data from individual flight lines.

The listing for the averaged output (microfiche), gives the mean value and the magnitude of the deviations from the mean for each averaged radiometric record along the entire flight line. The deviation from the mean is indicated by stars in the "rank" column of the listing. One, two, or three stars with no preceeding sign indicate one, two, or three sigma and greater deviations above the mean value. If the stars are preceeded by a minus sign, the deviations are below the mean.

Tables 1-6 list the mean values for each geologic type based on the data from a single line rather than from the entire area. The mean values for water are greater than zero because of sand bars, islands, etc. which occur in the water areas. This is particularly noticeable on the radiometric profiles of map lines 14, 17 and others crossing the bay area.

G. FREQUENCY DISTRIBUTIONS OF DATA FOR EACH GEOLOGIC TYPE

The six radiation variables were grouped according to geologic type and presented in the form of frequency distribution plots. These plots, which show the number of occurrences at a specific magnitude as a function of the magnitude, are included in Appendix I of Volume I. Data from all map lines and tie lines were used to determine these distributions. Statistically invalid values as determined according to Section III, Part D above, were not used in producing the distributions. The mean and standard deviations for each geologic type encountered in the Houston quadrangle are presented in Table 7 for easy reference.

H. MICROFICHE REPRODUCTION OF SINGLE RECORD AND AVERAGED RECORD LISTINGS

The output listings of the single point non-averaged and averaged computer programs have been reproduced on MICROFICHE, and are included in Volume I of this report. A 7-point weighted average was used to produce the listing of the six radiation variables. An example of both the single point and averaged listings is included in Appendix II for reference.

I. ALTITUDE AND GROUND SPEED HISTOGRAMS

A histogram of the ground speed and altitude of the aircraft for each map line and tie line is included in Appendix III. Certain lines passed over the Houston, Texas area and these lines are reflected in a double distribution in altitude.

	QAL	QB	QBB	QBI	QBY	QD	QM	QW
TL7	45	40			27		30	28
TL6	42	40					23	
TL5	39	39					23	
TL4	21	37		9				
TL3	20	35	16	17		34		
TL2	28	40						
TL1	22	41						
ML22	18	41	18			29	21	22
ML21	23	43	13		24	26	26	26
ML20	28	40	24		24	26	26	
ML19	30	39			30	34	23	
ML18	29	41			35		27	
ML17	28	35					30	
ML16	25	40	31				28	
ML15	37	44	17					
ML14	44	45						
ML13	45	54	17					
ML12	50	52						
ML11	56	55						
ML10	51	55						
ML9	56	52						
ML8	54	49						
ML7	55	54						
ML6	52	58		17				
ML5	54	57		15				
ML4	56	57	35	16				
ML3	57	57		17				
ML2	51	61						
ML1	55	58		18				

Table 1. Geologic Unit Average Value as a Function of Map Line for ^{208}Tl.

	QAL	QB	QBB	QBI	QBY	QD	QM	QW
TL7	109	98			66		86	70
TL6	109	92					63	
TL5	107	94					69	
TL4	64	90		44				
TL3	55	83	51	61		73		
TL2	85	97						
TL1	84	97						
ML22	61	98	41			62	60	60
ML21	67	98	42		73	63	67	64
ML20	72	90	58		68	69	66	
ML19	73	90			81	72	62	
ML18	73	92			73		69	
ML17	70	87					75	
ML16	70	96	78				74	
ML15	89	96	55					
ML14	93	90						
ML13	101	105	50					
ML12	108	100						
ML11	112	103						
ML10	107	107						
ML9	112	106						
ML8	103	95						
ML7	106	97						
ML6	109	108		54				
ML5	118	111		53				
ML4	130	119	119	54				
ML3	123	116		37				
ML2	115	124						
ML1	112	111		56				

Table 2. Geologic Unit Average Value as a Function of Map Line for ^{214}Bi

	QAL	QB	QBB	QBI	QBY	QD	QM	QW
TL7	101	48			15		51	15
TL6	108	50					15	
TL5	98	49					16	
TL4	54	40		38				
TL3	34	29	28	60		27		
TL2	43	31						
TL1	39	34						
ML22	30	29	13			40	15	14
ML21	40	32	17		14	34	16	16
ML20	42	30	16		13	20	16	
ML19	34	30			35	25	19	
ML18	57	31			73		18	
ML17	59	32					19	
ML16	51	39	27				17	
ML15	89	44	19					
ML14	114	69						
ML13	119	78	31					
ML12	148	72						
ML11	155	71						
ML10	119	69						
ML9	143	69						
ML8	142	65						
ML7	142	69						
ML6	136	69		62				
ML5	127	75		60				
ML4	132	78	78	61				
ML3	133	82		81				
ML2	130	84						
ML1	134	78		61				

Table 3. Geologic Unit Average Value as a Function of Map Line for ^{40}K.

	QAL	QB	QBB	QBI	QBY	QD	QM	QW
TL7	247	246			250		288	261
TL6	265	239					280	
TL5	277	250					304	
TL4	334	253		486				
TL3	278	249	358	381		227		
TL2	313	248						
TL1	293	242						
ML22	352	249	247			247	295	286
ML21	301	236	345		298	278	257	251
ML20	276	234	249		282	307	261	
ML19	263	236			278	272	275	
ML18	271	232			232		266	
ML17	265	254					253	
ML16	295	246	250				268	
ML15	256	228	328					
ML14	223	208						
ML13	236	206	309					
ML12	221	200						
ML11	202	194						
ML10	217	200						
ML9	205	210						
ML8	192	198						
ML7	201	187						
ML6	219	191		327				
ML5	223	199		338				
ML4	236	217	345	350				
ML3	226	210		224				
ML2	232	205						
ML1	207	196		327				

Table 4. Geologic Unit Average Value as a Function of Map Line for $^{214}Bi/^{208}Tl$

	QAL	QB	QBB	QBI	QBY	QD	QM	QW
TL7	1232	2121			4662		2656	5581
TL6	1061	1911					6468	
TL5	1146	2004					9079	
TL4	1386	2488		1175				
TL3	1673	3073	2160	1017		2875		
TL2	2172	3286						
TL1	1942	2996						
ML22	2956	3608	3793			1676	3187	4787
ML21	1816	3240	2546		5909	1960	4769	4693
ML20	1880	3220	3840		5936	3475	4951	
ML19	2236	3190			4704	3022	4011	
ML18	1758	3099			1905		4669	
ML17	1572	2937					3320	
ML16	1685	2806	2906				3265	
ML15	1195	2413	2856					
ML14	1132	1383						
ML13	1002	1458	1740					
ML12	779	1461						
ML11	791	1494						
ML10	1011	1603						
ML9	881	1578						
ML8	776	1514						
ML7	813	1504						
ML6	861	1641		948				
ML5	992	1564		882				
ML4	1054	1605	1566	941				
ML3	986	1518		466				
ML2	926	1569						
ML1	865	1496		1010				

Table 5. Geologic Unit Average Value as a Function of Map Line for $^{214}Bi/^{40}K$

	QAL	QB	QBB	QBI	QBY	QD	QM	QW
TL7	514	876			1903		941	2108
TL6	410	820					2194	
TL5	416	804					2717	
TL4	416	991		241				
TL3	623	1277	623	282		1288		
TL2	722	1358						
TL1	681	1248						
ML22	873	1458	1540			752	2778	1677
ML21	648	1389	785		2081	826	2885	1864
ML20	702	1399	1532		2105	1320	2924	
ML19	887	1371			1666	1406	2520	
ML18	648	1348			713		2830	
ML17	606	1188					2065	
ML16	570	1155	1154				2941	
ML15	470	1076	896					
ML14	495	682						
ML13	421	723	563					
ML12	352	739						
ML11	393	776						
ML10	500	807						
ML9	438	764						
ML8	407	772						
ML7	405	812						
ML6	401	861		295				
ML5	446	787		268				
ML4	460	759	457	275				
ML3	440	723		227				
ML2	403	759						
ML1	422	761		301				

Table 6. Geologic Unit Average Value as a Function of Map Line for $^{208}Tl/^{40}K$

GEOL. TYPE	Tl		Bi		K		Bi/Tl		Bi/K		Tl/K	
	$\bar{X}$	σ	$\bar{X}$	σ	$\bar{X}$	σ	$\bar{X}$	σ	$\bar{X}$	σ	$\bar{X}$	σ
QAL	43.12	17.23	97.74	32.28	102.06	53.26	2.45	.76	1.23	.72	.50	.23
QB	45.59	13.47	97.90	21.30	49.13	23.20	2.26	.58	2.43	1.21	1.07	.44
QBB	19.71	9.04	55.53	21.88	24.14	14.05	3.10	1.12	2.65	1.26	.92	.45
QBI	16.45	5.69	53.85	17.75	61.35	19.70	3.47	1.12	.93	.31	.28	.07
QBY	28.54	8.16	74.81	17.80	29.26	32.55	2.72	.66	4.83	6.16	1.75	1.65
QD	29.49	12.35	66.96	16.79	32.29	10.30	2.58	.97	2.33	1.09	1.01	.52
QM	25.88	6.43	67.37	14.46	17.93	10.55	2.70	.67	4.82	5.43	1.82	1.65
QW	24.26	5.70	63.86	13.13	15.28	7.41	2.72	.69	4.86	4.75	1.79	1.47

Table 7. Mean ($\bar{X}$) and Standard Deviation (σ) for Each Geologic Type.

Geologic Unit	^{208}Tl	^{214}Bi	$^{214}Bi/^{208}Tl$
Qal	42	21	32 (9)
Qd	Zero	Zero	1 (-)
Qb	89	70	61 (52)
Qbb	1	2	2 (-)
Qby	1	Zero	1 (-)
Qw	2	1	3 (-)
Qm	8	11	8 (2)

Table 8 - Summary of Anomalies in the Houston Quadrangle.

J. DATA INTERPRETATIONS

1. Analysis of Histograms

Radioactivity data for the various geologic units is presented as a series of histograms (Appendix I) with values in counts per second (c/s) plotted against frequency of events. The histograms should approximate a Gaussian distribution if the geologic unit is represented by facies of similar kind and geochemical content. Bimodal or polymodal distributions for the ^{208}Tl, ^{214}Bi and ^{40}K values may indicate variation in geologic or geochemical content, or large scale variations in hydrologic regimes of the soils. The latter may be significant in a coastal plain location.

Qal: Alluvium

The alluvium mapped as Qal on the Houston Geologic Map is extensive and the number of events is high. The histogram representing the ^{40}K values is bimodal, with modes at 40 c/s and 140 c/s. However, significant overlap between the tails of the two distributions prevents a consistent differentiation. Similarly, the bimodal ^{208}Tl histogram could not be separated due to considerable overlap between tails of the distributions. The ^{214}Bi values were unimodal.

The bimodal histograms for the alluvium may represent facies change(s) or soil hydrology change(s).

Qd: Deweyville Formation

The Deweyville Formation is not extensive, with less than 500 events. The ^{208}Tl distribution is bimodal, with modes at 15 c/s and 35 c/s. However, separation of the overlapping tails of the distributions is not plausible.

Qby: Bentley Formation

The three histograms for ^{40}K, ^{208}Tl and ^{214}Bi are polymodal with an elongated tail of relatively few events for the highest values. The total number of events is not high. Separation is possible in all the histograms; the critical parameter for ^{208}Tl is 45 c/s, for ^{214}Bi and ^{40}K the critical parameters are 102 c/s and 50 c/s respectively.

Qb: Beaumont Formation

The Beaumont Formation is the most extensive formation, with 38621 events forming the histograms. The ^{214}Bi and ^{208}Tl histograms are unimodal, whereas the ^{40}K histogram is bimodal with modes at 40 c/s and 70 c/s. However, the tails of the two overlapping distributions cannot be separated.

2. Discussion of the ^{208}Tl, ^{214}Bi and $^{214}Bi/^{208}Tl$ Anomalies

Anomalous ^{208}Tl and ^{214}Bi amounts and anomalous $^{214}Bi/^{208}Tl$ ratios were analyzed for the geologic units of the Houston Airbourne Radiometric Maps. An anomaly was considered to be: (1) a cluster of three or more values of one standard deviation or greater that was visually distinguishable on the map; (2) a juxtaposition of two or more two standard deviations; (3) one or more three standard deviation values. Only positive anomalies were considered for the ^{208}Tl and ^{214}Bi but both positive and negative anomalies were considered for the $^{214}Bi/^{208}Tl$ ratios. The anomalies based on the above three criteria are indicated by the red bars in Figures 9, 10 and 11 for ^{208}Tl, ^{214}Bi and $^{214}Bi/^{208}Tl$ respectively. In the case of the ratio, positive anomalies appear as bars above the line and negative anomalies appear as bars below the line. Table 8 summarizes the anomalies by variable, soil type and number encountered in the area.

A total of seven geologic units showed anomalous values, Qal, Qd, Qb, Qbb, Qby, Qm and Qw. The two units which were most extensive, Qal and Qb, had by far the greatest number of anomalies.

Qal: Alluvium

The Quaternary alluvium mapped in the unit Qal consists of a variety of clay, silt and sand deposited mainly during Recent times in environments which vary from stream channel to coastal marsh to beach. The anomalies are most frequent in the southwestern part of the mapsheet where the unit tends to lie in topographic lows and watertables are close to the surface, often forming marshy, poorly drained areas. High water content in soils over large parts of the unit may have reduced the average radioactivity count, allowing counts for the drier areas to appear as anomalous highs more frequently than would otherwise occur.

Anomalies in the ^{214}Bi and $^{214}Bi/^{208}Tl$ are probably associated with the migration of uranium isotopes in solution, both into and out of deposits. This would be facilitated by the near surface movement of groundwater and frequent inundation of alluvia by river or sea water flooding. The precipitation of isotopes through chemical absorption or isomorphous substitution would be concentrated in clays, organic matter and internally drained topographic lows.

Qb: Beaumont Formation

The widely distributed Beaumont Formation has a great number of anomalies. The unit consists mostly of clay, silt and sand deposited in stream channels, point bars, natural levees and back swamp environs. As with the Qal unit, variations in the water content of soils due to changes in texture and changes in topographic position probably affect radioactivity readings.

Concentration of soluble uranium isotopes through near-surface groundwater movement and in poorly drained depressions is probable. Removal of uranium isotopes resulting in a reversal of $^{214}Bi/^{208}Tl$ occur in other areas. Locii of likely concentration are clays and organic deposits in topographic lows. Soils with high clay content occur over large areas of the Beaumont Formation; these soils are classified as Pelluderts.

As with the Qal geologic unit concentration of uranium minerals may be associated in some instances with the upward escape of hydrogen sulphide and other gases from oil or gas reservoirs. The reducing environment produced by these gases may be suitable for uranium mineralization and deposition.

Montgomery Formation

The Montgomery Formation was formed in similar types of environment to the Beaumont and consists largely of fluviatile clay, silt and sand. The unit is older than the Beaumont, generally better drained and with greater depth to the watertable - an exception would be the area covered by Ochraqualf soils.

Variations in topography which affect the flow of groundwater and surface waters might explain the concentration or removal of uranium isotopes in the surficial deposits, with concentration of uranium isotopes in clayier depressions.

Well developed caliche/calcic deposits in the subsoil may be locii for trapping mobile uranium isotopes. The calcic horizons require thousands of years to develop and are usually present only in the soils of the older Quaternary deposits.

In many areas the naturally developed soils have experienced eluviation of clay to deeper horizons and the concentration of adsorbed uranium isotopes in argillic (clay-enriched) horizons may occur.

Qw: Willis Formation

The Willis Formation is the oldest of the Quaternary fluviatile formations and crops-out in the northwestern portion of the map sheet. The concentration of radioactivity anomalies seems slightly higher for this unit than for the others. The material is deeply weathered and lateritic; the soils are old and well developed. Although the heavy textured clays of the Beaumont are absent in the Willis, the formation of insitu clay has occurred over a long period of time. It is possible that some of these clayier horizons are the locii of the high ^{214}Bi counts.

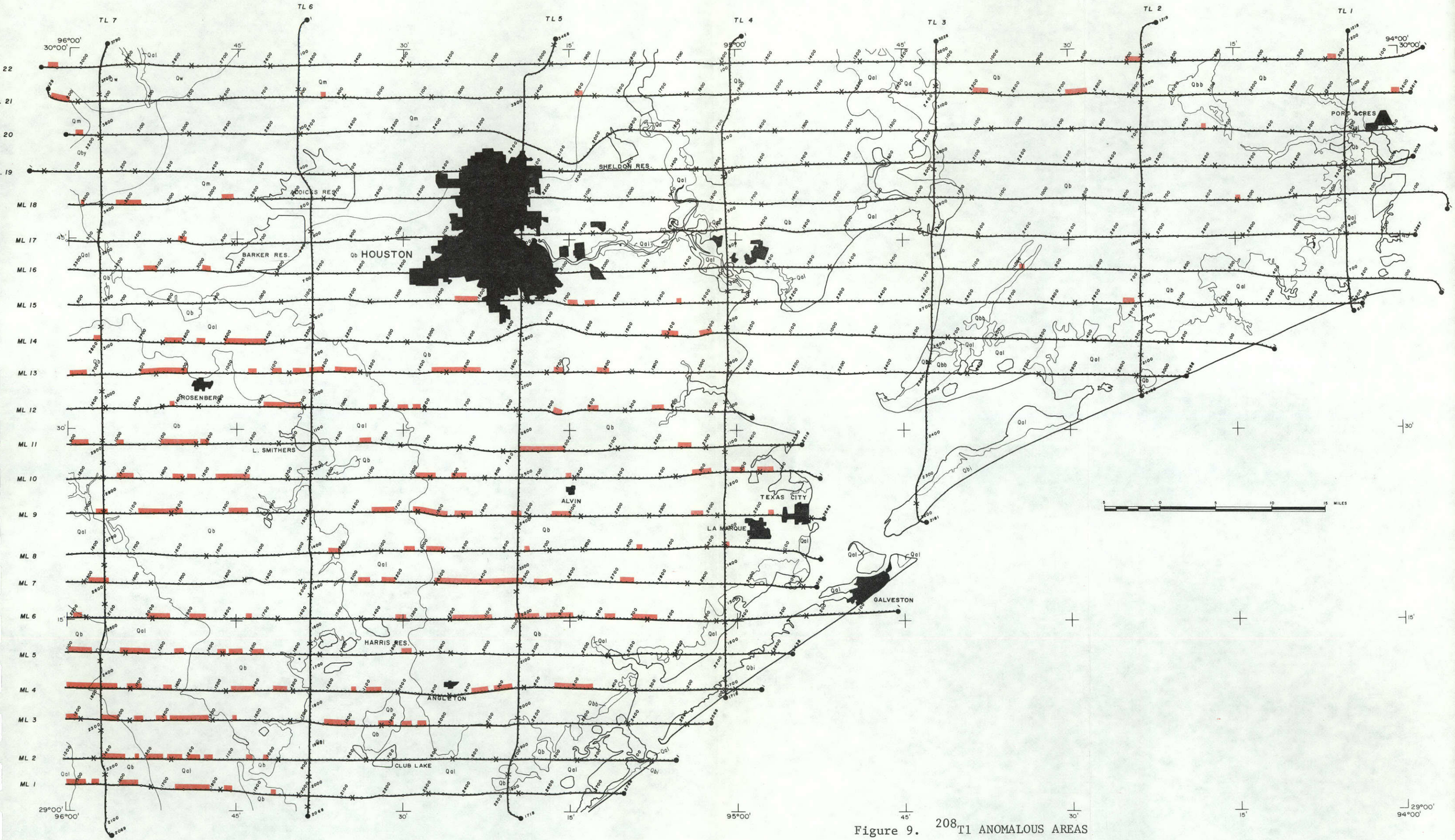

Figure 9. ^{208}T1 ANOMALOUS AREAS

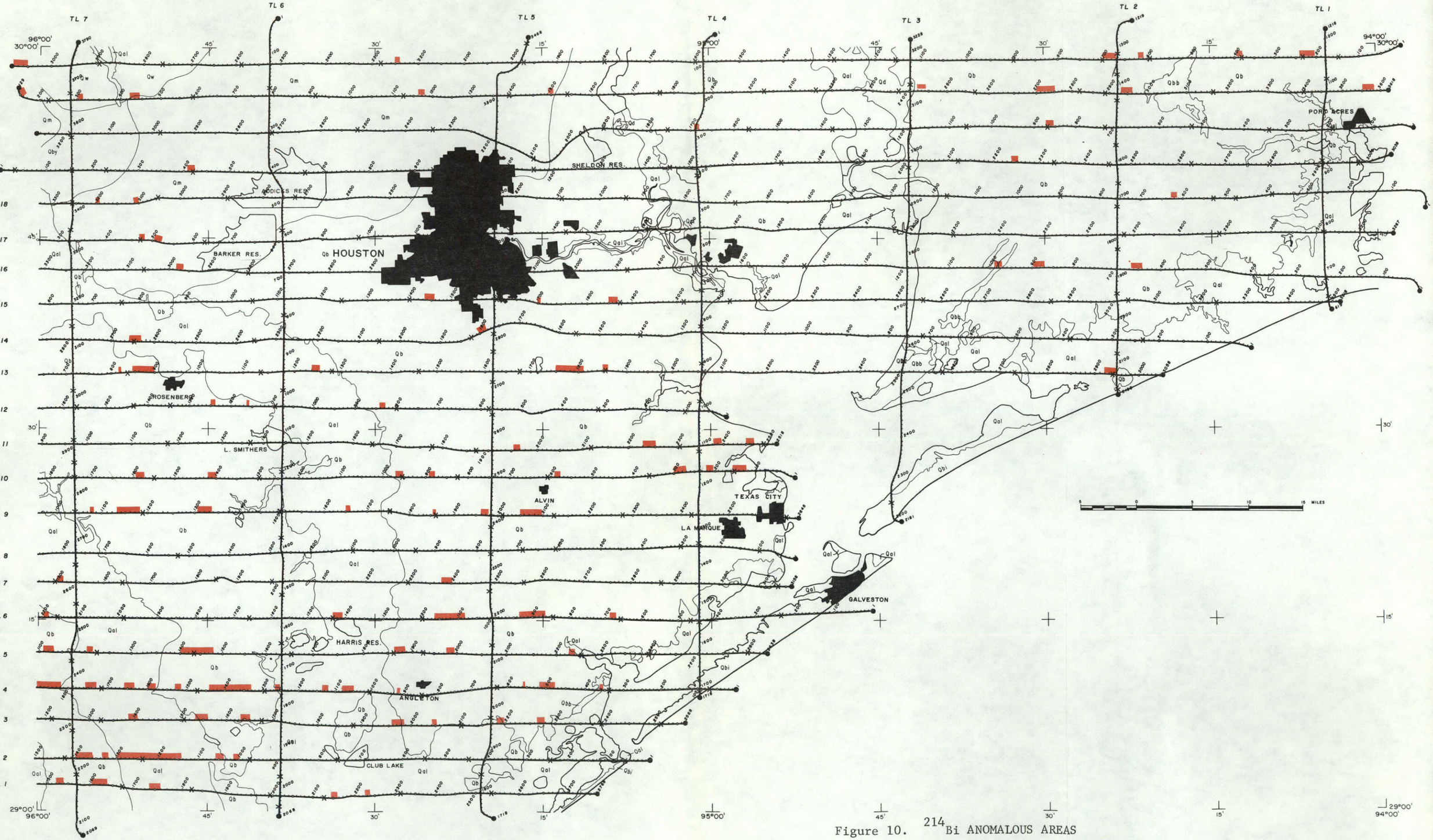

Figure 10. ^{214}Bi ANOMALOUS AREAS

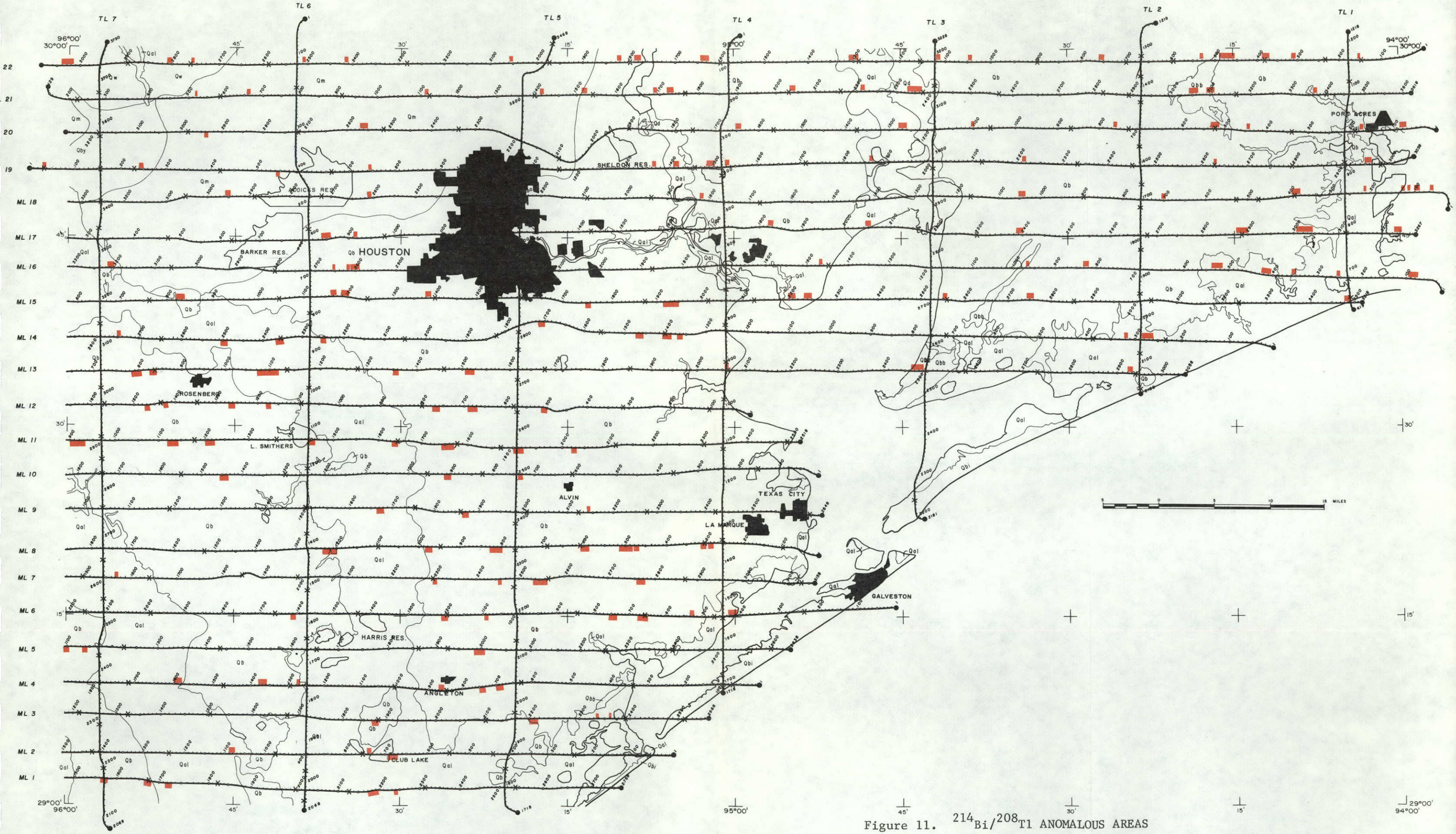

Figure 11. $^{214}Bi/^{208}Tl$ ANOMALOUS AREAS

3. Cultural Features

The major cultural features that might effect the radiometric data on the Houston Map Sheet are the City of Houston and several smaller towns such as Galveston, Texas City, La Marque, Port Acres, etc. Anomalies associated with these urban areas were ignored.

Large reservoirs and lakes that are man dammed were potential areas for negative anomalies; such anomalies were not analyzed.

The many small oil or gas fields are a cultural response to a natural geological event. The fields were included in the discussion of reasons for anomalies in individual geologic units. Reducing environments associated with the upward escape of hydrogen sulfide gas or other "reducing" gases can affect the deposition and location of uranium ions and mineralization.

4. Trends and Significant Results

The greatest concentration of anomalies is located in the southwestern portion of the map-sheet in the Beaumont Formation and in the alluvium of the flood plains. Many of the anomalies appear to be associated with oil fields or in close proximity to them. The fact that some anomalies cut across surface boundaries between geologic units suggests epigenic deposition possibly related to near surface water movement and the formation of localized environments conducive to ion concentration, perhaps mineralization.

A P P E N D I X I

FREQUENCY DISTRIBUTION OF RADIATION DATA

AS A FUNCTION OF GEOLOGIC UNIT

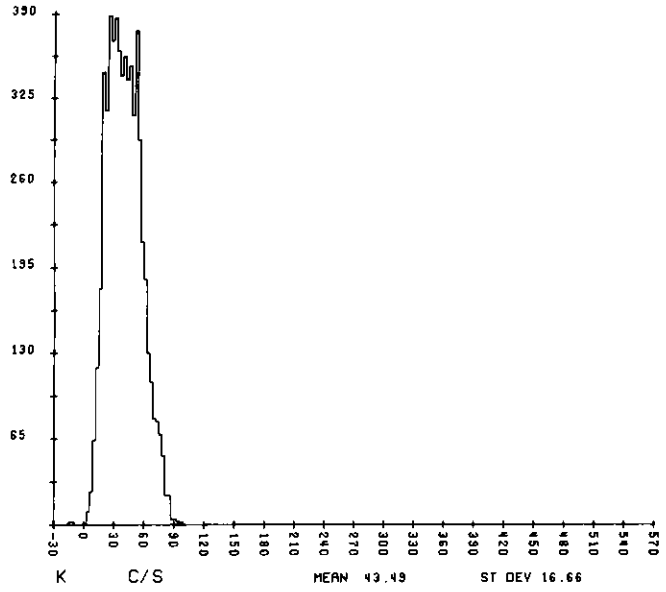
K C/S
MEAN 43.49
ST DEV 16.66

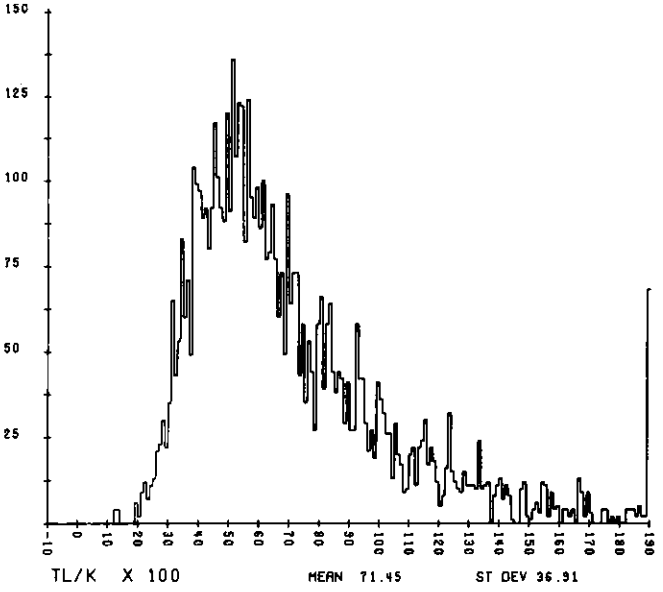
TL/K X 100
MEAN 71.45
ST DEV 36.91

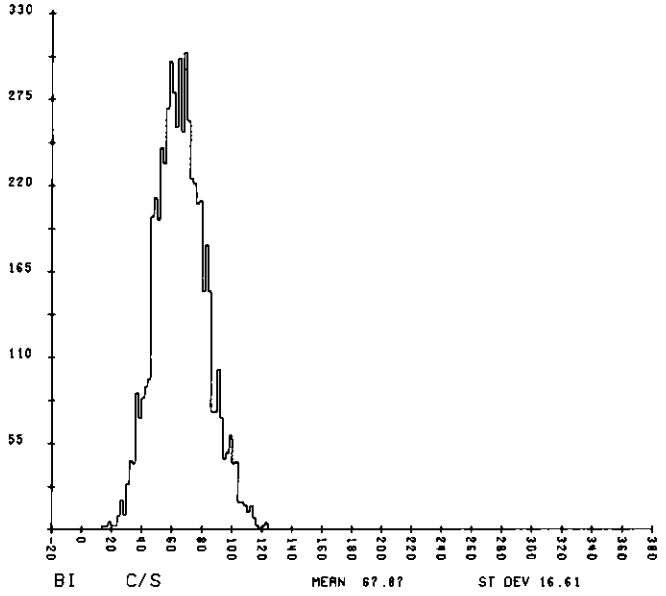
BI C/S
MEAN 67.87
ST DEV 16.61

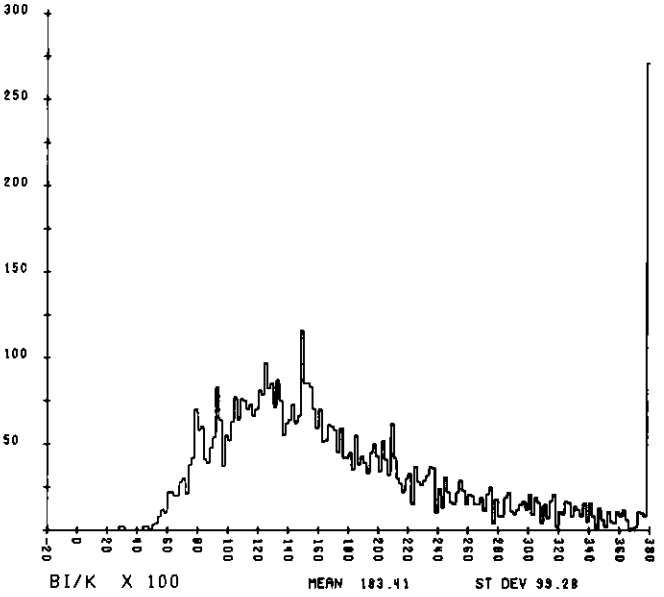
BI/K X 100
MEAN 183.41
ST DEV 99.28

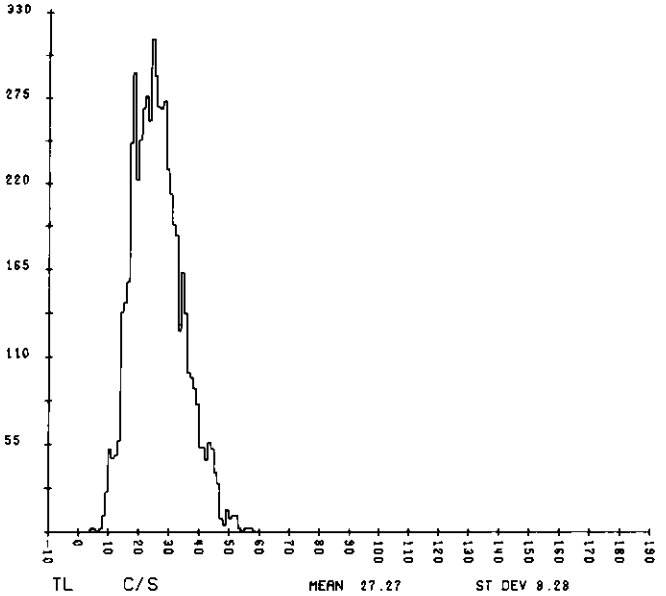
TL C/S
MEAN 27.27
ST DEV 8.28
GEOLOGIC UNIT CITY
TOTAL EVENTS 5906

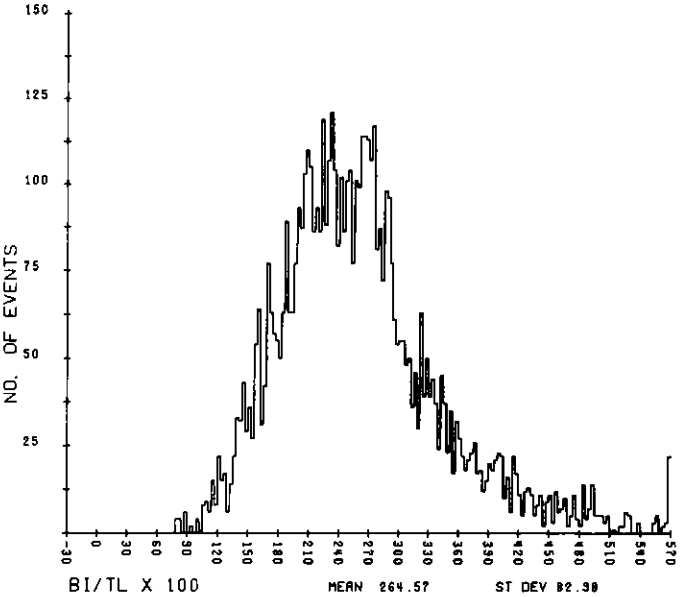
NO. OF EVENTS
BI/TL X 100
MEAN 264.57
ST DEV 82.38

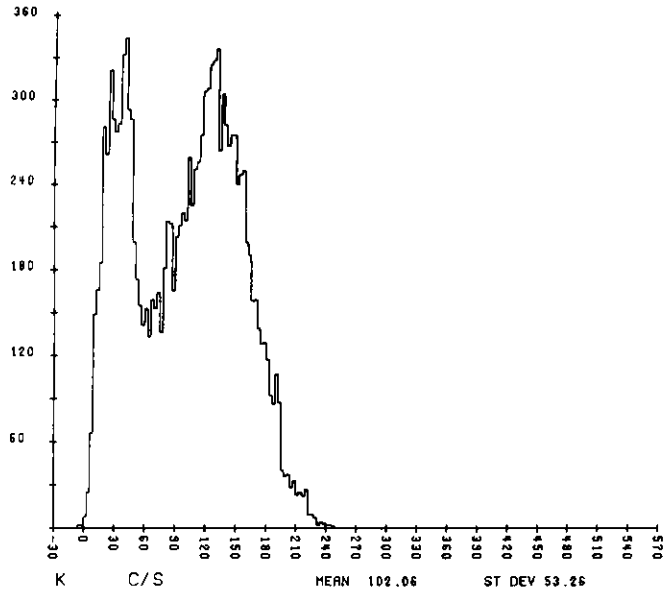
K C/S
MEAN 102.06
ST DEV 53.26

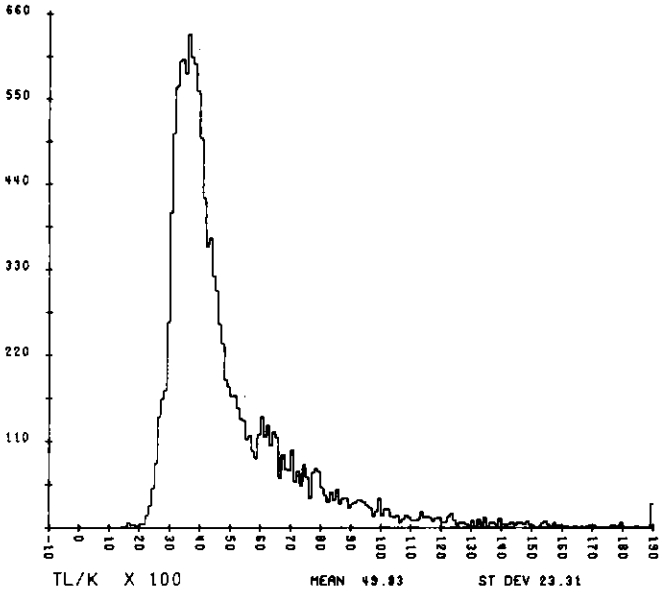
TL/K X 100
MEAN 49.83
ST DEV 23.31

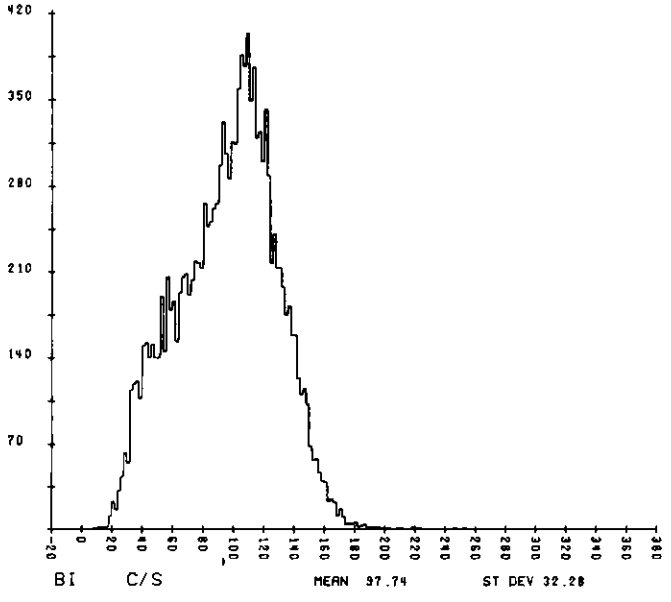
BI C/S
MEAN 97.74
ST DEV 32.28

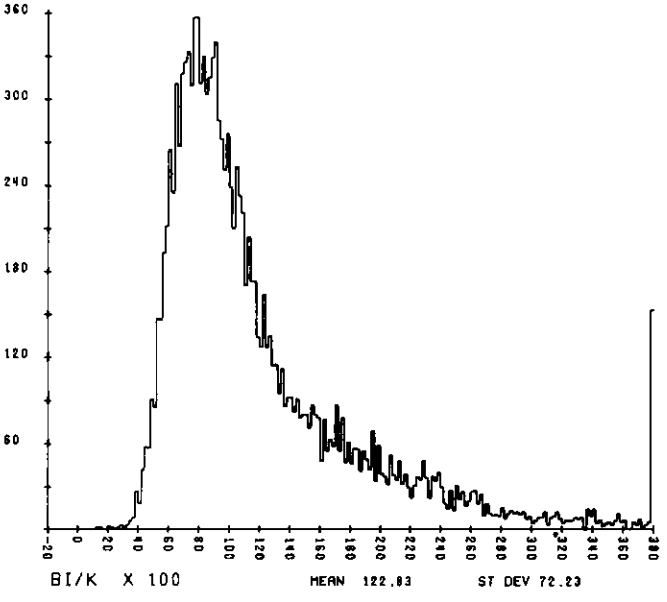
BI/K X 100
MEAN 122.83
ST DEV 72.23

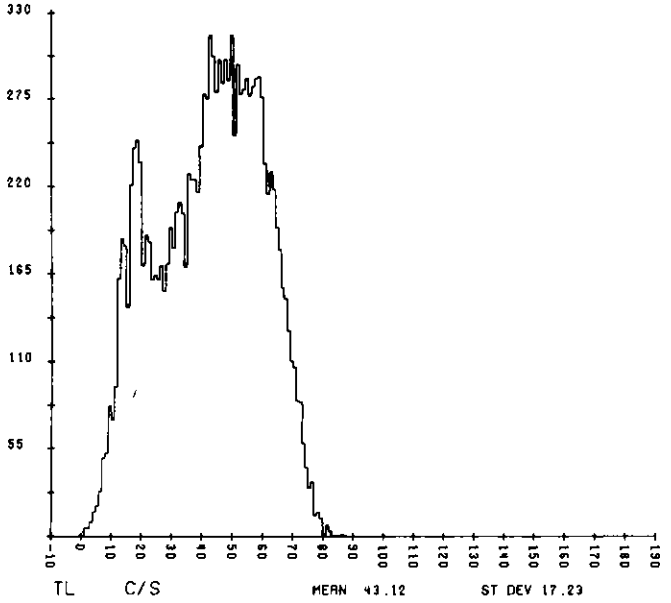
TL C/S
MEAN 43.12
ST DEV 17.23
GEOLOGIC UNIT QAL
TOTAL EVENTS 13925

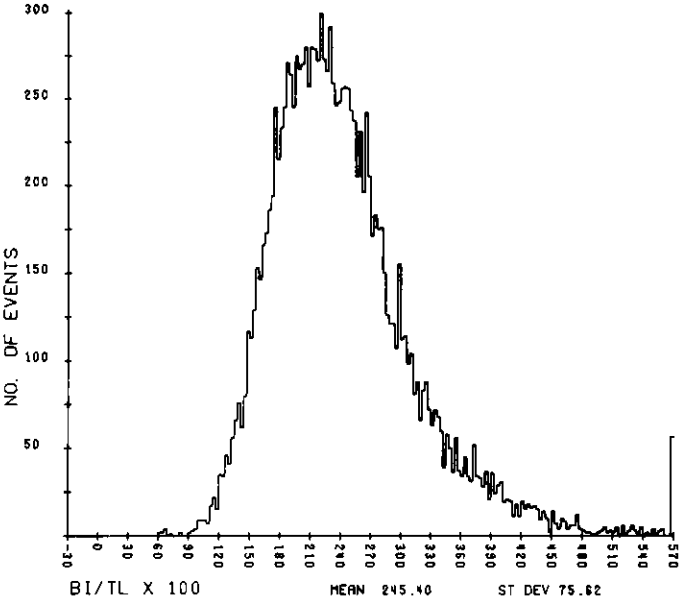
NO. OF EVENTS
BI/TL X 100
MEAN 245.40
ST DEV 75.82

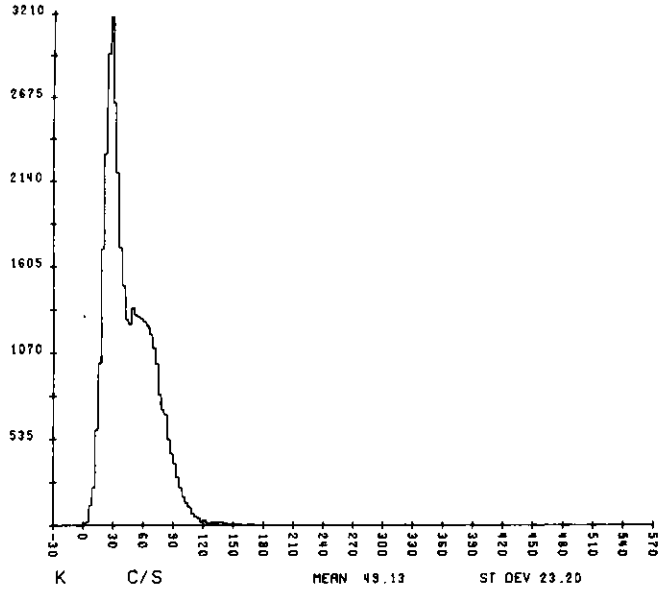
K C/S
MEAN 49.13
ST DEV 23.20

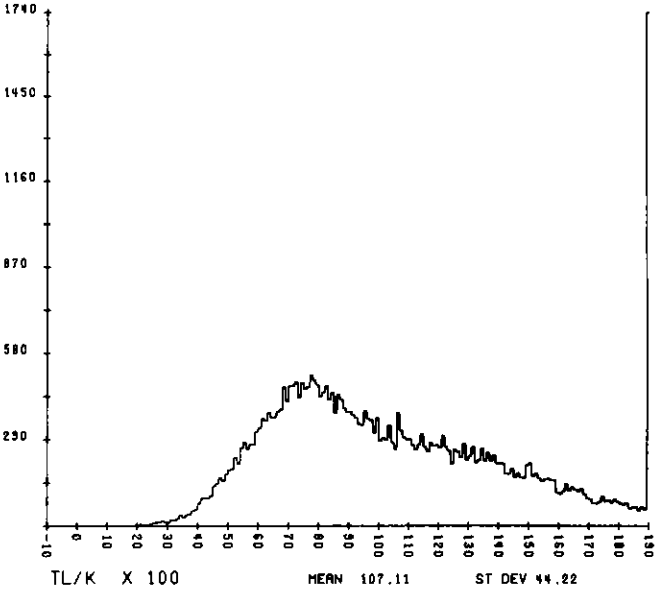
TL/K X 100
MEAN 107.11
ST DEV 44.22

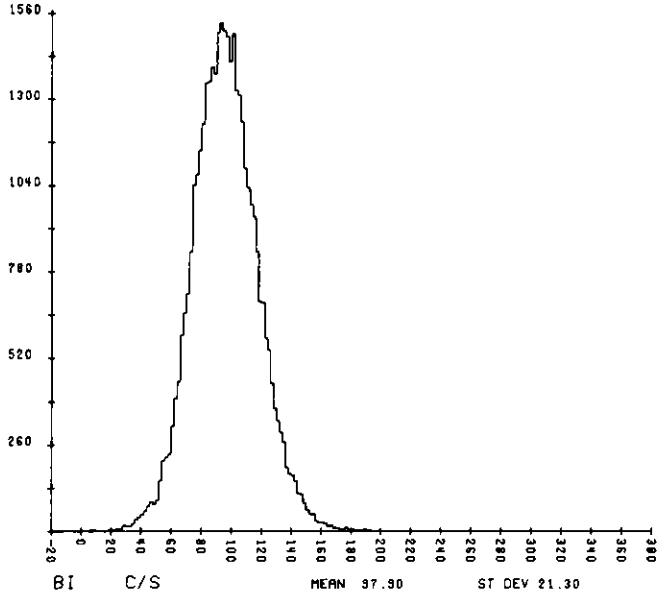
BI C/S
MEAN 97.90
ST DEV 21.30

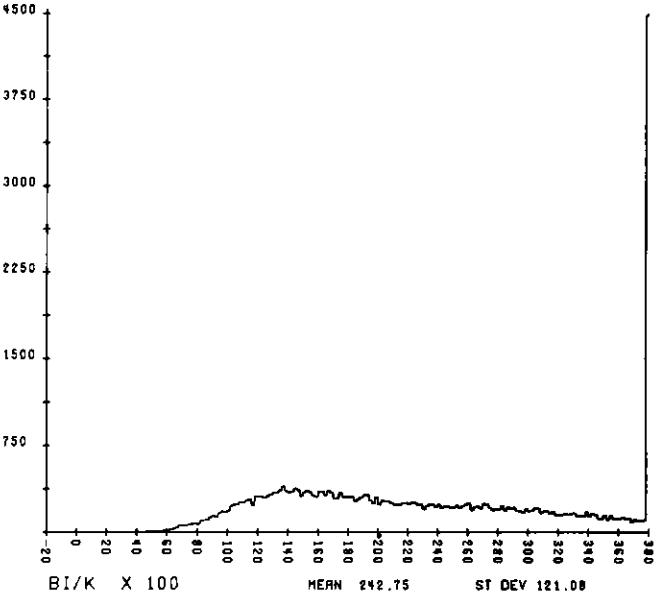
BI/K X 100
MEAN 242.75
ST DEV 121.08

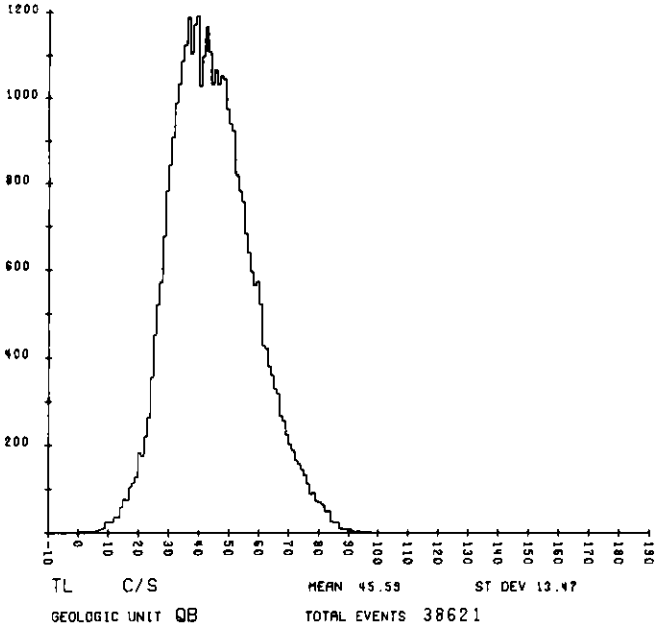
TL C/S
MEAN 45.59
ST DEV 13.47
GEOLOGIC UNIT QB
TOTAL EVENTS 38621

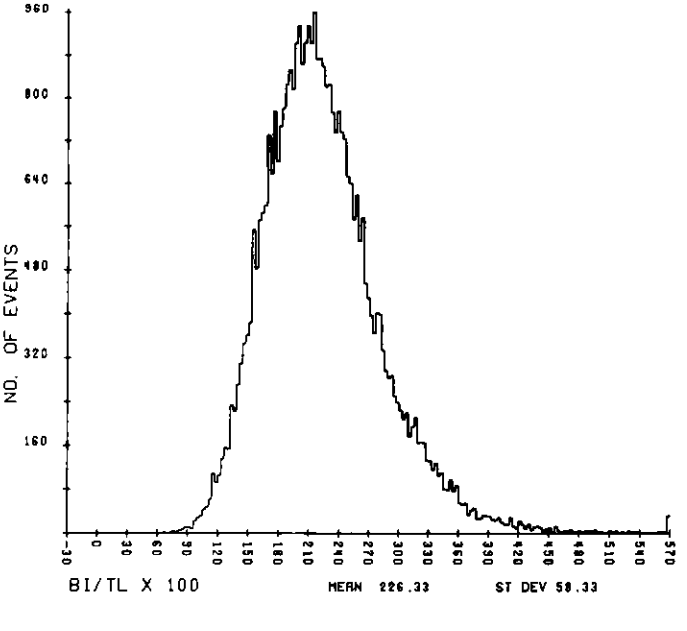
NO. OF EVENTS
BI/TL X 100
MEAN 226.33
ST DEV 58.33

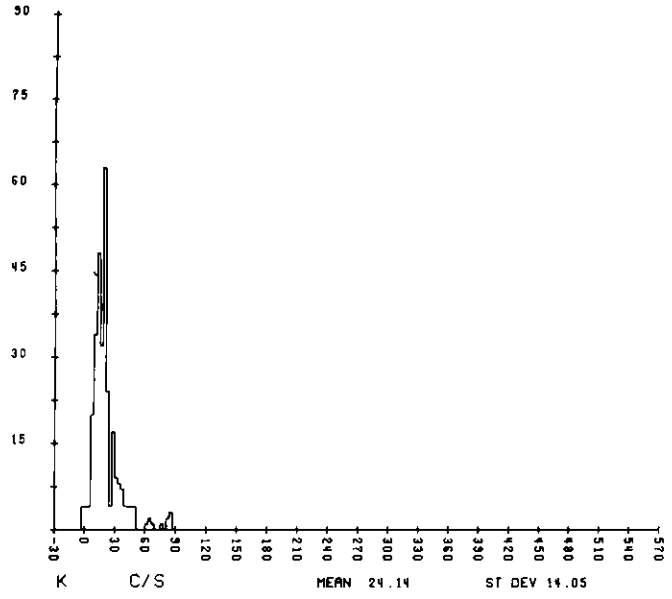
K C/S
MEAN 24.14
ST DEV 14.05

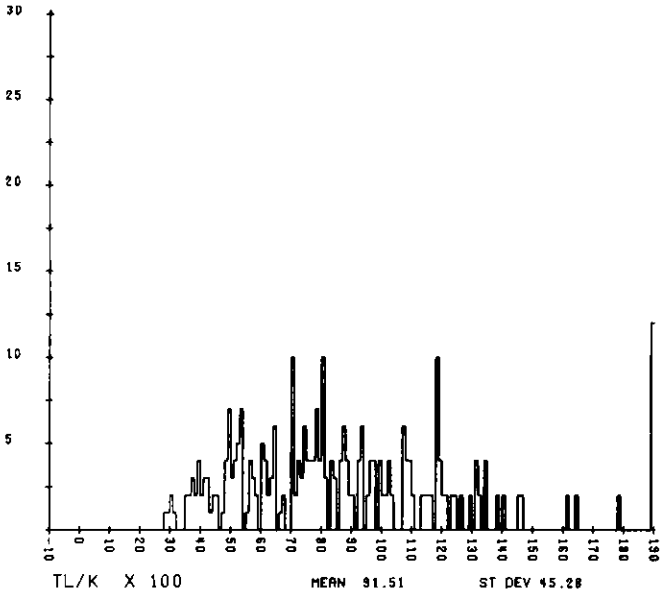
TL/K X 100
MEAN 91.51
ST DEV 45.28

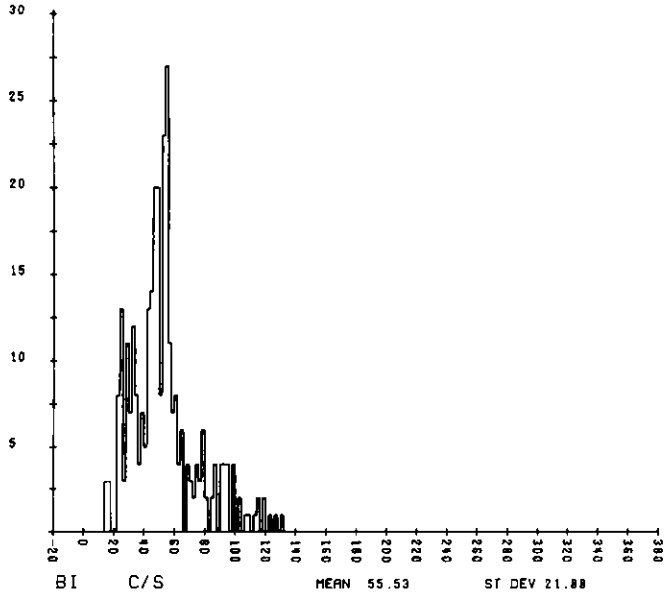
BI C/S
MEAN 55.53
ST DEV 21.88

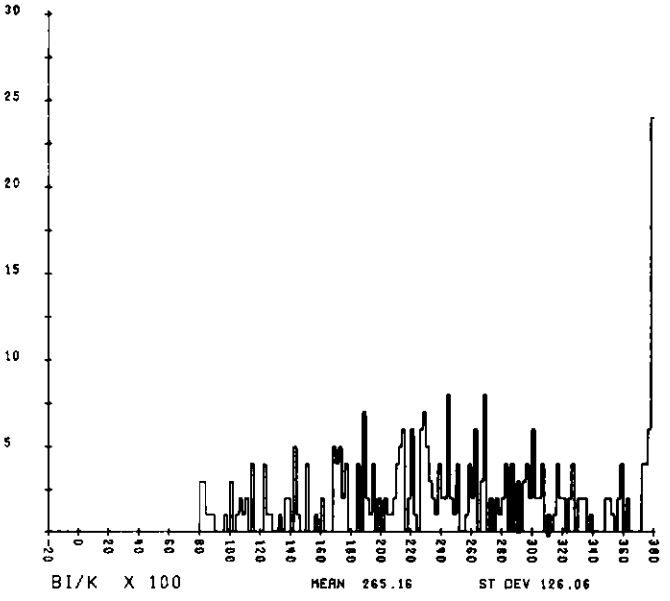
BI/K X 100
MEAN 265.16
ST DEV 126.06

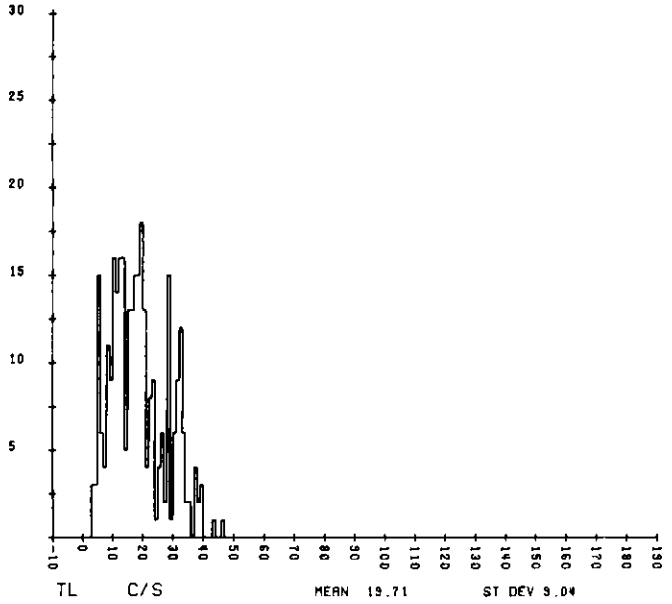
TL C/S
MEAN 19.71
ST DEV 9.04
GEOLOGIC UNIT QBB
TOTAL EVENTS 300

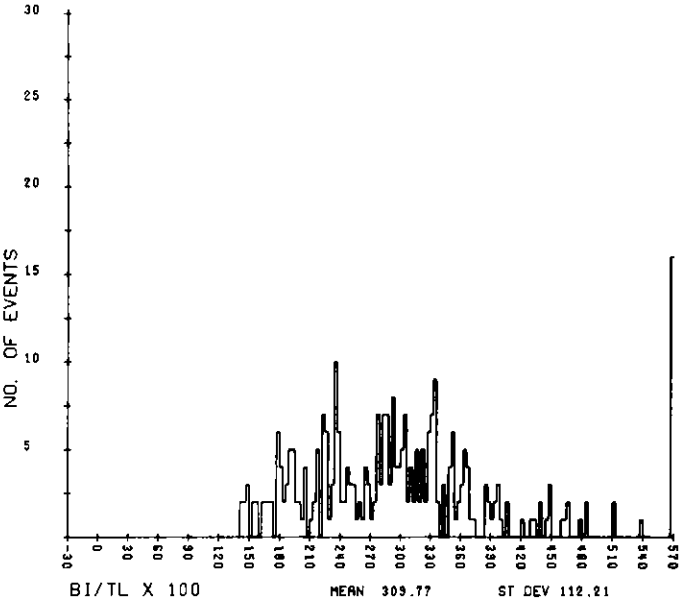
NO. OF EVENTS
BI/TL X 100
MEAN 309.77
ST DEV 112.21

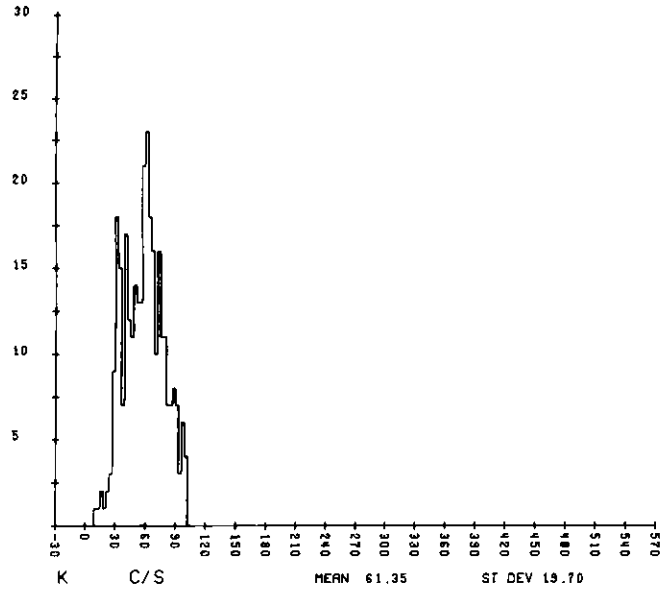
K C/S
MEAN 61.35
ST DEV 19.70

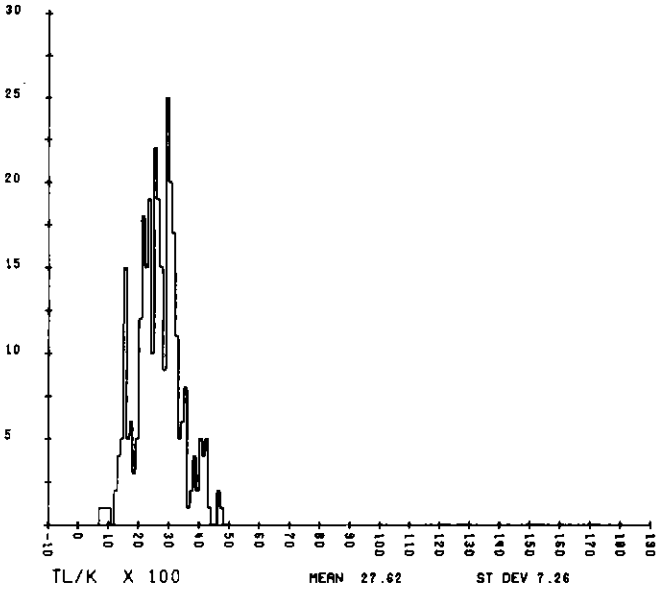
TL/K X 100
MEAN 27.62
ST DEV 7.26

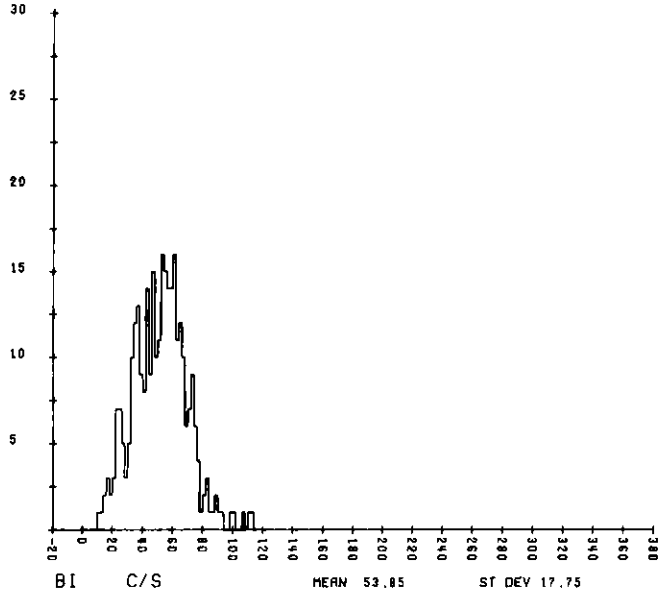
BI C/S
MEAN 53.85
ST DEV 17.75

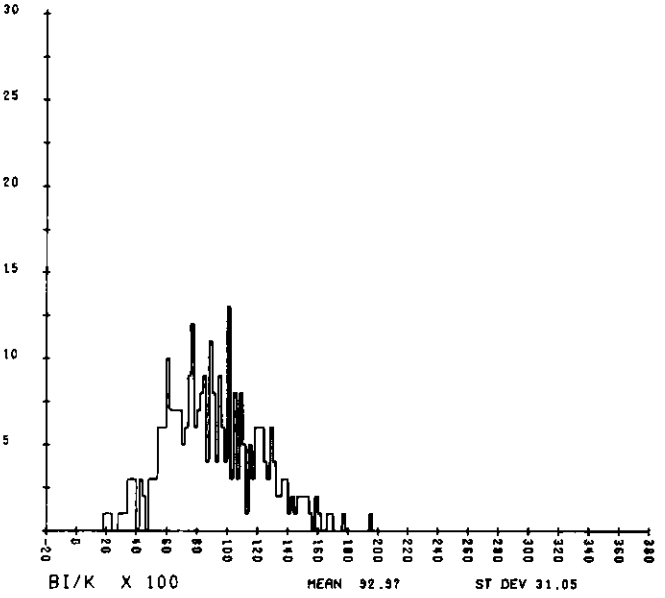
BI/K X 100
MEAN 92.97
ST DEV 31.05

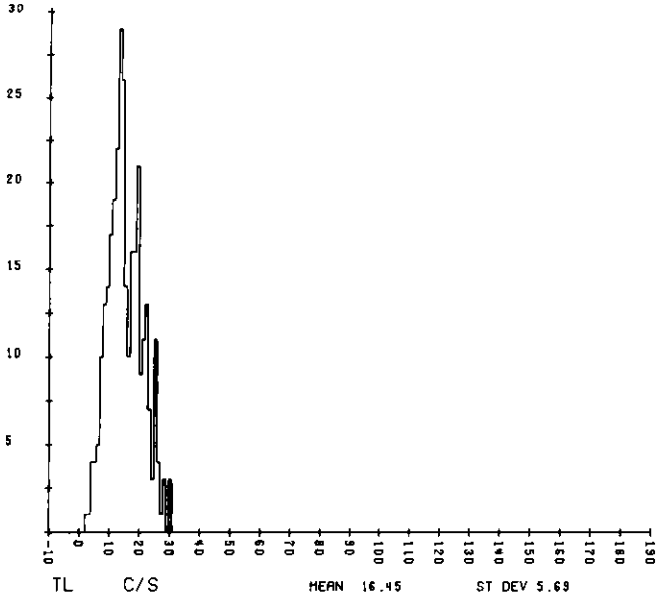
TL C/S
MEAN 16.45
ST DEV 5.69
GEOLOGIC UNIT QBI
TOTAL EVENTS 306

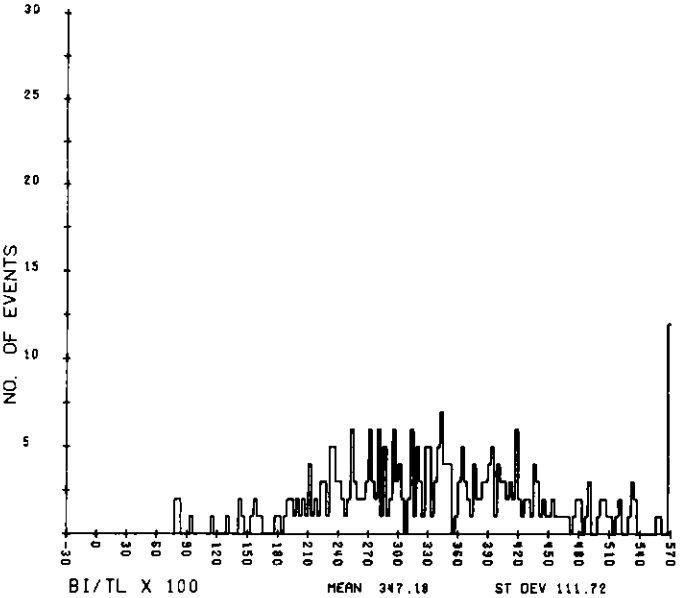
NO. OF EVENTS
BI/TL X 100
MEAN 347.18
ST DEV 111.72

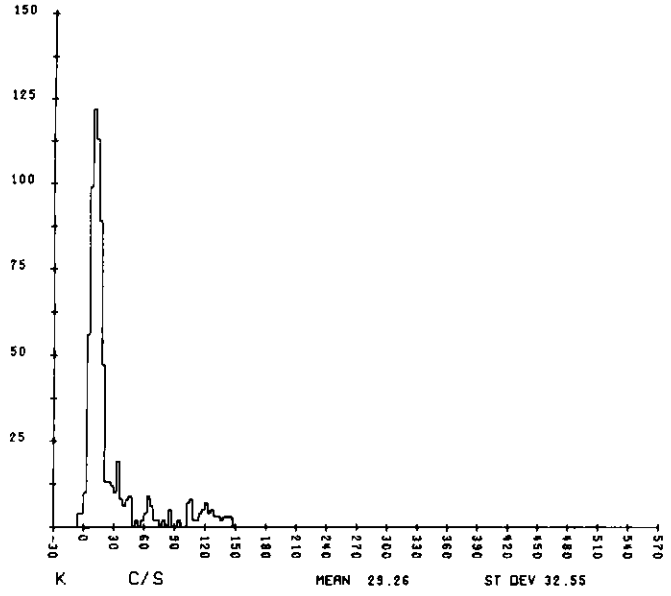
K C/S
MEAN 23.26
ST DEV 32.55

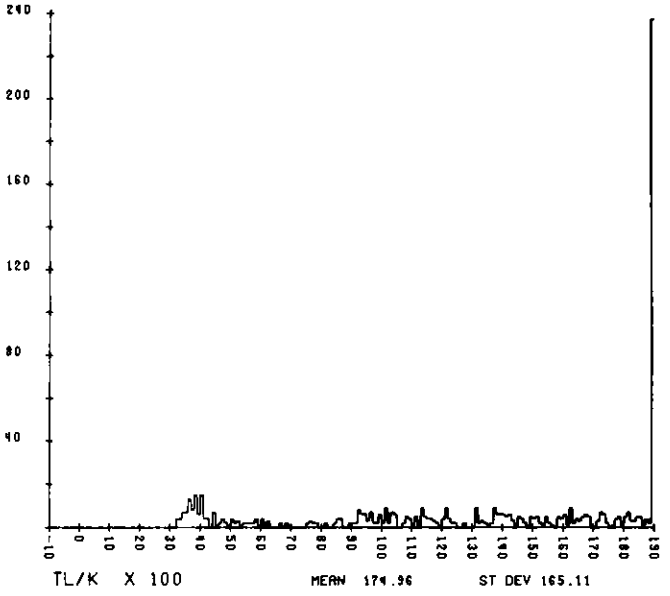
TL/K X 100
MEAN 174.96
ST DEV 165.11

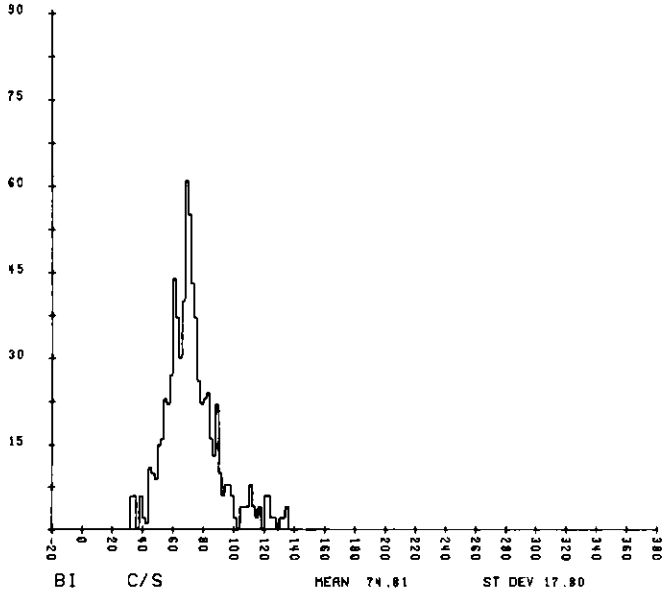
BI C/S
MEAN 74.81
ST DEV 17.80

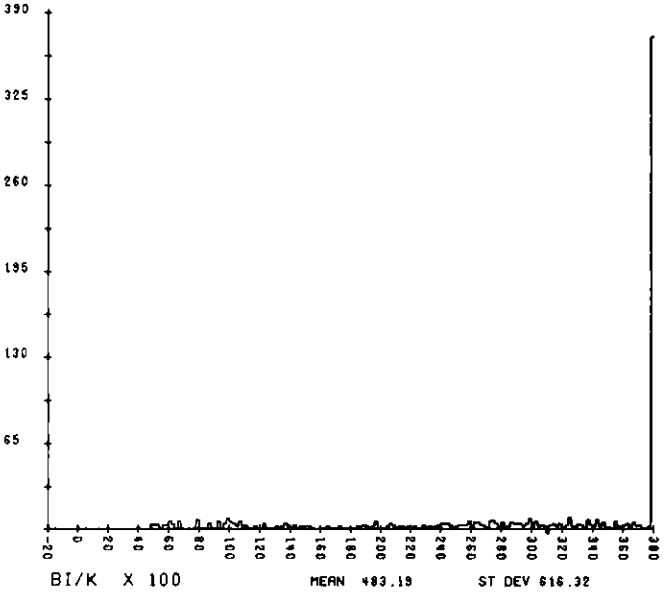
BI/K X 100
MEAN 483.19
ST DEV 616.32

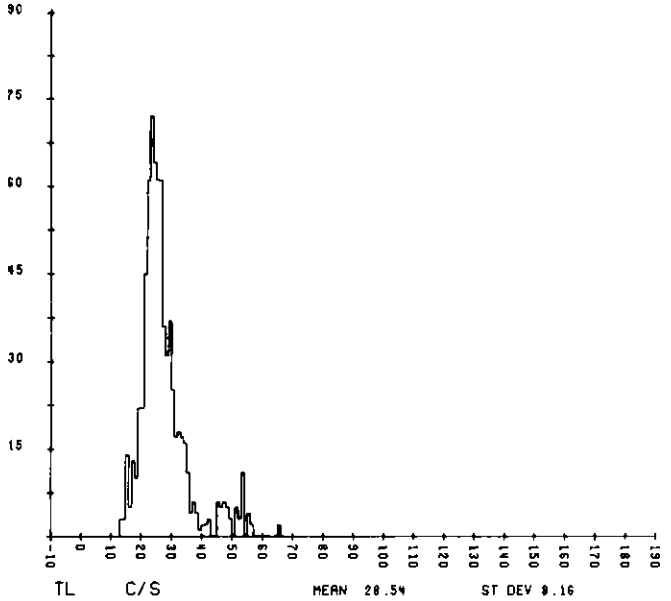
TL C/S
MEAN 28.54
ST DEV 9.16
GEOLOGIC UNIT QBY
TOTAL EVENTS 735

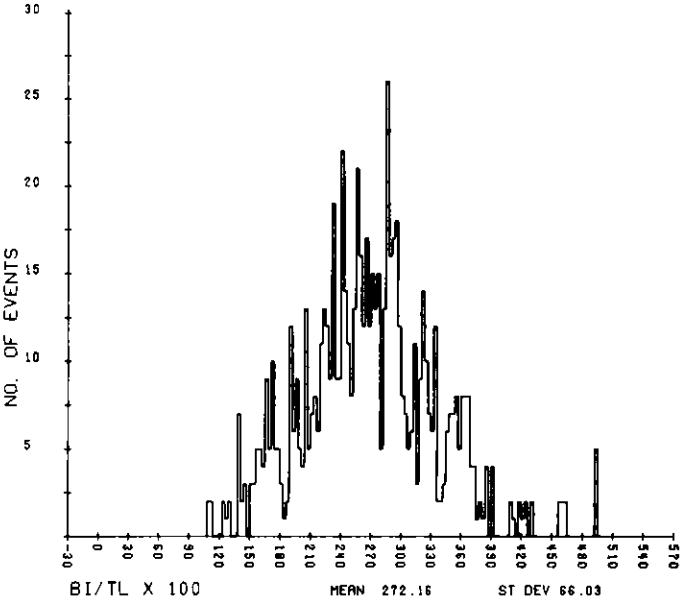
NO. OF EVENTS
BI/TL X 100
MEAN 272.16
ST DEV 66.03

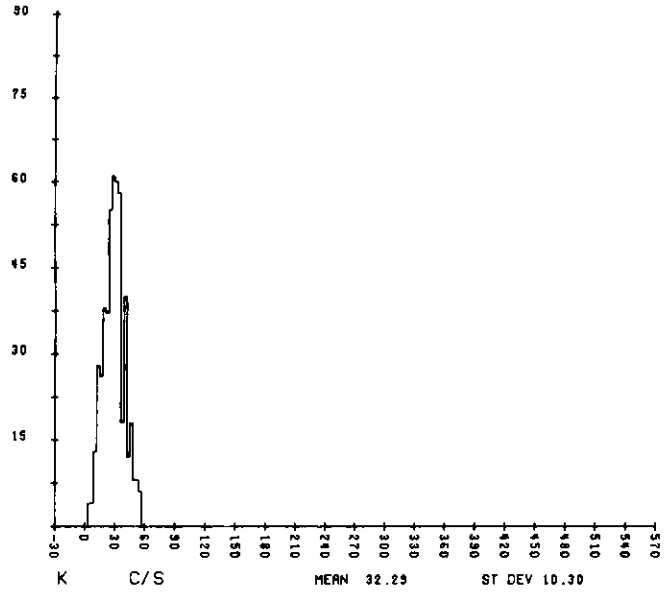
K C/S
MEAN 32.29
ST DEV 10.30

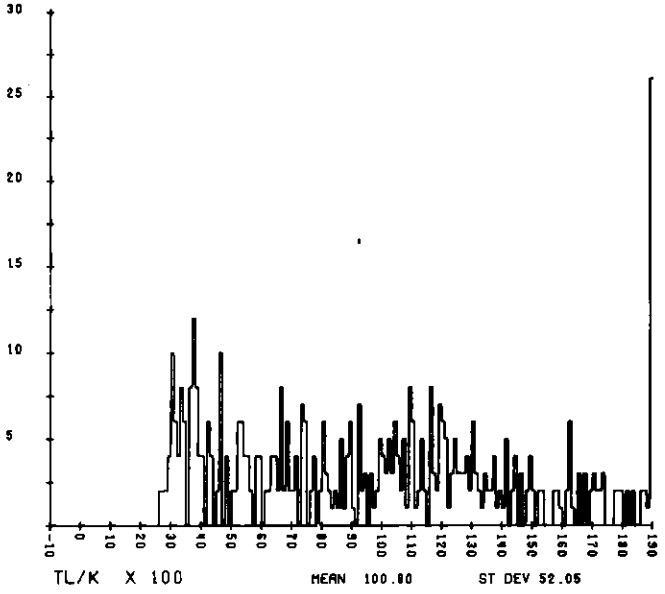
TL/K X 100
MEAN 100.80
ST DEV 52.05

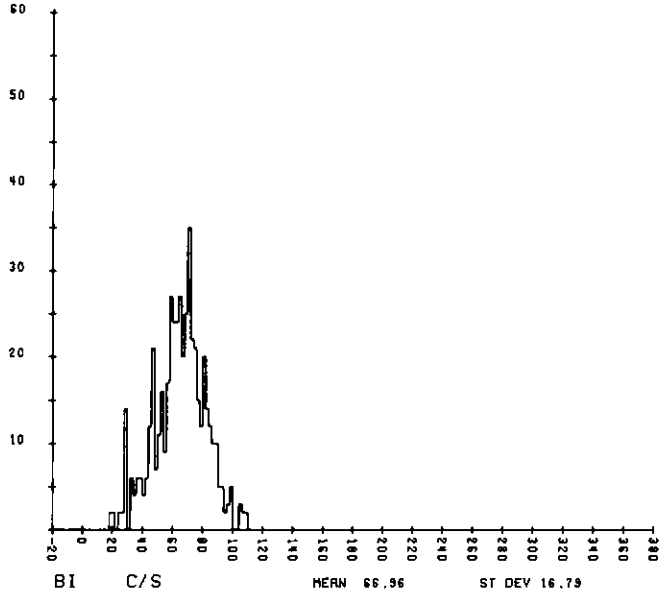
BI C/S
MEAN 66.96
ST DEV 16.79

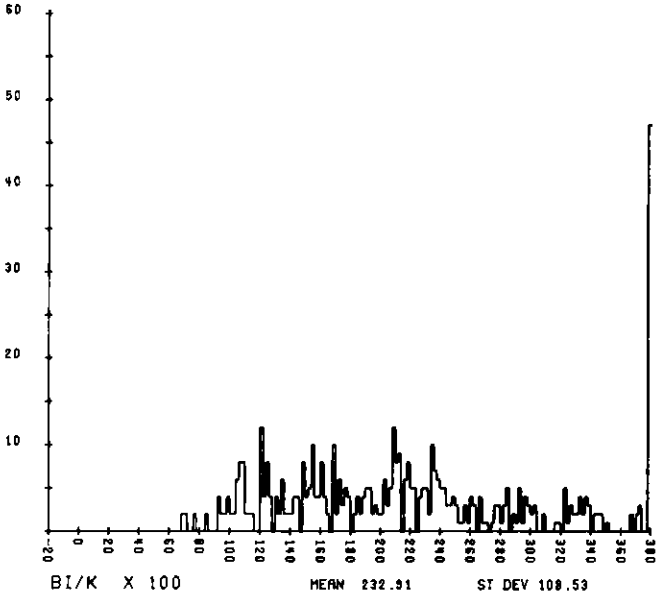
BI/K X 100
MEAN 232.91
ST DEV 108.53

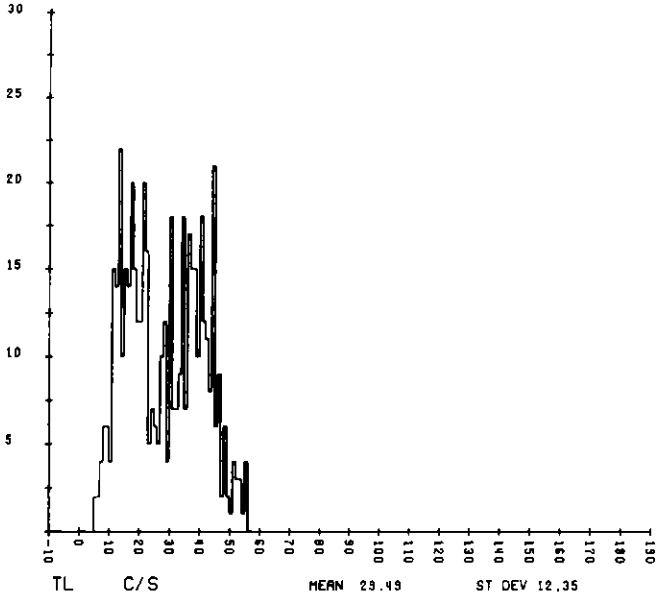
TL C/S
MEAN 29.49
ST DEV 12.35
GEOLOGIC UNIT QD
TOTAL EVENTS 490

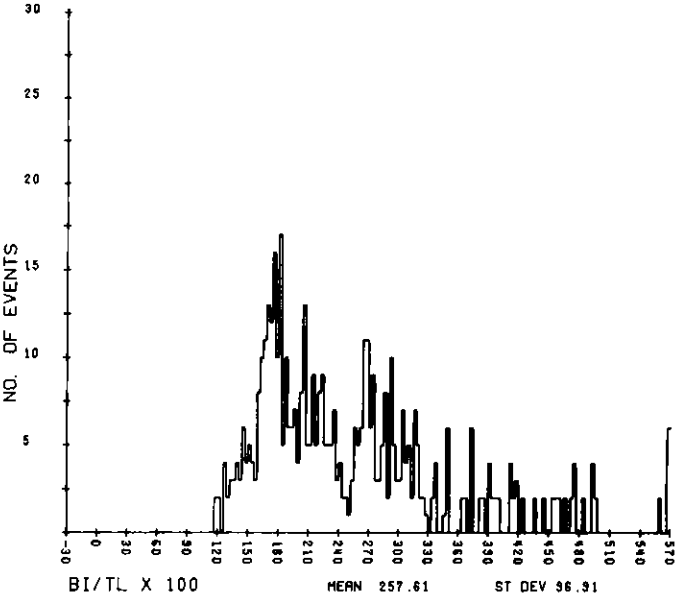
NO. OF EVENTS
BI/TL X 100
MEAN 257.61
ST DEV 96.91

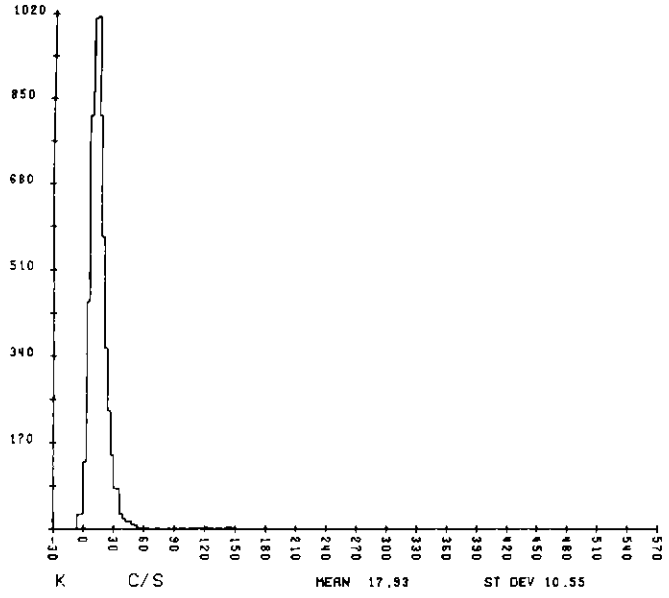
K C/S
MEAN 17.93
ST DEV 10.55

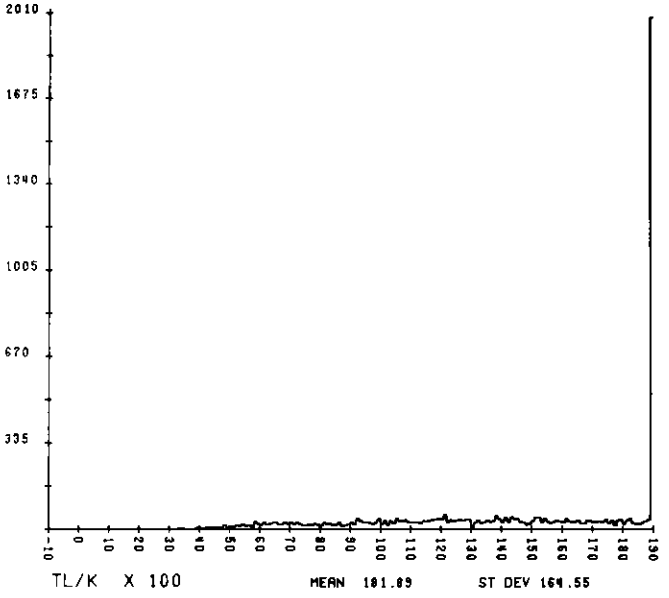
TL/K X 100
MEAN 181.89
ST DEV 164.55

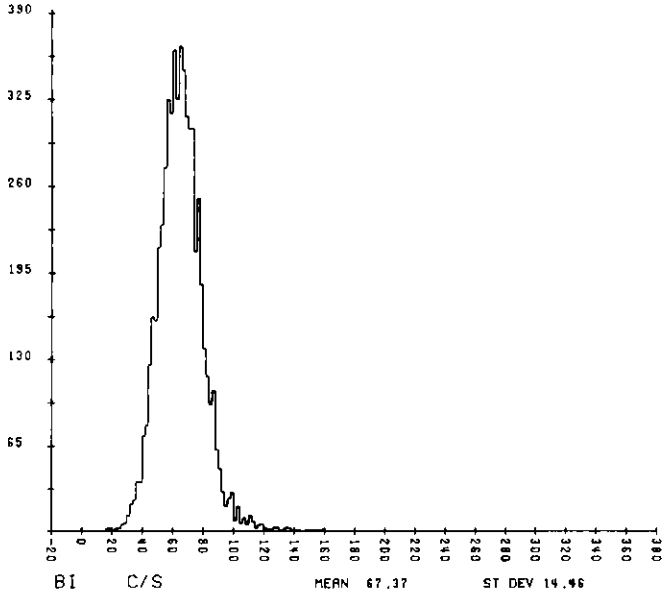
BI C/S
MEAN 67.37
ST DEV 14.96

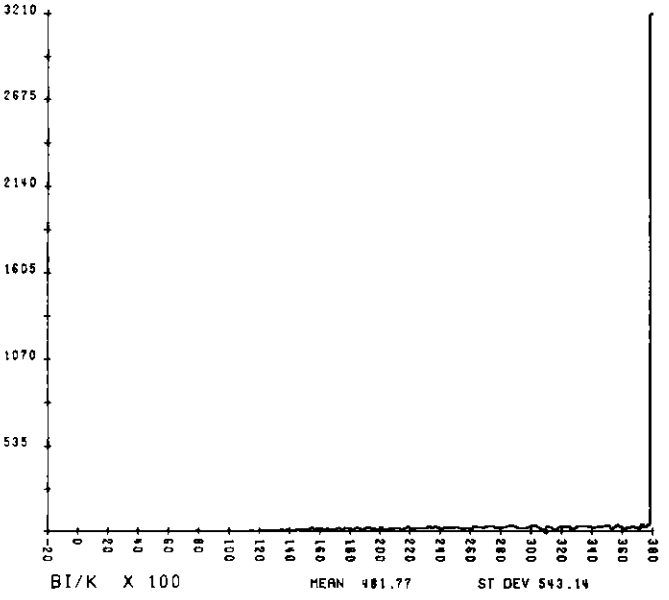
BI/K X 100
MEAN 481.77
ST DEV 543.14

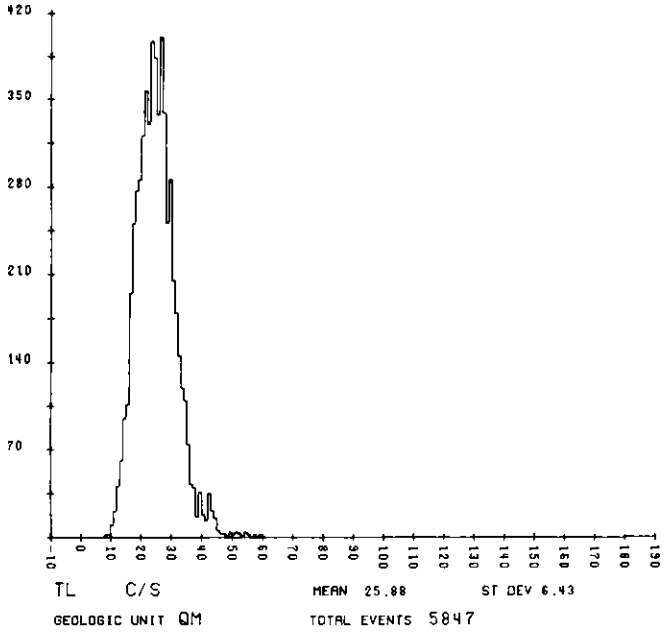
TL C/S
MEAN 25.88
ST DEV 6.43
GEOLOGIC UNIT QM
TOTAL EVENTS 5847

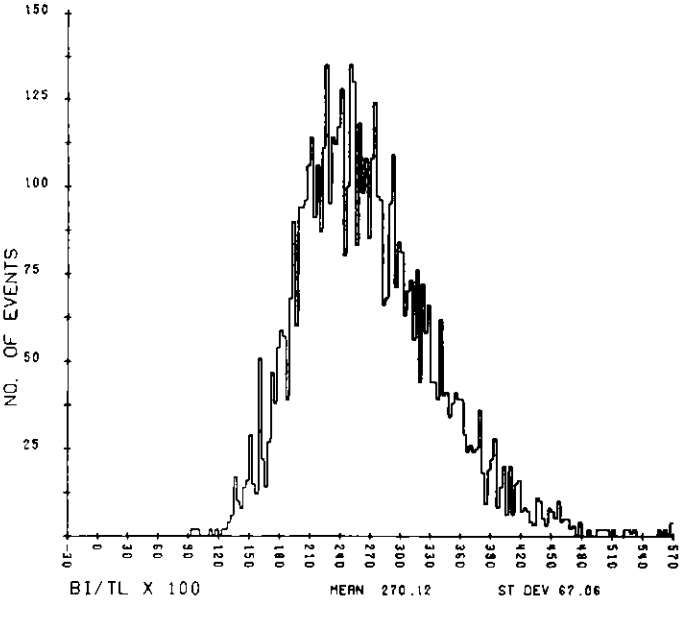
NO. OF EVENTS
BI/TL X 100
MEAN 270.12
ST DEV 67.06

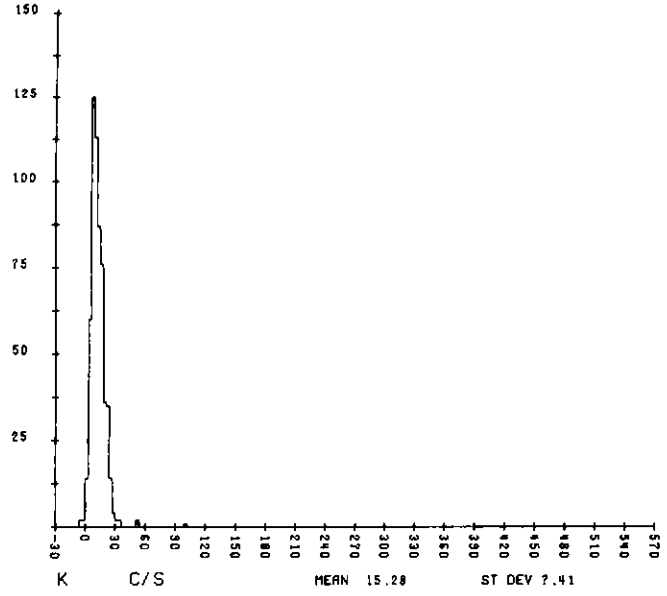
K C/S
MEAN 15.28
ST DEV 7.41

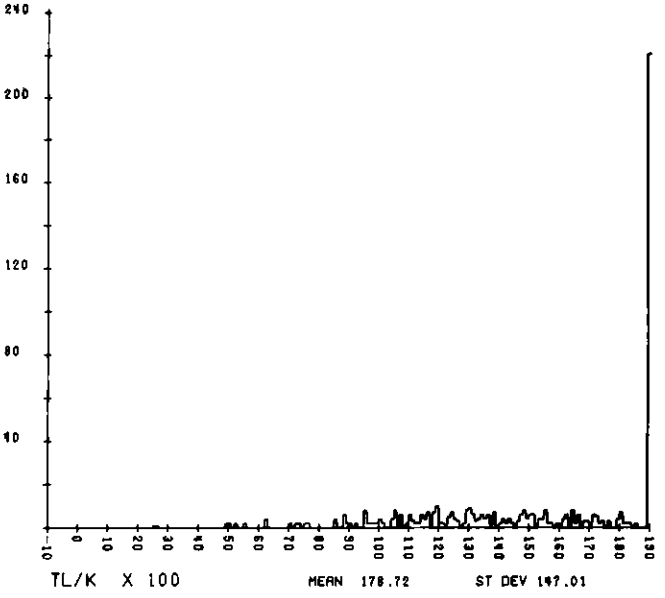
TL/K X 100
MEAN 178.72
ST DEV 147.01

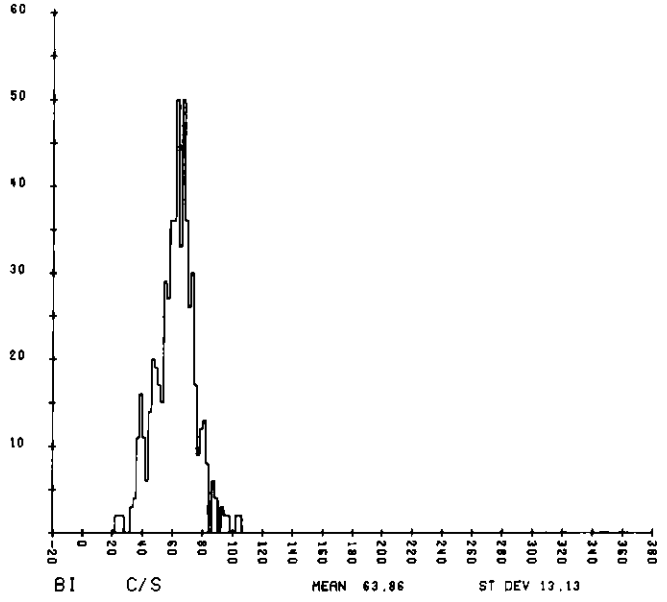
BI C/S
MEAN 63.86
ST DEV 13.13

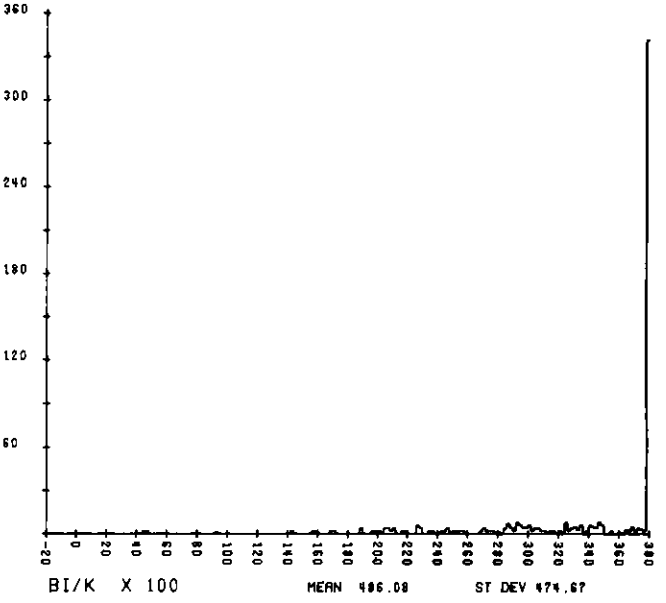
BI/K X 100
MEAN 486.08
ST DEV 474.67

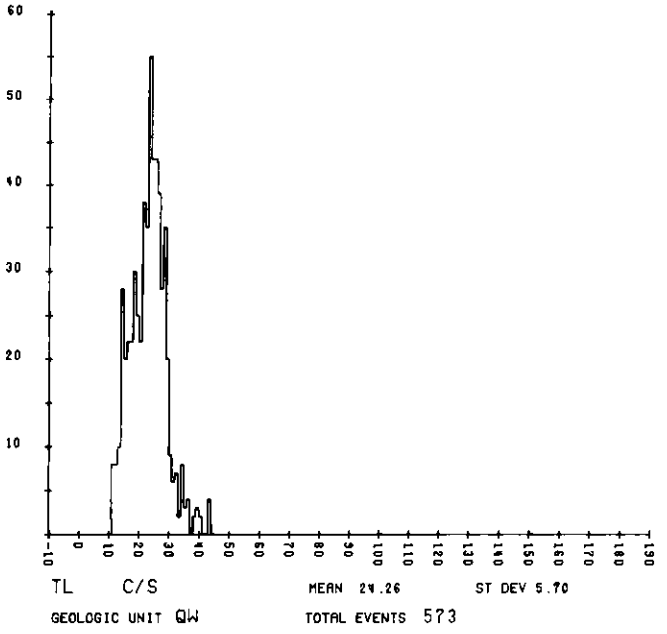
TL C/S
MEAN 24.26
ST DEV 5.70
GEOLOGIC UNIT QW
TOTAL EVENTS 573

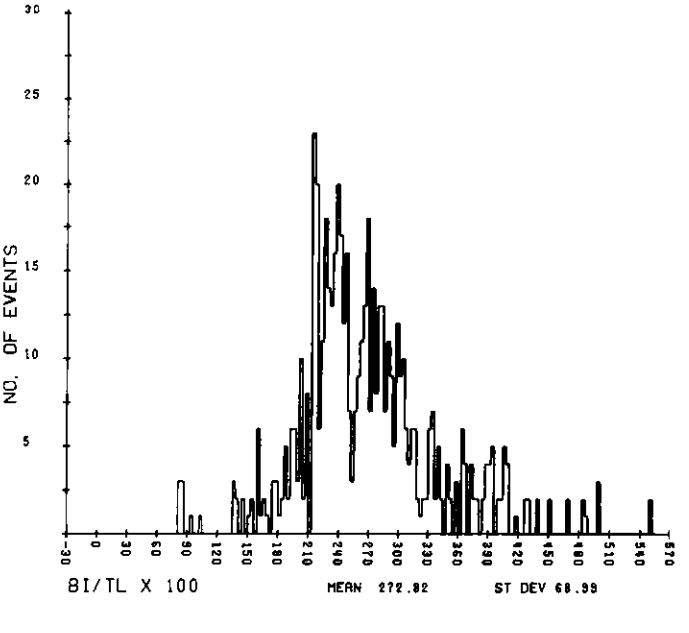
NO. OF EVENTS
BI/TL X 100
MEAN 272.82
ST DEV 68.99

A P P E N D I X II

DESCRIPTION OF MAGNETIC TAPES AND LISTINGS

APPENDIX II

A. DESCRIPTION OF MAGNETIC TAPES

Four separate tapes are furnished in the following specified formats. All tapes are 9-track EBCDIC Code 800 bpi. Each has a common header. The header format is as follows:

INFORMATION	FORMAT I
Map Line Number	I6
Beginning Record Number	I6
Ending Record Number	I6
Date Flown	I5
Subcontractor	10A6
Contract Number	10A6

A1. Single Record Reduced Data Tape

	TYPE VARIABLE	FORMAT
1.	Record identification number	I6
2.	Latitude in degrees to four decimal places	I10
3.	Longitude in degrees to four decimal places	I10
4.	Residual total magnetic intensity (IGRF removed) in gammas	I10
5.	Terrain clearance in feet	I5
6.	Surface geologic map unit	A6
7.	Quality flag code (for radiometric data)	4I2
8.	Integral gamma ray counts per second from the energy range 3.0 to 6.0 MeV	I10
9.	Gamma ray counts per second from atmospheric ^{214}Bi	I6
10.	Integral gamma ray counts per second in the energy range 0.4 to 3.0 MeV.	I6
11.	Gamma ray counts per second relative to terrestrial thorium (^{208}Tl)	I6
12.	Gamma ray counts per second relative to terrestrial uranium (^{214}Bi)	I6
13.	Gamma ray counts per second relative to terrestrial (^{40}K)	I6
14.	Uranium/thorium ratio	I6
15.	Uranium/potassium ratio	I6
16.	Thorium/potassium ratio	I6
17.	Outside air temperature	I6
18.	Barometric pressure	I6

A2. Raw Spectral Data Tapes

	TYPE VARIABLE	FORMAT
1.	Record identification number	I6
2.	Latitude in degrees to four decimal places	I10
3.	Longitude in degrees to four decimal places	I10
4.	Time of day	3I2
5.	Total magnetic field intensity data	I10
6.	Terrain clearance in feet (from radar altimeter)	I5
7.	Barometric pressure reading	I5
8.	Outside flight level air temperature reading	I5
9.	Quality flag code (for altitude data)	4I1
10.	Raw count data for all channels (0-3.0 MeV) 4π detector	255I4
11.	Dead time counting period for each sample in seconds - 4π detector	I10
12.	Raw count data for all channels (0-3.0 MeV) 2π detector	255I4
13.	Dead time counting period for each sample in seconds - 2π detector	I10
14.	Cosmic spectral summed data (3.0-6.0 MeV) 4π detector	I10
15.	Cosmic spectral summed data (3.0-6.0 MeV) 2π detector	I10

A3. Statistical Analysis Data Tape

Additional Header Information

Information	Format
Tl Sigma	F10.4
Tl Mean	F10.1
Bi Sigma	F10.4
Bi Mean	F10.1
K Sigma	F10.4
K Mean	F10.1
Bi/Tl Sigma	F10.4
Bi/Tl Mean	F10.4
Bi/K Sigma	F10.4
Bi/K Mean	F10.4
Tl/K Sigma	F10.4
Tl/K Mean	F10.4
Number of Events	7.0
Geologic Unit	A5

This information is based on data from the entire NTMS quad.

	TYPE VARIABLE	FORMAT
1.	Record identification number (on central record)	I6
2.	Latitude in degrees to four decimal places	I10

3.	Longitude in degrees to four decimal places	I10
4.	Residual total magnetic intensity in gammas (IGRF removed)	I10
5.	Surface geologic map unit	A6
6.	Quality flag code (for radiometric data)	4I1
7.	Integral gamma ray measurements in counts per second in the energy range 0.4 to 3.0 MeV	I6
8.	Gamma ray counts per second relative to terrestrial thorium (^{208}Tl)	
9.	Thorium standard deviations from the mean, signed (±)	I6
10.	Gamma ray counts per second relative to terrestrial uranium (^{214}Bi)	I6
11.	Uranium standard deviations from the mean, signed (±)	I6
12.	Gamma ray counts per second relative to terrestrial potassium (^{40}K)	I6
13.	Potassium standard deviations from the mean, signed (±)	I6
14.	Uranium/thorium ratio and standard deviations from the mean, signed (±)	I6
15.	Uranium/potassium ratio and standard deviations from the mean, signed (±)	I6
16.	Thorium/potassium ratio and standard deviations from the mean, signed (±)	I6

A4. Magnetic Data Tape

	TYPE VARIABLE	FORMAT
1.	Record identification number	I10
2.	Latitude in degrees to four decimal places	I10
3.	Longitude in degrees to four decimal places	3I2
4.	Time of day (hour, minutes, seconds)	I6
5.	Terrain clearance in feet	I6
6.	Barometric pressure reading	I6
7.	Surface geologic map unit	A6
8.	Total magnetic field intensity in gammas (not averaged)	I10
9.	Residual total magnetic intensity (IGRF removed)	I10
10.	Ground magnetic base station	I10

B. DESCRIPTION OF LISTINGS

B1. Single Point Unaveraged listings include the following information:

ITEM	DESCRIPTION
RCN	Sequential record number
AKUT	Quality flag codes; A - Altitude; K - Potassium; U - Uranium; T - Thorium - Results of statistical adequacy test. For A: 0-OK, 1-700' to 1000', 2 - G.T. 1000'

Long	Longitude
Lat	Latitude
Hr	Hour
Min	Minute
LTC	4π live time
BiAir	Airborne ^{214}Bi, 4π data
Alt	Surface altitude
GC	Gross Count, .4 MeV - 3.0 MeV
COS	Cosmic c/s
Tl	Tl c/s
Bi	Bi c/s
K	K c/s
Mag	Magnetic field, gammas
RMag	Residual magnetic field, gammas
Temp	Outside air temperature, C.
B.P.	Barometric pressure, in - Hg

B2. Averaged, 7-point, listings include the following information:

ITEM	DESCRIPTION
RCN	Sequential record number
Long	Longitude
Lat	Latitude
RMag	Residual magnetic field, gammas
GC	Gross count, c/s, 0.4 - 3.0 MeV
GEOL UNIT	Geologic type
Tl	Tl value, c/s
Rank	Tl standard deviation rank
Bi	Bi value, c/s
Rank	Bi standard deviation rank
K	K value, c/s
Rank	K standard deviation rank
Bi/Tl	Ratio value
Rank	Bi/Tl standard deviation rank
Bi/K	Ratio value
Rank	Bi/K standard deviation rank
Tl/K	Ratio value
Rank	Tl/K standard deviation rank
Cnt	5-counts indicating data shown on NGRMS maps.
AKUT	Quality flag codes; A - Altitude; K - Potassium; U - Uranium; T - Thorium - Results of statistical adequacy test. For A: 0-OK, 1-700' to 1000', 2 - G. T. 1000'.

HOUSTON AREA

RCN	AKUT	X	Y	LONG	LAT	HRMIN	LTC	BIAIR	ALT	GC	FL COS	1 TL	MAP BI	LINE K	1 MAG	RMA@	TEMP	B.P.
273	0010	.4560	.0342	96.7911	29.0291	9 46	926	88.6	407	1148	39	52	10	58	50093.6	=370.2	15.8	28.88
274	0000	.4654	.0342	96.7905	29.0291	9 46	936	88.4	403	1113	42	33	76	36	50094.1	=369.8	15.8	28.89
275	0000	.4747	.0371	96.7899	29.0293	9 46	938	88.3	402	1084	50	25	49	97	50094.7	=369.4	15.8	28.89
276	0000	.4838	.0371	96.7893	29.0293	9 46	830	92.6	402	1122	39	54	39	46	50095.4	=368.8	15.7	28.89
277	0100	.4931	.0371	96.7886	29.0293	9 46	835	92.7	405	969	40	25	81	7	50096.1	=368.1	15.7	28.89
278	0000	.5025	.0371	96.7880	29.0293	9 46	828	92.8	405	1030	43	41	41	42	50096.9	=367.4	15.7	28.89
279	0000	.5116	.0371	96.7874	29.0292	9 46	843	93.2	414	978	39	25	73	16	50097.7	=366.5	15.7	28.89
280	0100	.5209	.0371	96.7868	29.0292	9 46	840	93.5	421	964	41	36	68	0	50098.5	=365.8	15.7	28.89
281	0000	.5303	.0371	96.7862	29.0292	9 46	845	93.7	426	988	46	21	32	61	50099.4	=364.7	15.7	28.89
282	0000	.5396	.0342	96.7856	29.0290	9 46	840	93.7	425	1007	37	41	39	18	50100.5	=363.7	15.7	28.88
283	0100	.5490	.0342	96.7850	29.0290	9 46	832	93.5	420	946	43	37	49	8	50101.6	=362.8	15.7	28.88
284	0100	.5580	.0314	96.7844	29.0289	9 46	841	93.5	421	1014	37	28	80	15	50102.7	=361.5	15.7	28.88
285	0010	.5674	.0314	96.7838	29.0289	9 46	832	93.4	419	984	38	37	20	34	50104.0	=360.4	15.7	28.88
286	0100	.5767	.0285	96.7832	29.0287	9 46	840	93.5	420	984	41	17	147	1	50105.4	=358.9	15.7	28.88
287	0000	.5861	.0285	96.7826	29.0287	9 46	935	93.6	423	1071	38	31	53	34	50106.9	=357.4	15.7	28.88
288	0010	.5954	.0256	96.7820	29.0285	9 46	829	93.7	424	993	50	40	16	38	50108.5	=355.8	15.7	28.88
289	0100	.6048	.0256	96.7814	29.0285	9 46	925	93.9	430	984	44	43	59	6	50109.6	=354.7	15.7	28.88
290	0010	.6141	.0228	96.7808	29.0283	9 46	837	94.0	431	1047	49	23	5	59	50110.5	=353.7	15.7	28.88
291	0100	.6235	.0228	96.7802	29.0283	9 46	838	94.1	433	1089	44	43	88	=18	50111.3	=353.1	15.6	28.88
292	0000	.6328	.0228	96.7795	29.0283	9 46	835	94.1	434	1050	47	33	44	28	50112.0	=352.3	15.6	28.87
293	0000	.6421	.0228	96.7789	29.0283	9 46	826	94.6	443	1081	43	34	40	53	50112.9	=351.5	15.6	28.87
294	0000	.6515	.0228	96.7783	29.0283	9 46	832	94.7	445	1008	48	33	32	41	50113.7	=350.8	15.7	28.86
295	0000	.6608	.0228	96.7777	29.0283	9 46	837	88.4	440	1045	44	33	31	71	50114.4	=350.1	15.7	28.86
296	0100	.6702	.0228	96.7771	29.0282	9 46	843	88.3	438	1025	37	28	110	=6	50115.2	=349.4	15.7	28.86
297	0000	.6795	.0256	96.7765	29.0284	9 46	835	88.3	439	963	42	23	51	40	50116.1	=348.6	15.7	28.86
298	0000	.6889	.0256	96.7759	29.0284	9 46	832	88.5	443	1059	43	24	59	24	50117.1	=347.7	15.7	28.86
299	0100	.6980	.0256	96.7753	29.0284	9 46	839	88.6	446	1024	44	28	104	=9	50118.3	=346.6	15.7	28.85
300	0000	.7073	.0256	96.7747	29.0284	9 46	840	88.6	445	1072	44	28	57	39	50119.4	=345.5	15.7	28.85
301	0100	.7166	.0256	96.7741	29.0283	9 46	830	88.4	441	1056	45	55	53	1	50120.5	=344.5	15.8	28.85
302	0000	.7268	.0285	96.7734	29.0285	9 46	840	88.3	439	1063	45	31	53	35	50121.5	=343.7	15.8	28.85
303	0000	.7397	.0285	96.7725	29.0285	9 46	839	88.3	439	1127	49	34	53	36	50122.5	=343.0	15.8	28.85
304	0100	.7525	.0314	96.7717	29.0286	9 46	839	88.3	438	1072	40	35	109	14	50123.2	=342.3	15.9	28.85
305	0000	.7657	.0314	96.7708	29.0286	9 46	831	88.1	435	1101	45	37	64	27	50123.9	=341.8	15.9	28.85
306	0000	.7789	.0314	96.7700	29.0286	9 46	828	88.0	432	1091	43	13	132	29	50124.5	=341.3	15.9	28.85
307	0000	.7919	.0314	96.7691	29.0286	9 46	827	87.9	429	1057	40	21	78	33	50125.2	=340.7	15.9	28.86
308	0010	.8049	.0314	96.7683	29.0286	9 46	837	87.7	425	1014	48	26	19	67	50125.9	=340.1	15.9	28.86
309	0000	.8179	.0314	96.7674	29.0286	9 46	853	87.7	424	972	42	15	73	18	50126.5	=339.6	15.9	28.86
310	0100	.8311	.0314	96.7666	29.0285	9 46	839	87.6	423	997	41	43	50	5	50126.9	=339.3	15.9	28.87
311	0000	.8441	.0314	96.7657	29.0285	9 46	839	87.6	422	1042	44	32	36	43	50127.7	=338.5	15.9	28.87
312	0000	.8571	.0314	96.7649	29.0285	9 46	840	87.5	420	994	44	31	41	18	50128.4	=338.0	15.9	28.87
313	0010	.8690	.0314	96.7641	29.0285	9 46	844	87.6	424	973	39	40	2	41	50129.1	=337.3	15.9	28.87
314	0000	.8784	.0342	96.7635	29.0286	9 46	849	84.8	423	953	39	32	49	42	50129.9	=336.8	15.9	28.87
315	0000	.8880	.0342	96.7628	29.0286	9 46	844	84.7	420	981	50	18	91	18	50130.5	=336.2	15.8	28.87
316	0000	.8970	.0342	96.7622	29.0286	9 46	842	84.6	419	1005	41	13	91	30	50131.2	=335.6	15.9	28.87
317	0000	.9064	.0342	96.7616	29.0286	9 46	835	84.6	419	928	45	20	64	28	50131.9	=334.9	15.9	28.87
318	0010	.9157	.0342	96.7610	29.0286	9 46	848	84.6	420	917	39	26	7	60	50132.8	=334.1	15.9	28.88
319	0100	.9251	.0342	96.7604	29.0286	9 46	847	84.7	421	885	40	18	92	11	50133.7	=333.3	15.9	28.88
320	0000	.9347	.0342	96.7598	29.0286	9 46	840	84.9	425	873	45	16	36	32	50134.6	=332.4	15.9	28.88
321	0000	.9438	.0342	96.7592	29.0286	9 46	847	85.1	429	838	34	22	43	21	50135.5	=331.6	15.9	28.87
322	0010	.9531	.0342	96.7586	29.0286	9 46	845	85.1	431	874	38	38	=1	33	50136.3	=330.8	15.9	28.87
323	0000	.9625	.0342	96.7580	29.0285	9 46	852	85.3	435	902	43	19	45	18	50137.0	=330.2	15.9	28.87
324	0000	.9718	.0342	96.7574	29.0285	9 46	849	85.4	436	939	48	9	76	39	50137.8	=329.4	15.9	28.87
325	0101	.9811	.0342	96.7567	29.0285	9 46	850	85.4	436	778	44	4	75	0	50138.5	=328.7	15.9	28.86
326	0010	.9905	.0371	96.7561	29.0287	9 46	855	85.3	436	807	44	9	1	58	50139.3	=328.2	15.9	28.86
327	0100	.9998	.0371	96.7555	29.0287	9 46	849	85.1	430	773	43	18	56	=1	50140.0	=327.0	15.9	28.86

HOUSTON
MAP LINE 1

RCN / GEOL UNIT	A K U T	TL RANK	BI RANK	LONG	K RANK	LAT	BI/TL RANK	HR MIN DAY MO YR	BI/K RANK	ALT	TL/K RANK	MAG	RMAG	BPRESS	CNT	TEMP	GC
1496	0 0 0 0			95,9880		29,0342	10 6 4	4 77		413		5035 4,5	-207,2	29,93		15,6	1657
GAL		72 *	733 *		83*		1,849*		1,431		,774 *						
1497	0 0 0 0			95,9875		29,0342	10 6 4	4 77		407		5035 4,4	-207,4	29,93		15,6	1663
GAL		72 *	735 *		70*		1,879*		1,687		,898 *						
1498	0 0 0 0			95,9869		29,0342	10 6 4	4 77		405		5035 4,4	-207,5	29,93		15,5	1633
GB		71 *	729 *		67		1,806*		1,666*		,922-						
1499	0 0 0 0			95,9862		29,0342	10 6 4	4 77		402		5035 4,4	-207,6	29,94		15,5	1581
GB		70 *	721 *		70		1,726*		1,506*		,873-				5		
1500	0 0 0 0			95,9857		29,0342	10 6 4	4 77		407		5035 4,4	-207,6	29,94		15,5	1594
GB		70 *	713		76 *		1,612**		1,317*		,817-						
1501	0 0 0 0			95,9851		29,0342	10 6 4	4 77		410		5035 4,4	-207,6	29,94		15,6	1529
GB		71 *	709		83 *		1,535**		1,170**		,782-						
1502	0 0 0 0			95,9845		29,0341	10 6 4	4 77		420		5035 4,4	-207,6	29,94		15,6	1560
GB		71 *	712		92 *		1,581**		1,096**		,693-						
1503	0 0 0 0			95,9839		29,0341	10 6 4	4 77		416		5035 4,4	-207,7	29,93		15,6	1700
GB		73 **	717		97 **		1,609**		1,095**		,681-						
1504	0 0 0 0			95,9833		29,0341	10 7 4	4 77		412		5035 4,4	-207,8	29,92		15,6	1675
GB		73 **	717		103 **		1,593**		1,036**		,650-				5		
1505	0 0 0 0			95,9827		29,0341	10 7 4	4 77		409		5035 4,4	-207,9	29,93		15,5	1625
GB		73 **	714		108 **		1,561**		,966**		,619-*						
1506	0 0 0 0			95,9821		29,0341	10 7 4	4 77		408		5035 4,5	-207,9	29,93		15,5	1617
GB		74 **	716		103 **		1,581**		1,030**		,660-						
1507	0 0 0 0			95,9815		29,0341	10 7 4	4 77		411		5035 4,6	-207,8	29,93		15,5	1630
GB		72 **	721 *		99 **		1,670**		1,109**		,664-						
1508	0 0 0 0			95,9809		29,0342	10 7 4	4 77		410		5035 4,6	-208,0	29,93		15,5	1643
GB		71 *	726 *		91 *		1,758*		1,249*		,710-						
1509	0 0 0 0			95,9803		29,0342	10 7 4	4 77		411		5035 4,6	-208,0	29,93		15,5	1687
GB		71 *	729 *		82 *		1,811*		1,402*		,774-				5		
1510	0 0 0 0			95,9797		29,0342	10 7 4	4 77		411		5035 4,7	-208,0	29,93		15,5	1592
GB		70 *	723 *		78 *		1,745*		1,404*		,805-						
1511	0 0 0 0			95,9791		29,0342	10 7 4	4 77		412		5035 4,8	-207,9	29,93		15,5	1601
GB		72 *	710		75 *		1,528**		1,286*		,842-						
1512	0 0 0 0			95,9785		29,0342	10 7 4	4 77		412		5035 4,9	-207,9	29,93		15,5	1478
GB		70 *	706		74 *		1,504**		1,265*		,842-						
1513	0 0 0 0			95,9779		29,0342	10 7 4	4 77		415		5035 5,1	-207,7	29,92		15,6	1534
GB		70 *	702		76 *		1,447**		1,176**		,813-						
1514	0 0 0 0			95,9773		29,0342	10 7 4	4 77		422		5035 5,2	-207,7	29,92		15,5	1511
GB		68 *	701		81 *		1,482**		1,110**		,749-						
1515	0 0 0 0			95,9767		29,0342	10 7 4	4 77		427		5035 5,3	-207,6	29,92		15,6	1575
GB		66 *	706		85 *		1,603**		1,120**		,699-				5		
1516	0 0 0 0			95,9761		29,0342	10 7 4	4 77		424		5035 5,4	-207,6	29,91		15,6	1487
GB		65 *	704		91 *		1,597**		1,031**		,645-						
1517	0 0 0 0			95,9755		29,0341	10 7 4	4 77		428		5035 5,4	-207,6	29,92		15,5	1501
GB		62 *	715		89 *		1,859*		1,161**		,625-*						
1518	0 0 0 0			95,9749		29,0341	10 7 4	4 77		418		5035 5,4	-207,7	29,92		15,5	1480
GB		59 *	724 *		84 *		2,092*		1,309*		,626-*						
1519	0 0 0 0			95,9743		29,0341	10 7 4	4 77		412		5035 5,5	-207,8	29,92		15,5	1493
GB		55	731 *		81 *		2,376		1,440*		,606-*						
1520	0 0 0 0			95,9737		29,0341	10 7 4	4 77		413		5035 5,6	-207,7	29,93		15,5	1477
GB		52	736 *		75 *		2,583		1,595*		,618-*				50		
1521	0 0 0 0			95,9731		29,0343	10 7 4	4 77		410		5035 5,6	-207,9	29,93		15,5	1434
GB		52	729 *		76 *		2,437		1,491*		,612-*						
1522	0 0 0 0			95,9725		29,0343	10 7 4	4 77		409		5035 5,6	-207,9	29,93		15,5	1540
GB		52	723 *		76 *		2,344		1,437*		,613-*						

EVENTS PER INTERVAL
2100
1800
1500
1200
900
600
300
0
0
60
120
180
240
300
360
420
ML 1
SPEED IN MPH

EVENTS PER INTERVAL
2100
1800
1500
1200
900
600
300
0
0
60
120
180
240
300
360
420
ML 2
SPEED IN MPH

EVENTS PER INTERVAL
2100
1800
1500
1200
900
600
300
0
0
60
120
180
240
300
360
420
ML 3
SPEED IN MPH

EVENTS PER INTERVAL
2100
1800
1500
1200
900
600
300
0
0
60
120
180
240
300
360
420
ML 4
SPEED IN MPH

EVENTS PER INTERVAL
4200
3600
3000
2400
1800
1200
600
0
0
200
400
600
800
1000
1200
1400
ML 1
ALTITUDE IN FEET

EVENTS PER INTERVAL
4200
3600
3000
2400
1800
1200
600
0
0
200
400
600
800
1000
1200
1400
ML 2
ALTITUDE IN FEET

EVENTS PER INTERVAL
4200
3600
3000
2400
1800
1200
600
0
0
200
400
600
800
1000
1200
1400
ML 3
ALTITUDE IN FEET

EVENTS PER INTERVAL
4200
3600
3000
2400
1800
1200
600
0
0
200
400
600
800
1000
1200
1400
ML 4
ALTITUDE IN FEET

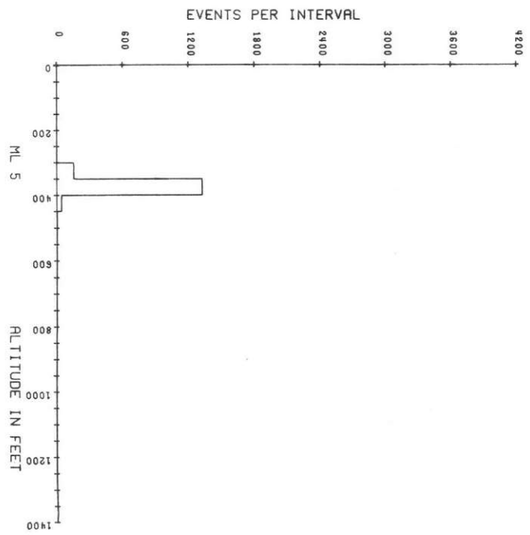
EVENTS PER INTERVAL
0
600
1200
1800
2400
3000
3600
4200
ML 5
ALTITUDE IN FEET
0
200
400
600
800
1000
1200
1400

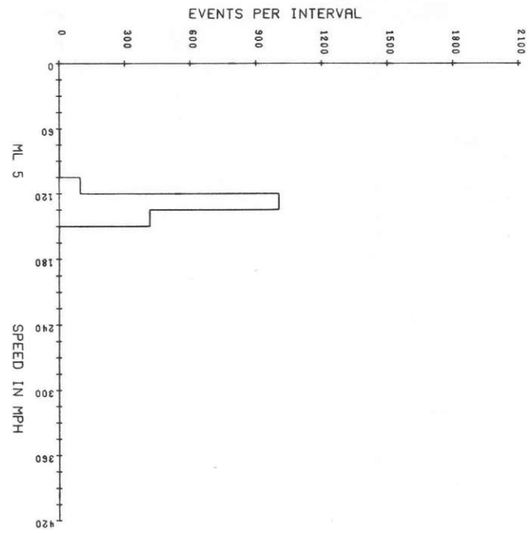
EVENTS PER INTERVAL
0
300
600
900
1200
1500
1800
2100
ML 5
SPEED IN MPH
0
60
120
180
240
300
360
420

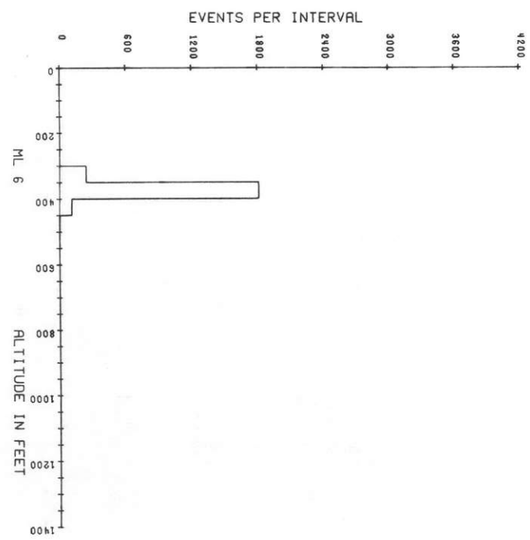
EVENTS PER INTERVAL
0
600
1200
1800
2400
3000
3600
4200
ML 6
ALTITUDE IN FEET
0
200
400
600
800
1000
1200
1400

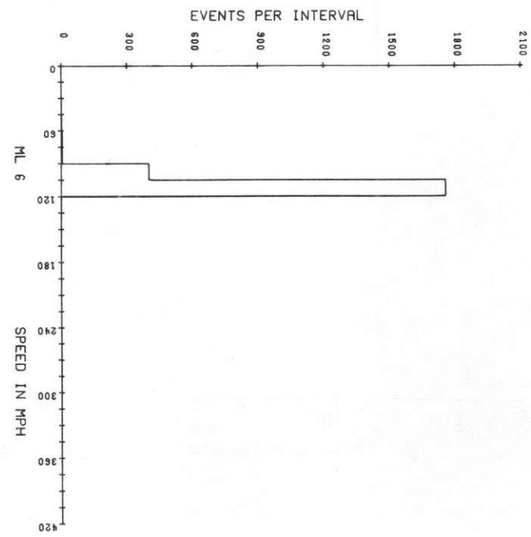
EVENTS PER INTERVAL
0
300
600
900
1200
1500
1800
2100
ML 6
SPEED IN MPH
0
60
120
180
240
300
360
420

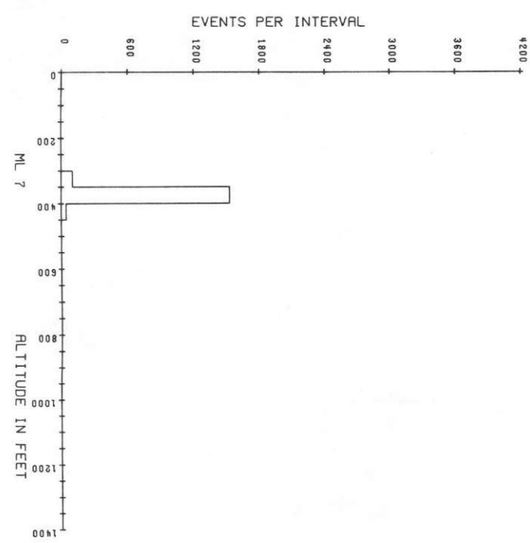
EVENTS PER INTERVAL
0
600
1200
1800
2400
3000
3600
4200
ML 7
ALTITUDE IN FEET
0
200
400
600
800
1000
1200
1400

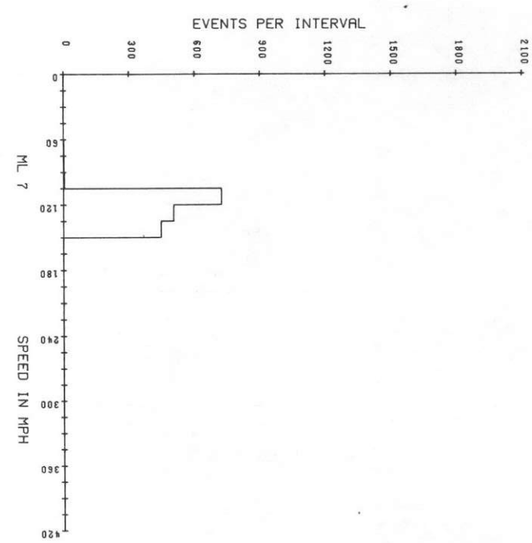
EVENTS PER INTERVAL
0
300
600
900
1200
1500
1800
2100
ML 7
SPEED IN MPH
0
60
120
180
240
300
360
420

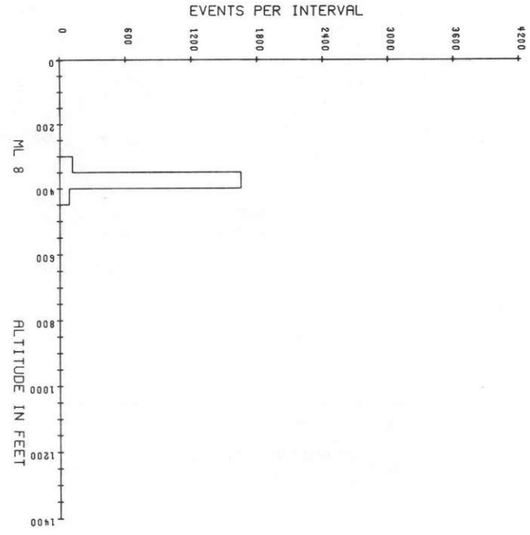
EVENTS PER INTERVAL
0
600
1200
1800
2400
3000
3600
4200
ML 8
ALTITUDE IN FEET
0
200
400
600
800
1000
1200
1400

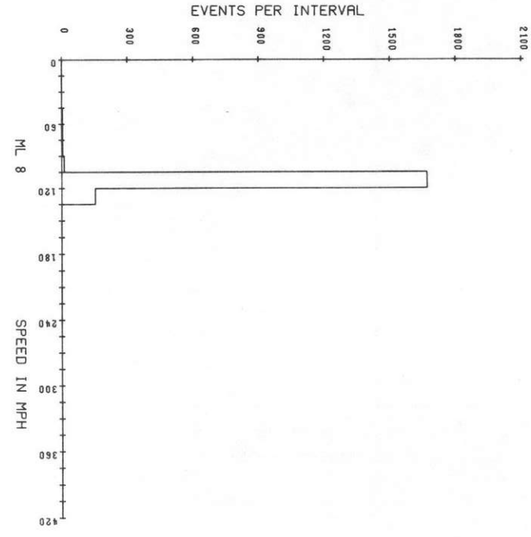
EVENTS PER INTERVAL
0
300
600
900
1200
1500
1800
2100
ML 8
SPEED IN MPH
0
60
120
180
240
300
360
420

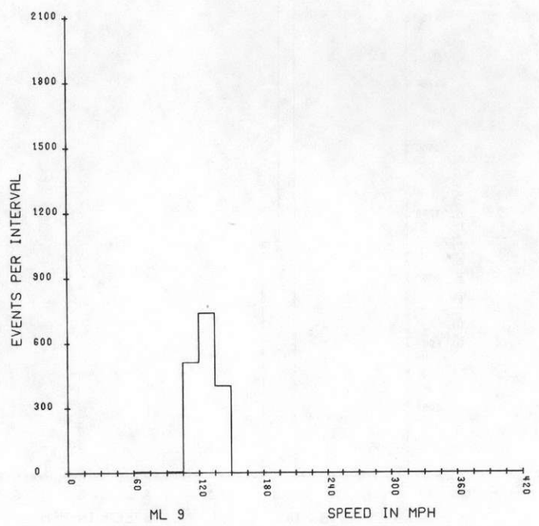
EVENTS PER INTERVAL
2100
1800
1500
1200
900
600
300
0
0
60
120
180
240
300
360
420
ML 9
SPEED IN MPH

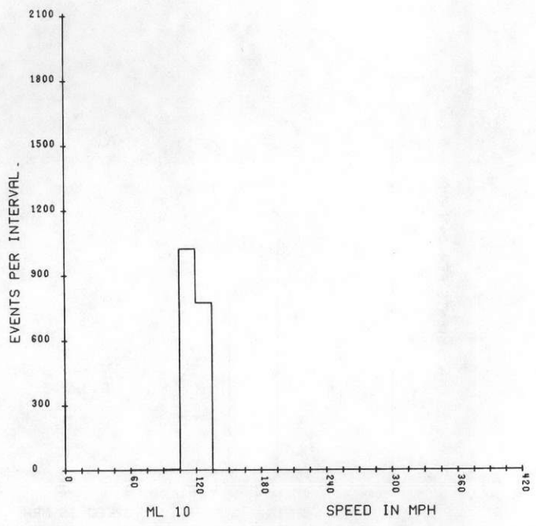
EVENTS PER INTERVAL
2100
1800
1500
1200
900
600
300
0
0
60
120
180
240
300
360
420
ML 10
SPEED IN MPH

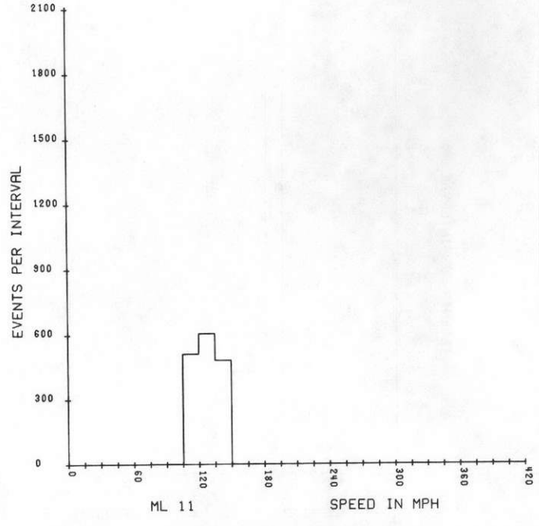
EVENTS PER INTERVAL
2100
1800
1500
1200
900
600
300
0
0
60
120
180
240
300
360
420
ML 11
SPEED IN MPH

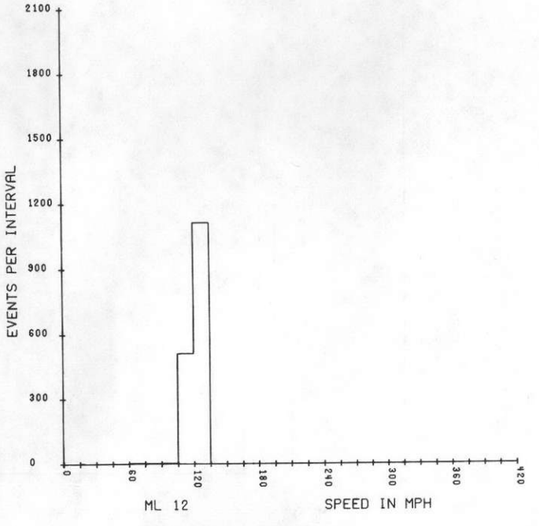
EVENTS PER INTERVAL
2100
1800
1500
1200
900
600
300
0
0
60
120
180
240
300
360
420
ML 12
SPEED IN MPH

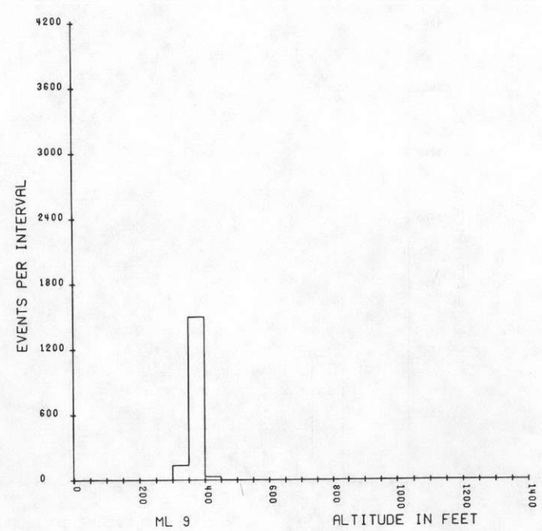
EVENTS PER INTERVAL
4200
3600
3000
2400
1800
1200
600
0
0
200
400
600
800
1000
1200
1400
ML 9
ALTITUDE IN FEET

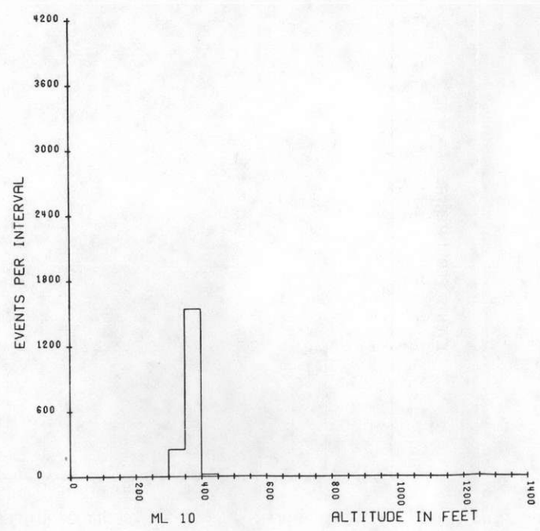
EVENTS PER INTERVAL
4200
3600
3000
2400
1800
1200
600
0
0
200
400
600
800
1000
1200
1400
ML 10
ALTITUDE IN FEET

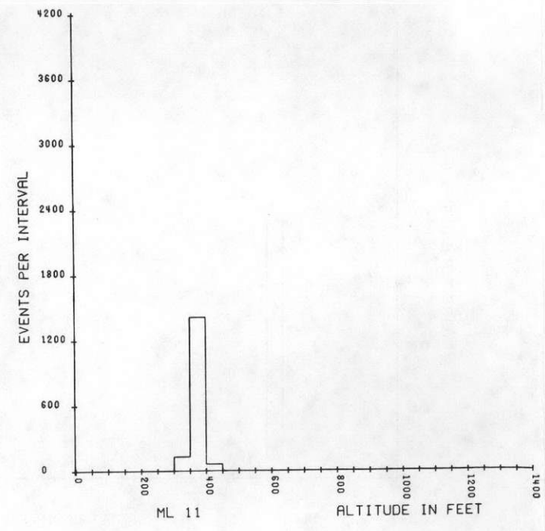
EVENTS PER INTERVAL
4200
3600
3000
2400
1800
1200
600
0
0
200
400
600
800
1000
1200
1400
ML 11
ALTITUDE IN FEET

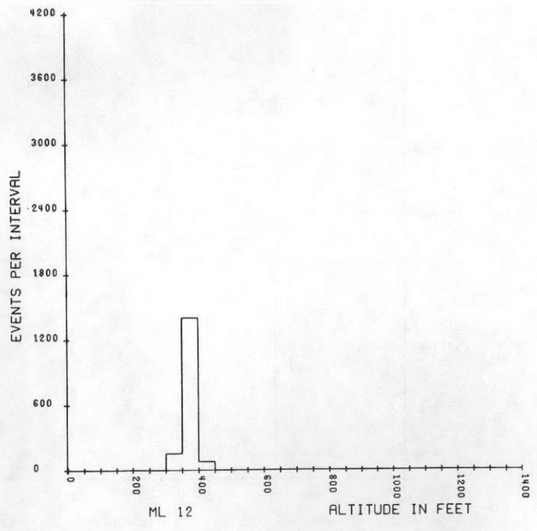
EVENTS PER INTERVAL
4200
3600
3000
2400
1800
1200
600
0
0
200
400
600
800
1000
1200
1400
ML 12
ALTITUDE IN FEET

EVENTS PER INTERVAL
2100
1800
1500
1200
900
600
300
0
0
60
120
180
240
300
360
420
ML 13
SPEED IN MPH

EVENTS PER INTERVAL
2100
1800
1500
1200
900
600
300
0
0
60
120
180
240
300
360
420
ML 14
SPEED IN MPH

EVENTS PER INTERVAL
2100
1800
1500
1200
900
600
300
0
0
60
120
180
240
300
360
420
ML 15
SPEED IN MPH

EVENTS PER INTERVAL
2100
1800
1500
1200
900
600
300
0
0
60
120
180
240
300
360
420
ML 16
SPEED IN MPH

EVENTS PER INTERVAL
4200
3600
3000
2400
1800
1200
600
0
0
200
400
600
800
1000
1200
1400
ML 13
ALTITUDE IN FEET

EVENTS PER INTERVAL
4200
3600
3000
2400
1800
1200
600
0
0
200
400
600
800
1000
1200
1400
ML 14
ALTITUDE IN FEET

EVENTS PER INTERVAL
4200
3600
3000
2400
1800
1200
600
0
0
200
400
600
800
1000
1200
1400
ML 15
ALTITUDE IN FEET

EVENTS PER INTERVAL
4200
3600
3000
2400
1800
1200
600
0
0
200
400
600
800
1000
1200
1400
ML 16
ALTITUDE IN FEET

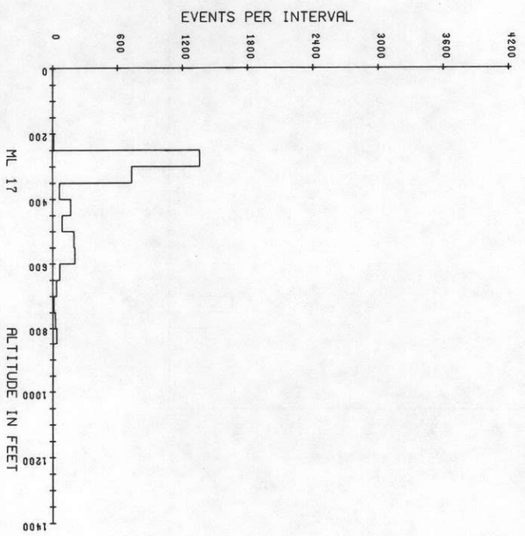
EVENTS PER INTERVAL
0
600
1200
1800
2400
3000
3600
4200
ML 17
ALTITUDE IN FEET
200
400
600
800
1000
1200
1400

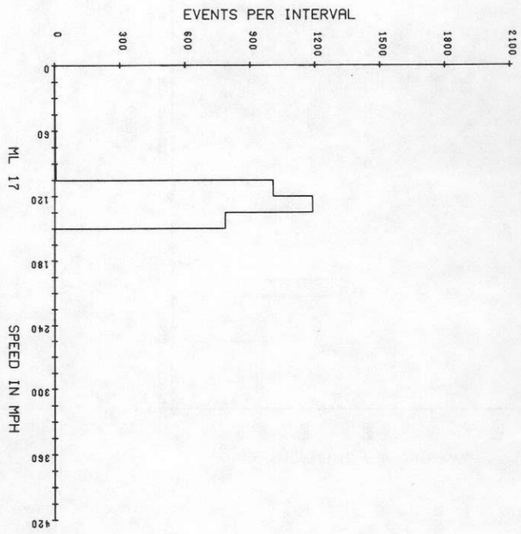
EVENTS PER INTERVAL
0
300
600
900
1200
1500
1800
2100
ML 17
SPEED IN MPH
60
120
180
240
300
360
420

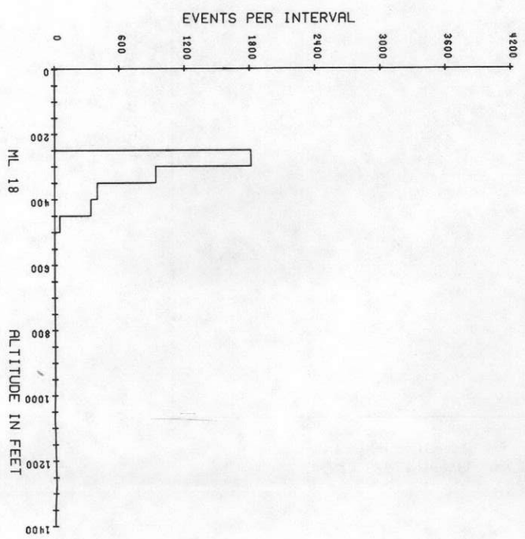
EVENTS PER INTERVAL
0
600
1200
1800
2400
3000
3600
4200
ML 18
ALTITUDE IN FEET
200
400
600
800
1000
1200
1400

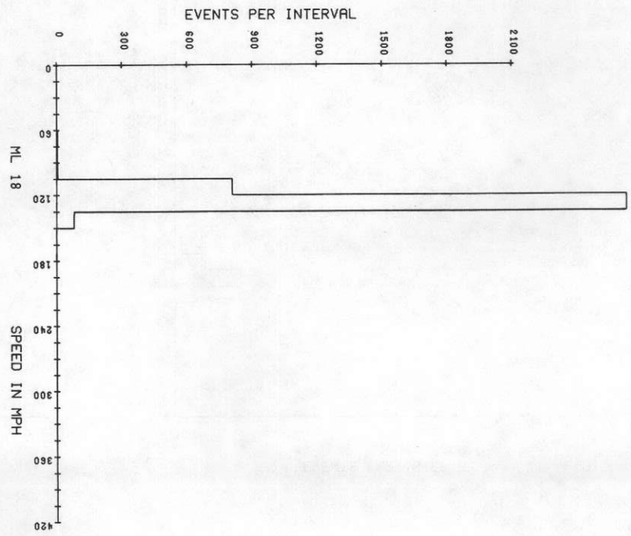
EVENTS PER INTERVAL
0
300
600
900
1200
1500
1800
2100
ML 18
SPEED IN MPH
60
120
180
240
300
360
420

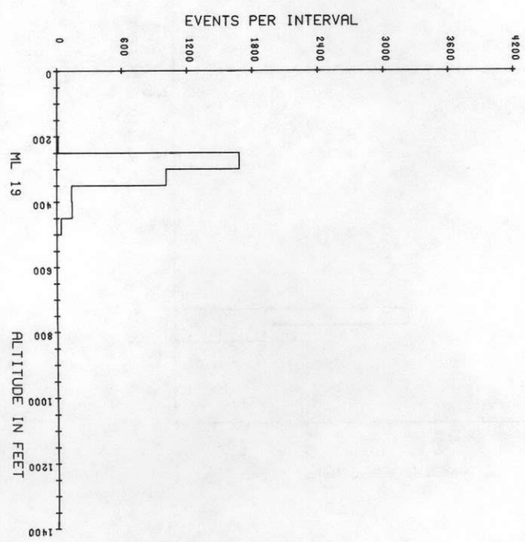
EVENTS PER INTERVAL
0
600
1200
1800
2400
3000
3600
4200
ML 19
ALTITUDE IN FEET
200
400
600
800
1000
1200
1400

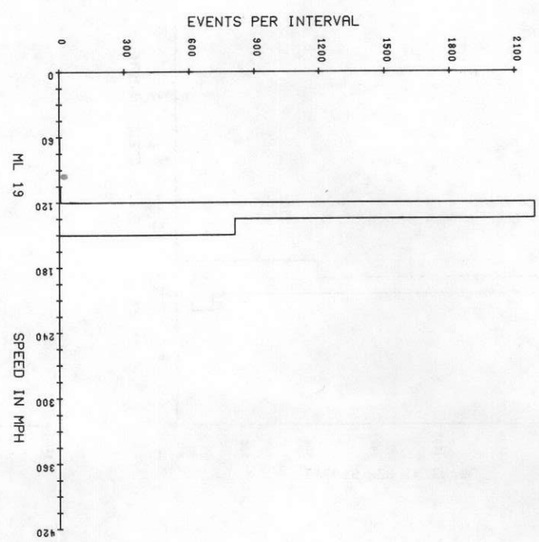
EVENTS PER INTERVAL
0
300
600
900
1200
1500
1800
2100
ML 19
SPEED IN MPH
60
120
180
240
300
360
420

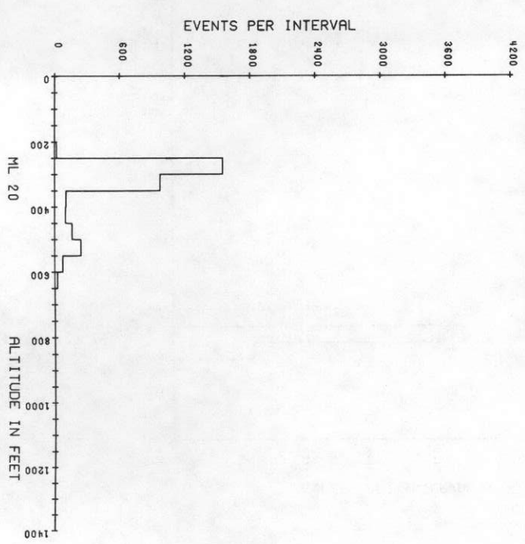
EVENTS PER INTERVAL
0
600
1200
1800
2400
3000
3600
4200
ML 20
ALTITUDE IN FEET
200
400
600
800
1000
1200
1400

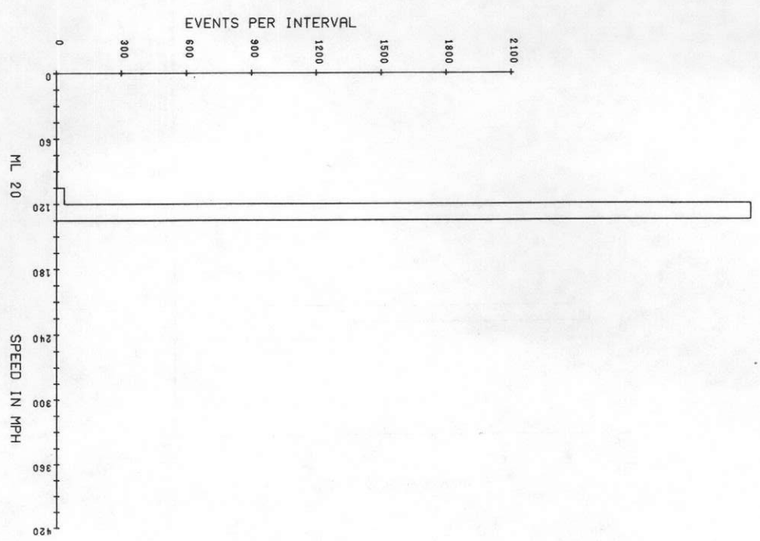
EVENTS PER INTERVAL
0
300
600
900
1200
1500
1800
2100
ML 20
SPEED IN MPH
60
120
180
240
300
360
420

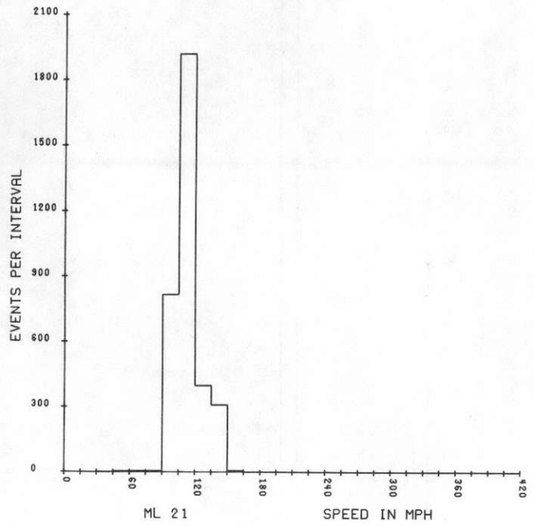
EVENTS PER INTERVAL
2100
1800
1500
1200
900
600
300
0
0
60
120
180
240
300
360
420
ML 21
SPEED IN MPH

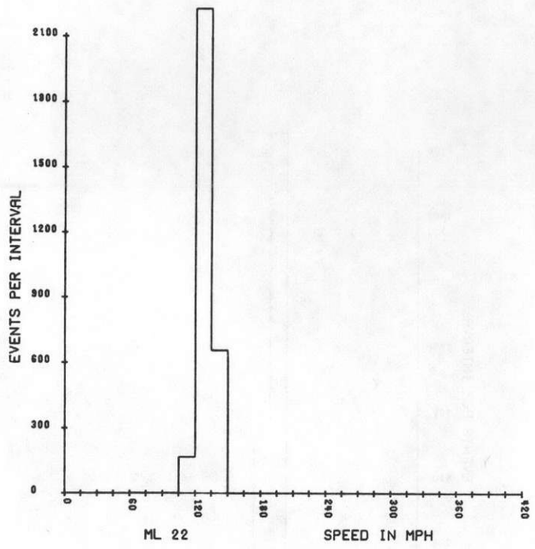
EVENTS PER INTERVAL
2100
1800
1500
1200
900
600
300
0
0
60
120
180
240
300
360
420
ML 22
SPEED IN MPH

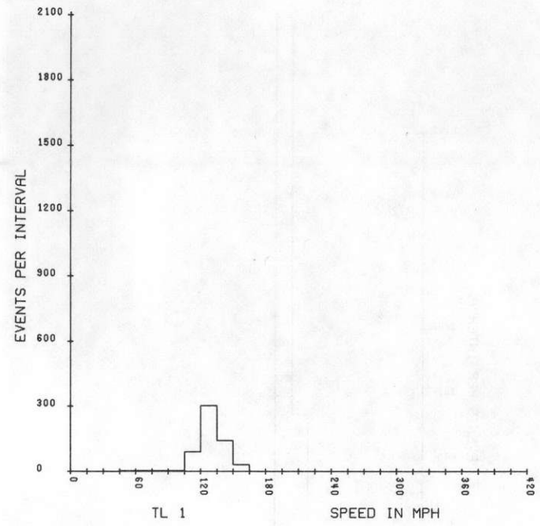
EVENTS PER INTERVAL
2100
1800
1500
1200
900
600
300
0
0
60
120
180
240
300
360
420
TL 1
SPEED IN MPH

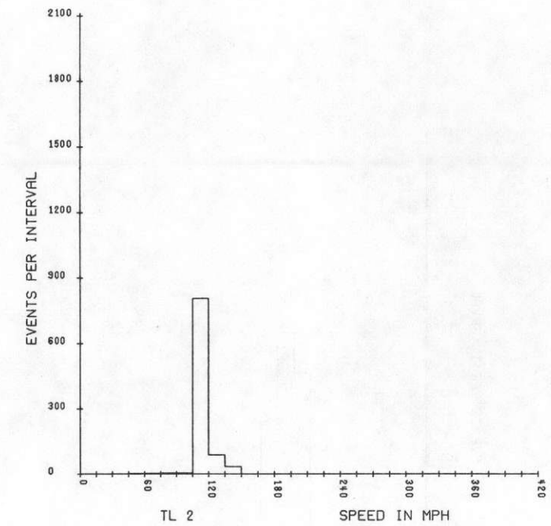
EVENTS PER INTERVAL
2100
1800
1500
1200
900
600
300
0
0
60
120
180
240
300
360
420
TL 2
SPEED IN MPH

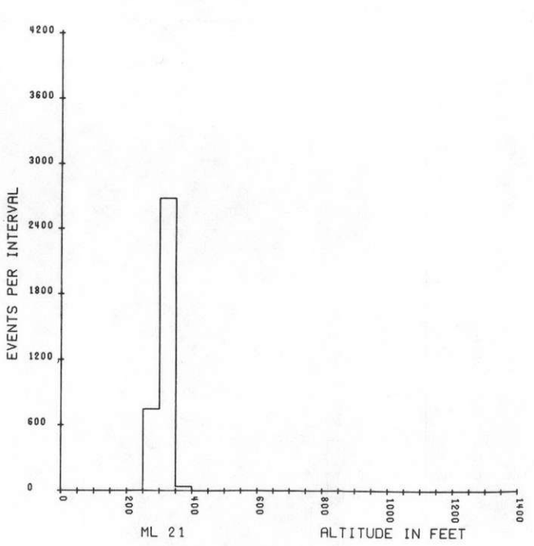
EVENTS PER INTERVAL
4200
3600
3000
2400
1800
1200
600
0
0
200
400
600
800
1000
1200
1400
ML 21
ALTITUDE IN FEET

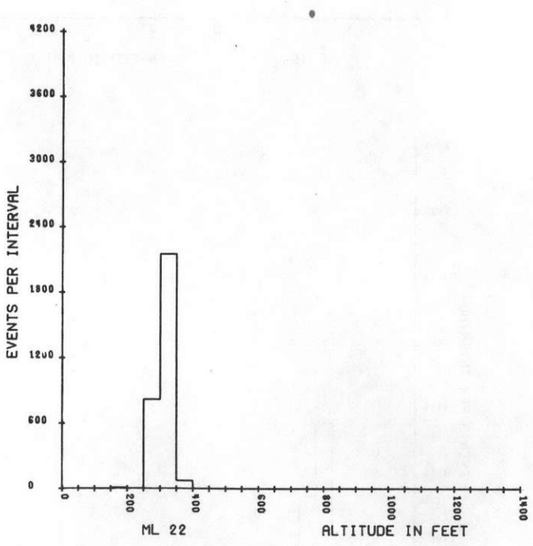
EVENTS PER INTERVAL
4200
3600
3000
2400
1800
1200
600
0
0
200
400
600
800
1000
1200
1400
ML 22
ALTITUDE IN FEET

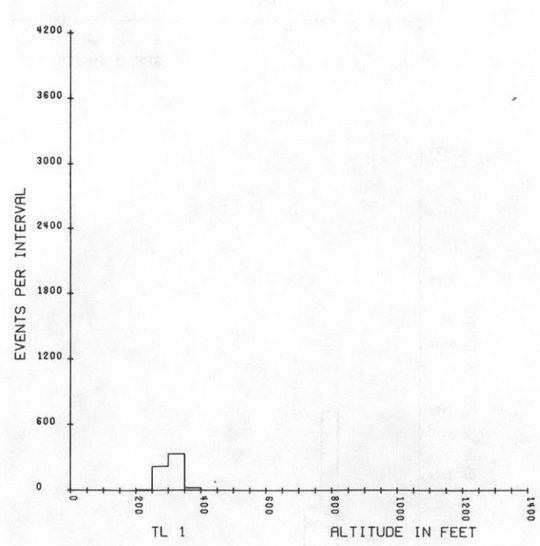
EVENTS PER INTERVAL
4200
3600
3000
2400
1800
1200
600
0
0
200
400
600
800
1000
1200
1400
TL 1
ALTITUDE IN FEET

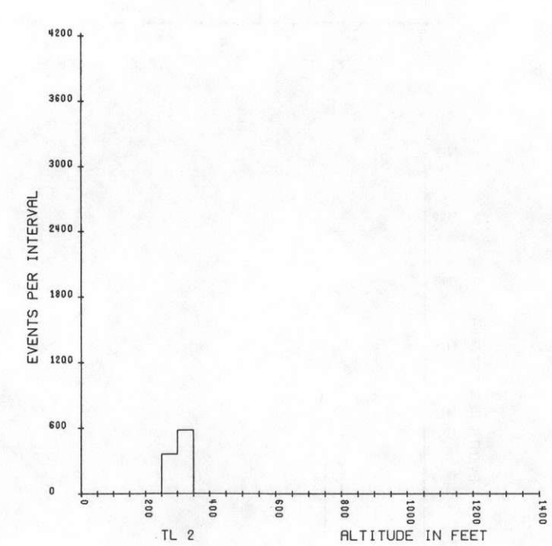
EVENTS PER INTERVAL
4200
3600
3000
2400
1800
1200
600
0
0
200
400
600
800
1000
1200
1400
TL 2
ALTITUDE IN FEET

EVENTS PER INTERVAL
2100
1800
1500
1200
900
600
300
0
0
60
120
180
240
300
360
420
TL 3
SPEED IN MPH

EVENTS PER INTERVAL
2100
1800
1500
1200
900
600
300
0
0
60
120
180
240
300
360
420
TL 4
SPEED IN MPH

EVENTS PER INTERVAL
2100
1800
1500
1200
900
600
300
0
0
60
120
180
240
300
360
420
TL 5
SPEED IN MPH

EVENTS PER INTERVAL
2100
1800
1500
1200
900
600
300
0
0
60
120
180
240
300
360
420
TL 6
SPEED IN MPH

EVENTS PER INTERVAL
4200
3600
3000
2400
1800
1200
600
0
0
200
400
600
800
1000
1200
1400
TL 3
ALTITUDE IN FEET

EVENTS PER INTERVAL
4200
3600
3000
2400
1800
1200
600
0
0
200
400
600
800
1000
1200
1400
TL 4
ALTITUDE IN FEET

EVENTS PER INTERVAL
4200
3600
3000
2400
1800
1200
600
0
0
200
400
600
800
1000
1200
1400
TL 5
ALTITUDE IN FEET

EVENTS PER INTERVAL
4200
3600
3000
2400
1800
1200
600
0
0
200
400
600
800
1000
1200
1400
TL 6
ALTITUDE IN FEET

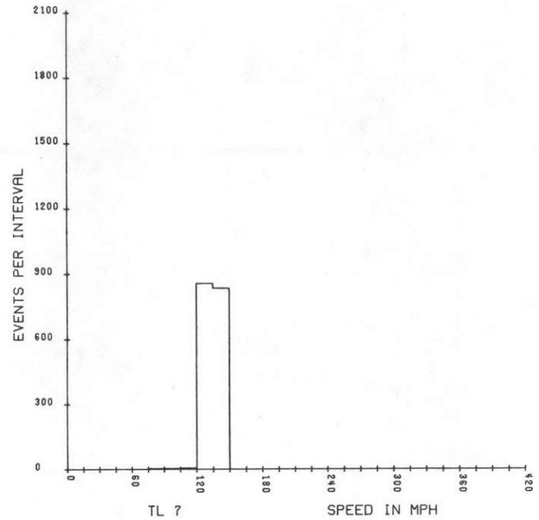
2100
1800
1500
1200
900
600
300
0
EVENTS PER INTERVAL
0
60
120
180
240
300
360
420
TL 7
SPEED IN MPH

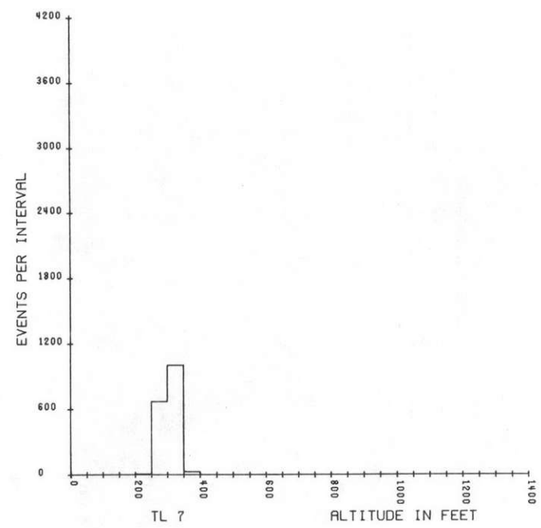
4200
3600
3000
2400
1800
1200
600
0
EVENTS PER INTERVAL
0
200
400
600
800
1000
1200
1400
TL 7
ALTITUDE IN FEET

APPENDIX III

PRODUCTION SUMMARY

APPENDIX III

A. FLIGHT OPERATIONS

The Houston quadrangle survey began on April 4, 1977 and was completed on April 12, 1977. A total of 22 map lines and seven tie lines were flown.

DATE	MAP/TIE LINES	LINE MILES FLOWN
4-04-77	ML 1 - 6	632
4-05-77	ML 7 -14	863
4-06-77	ML 15 -20	771
4-12-77	ML 21 -22, TL 1-7	613
	TOTAL...	2,879 S.M.

B. PRELIMINARY PROCESSING

Each morning following a flight survey day, the field data tapes were reformatted and the end-of-flight-line spectra (EOFL) were plotted to check resolution and calibration. In addition, spot dumps were made of the tapes to check such items as live time, magnetometer, altimeter, etc. If no problems were evident, the flight crew was informed to continue on plan. The 35-mm film was developed upon arrival.

C. TEST LINE RESULTS

The test line was flown before the start and upon completion of each day's survey. The results are given in Table A3-1. Between 4/6 and 4/12 the test line location was changed to a new area. The new area contained different surface amounts of Bi and K as is evidenced in the Table.

D. HISTOGRAMS

The histograms of aircraft ground speed and altitude above the surface for each map line and tie line are given in this appendix.

E. DATA REDUCTION AND INTERPRETATION

The flight maps and geologic overlays were completed for the Houston quadrangle in November, 1977. The final processing was completed in March, 1978.

DATE	PRE Tl	POST Tl	PRE Bi	POST Bi	PRE K	POST K	PRE Bi/Tl	POST Bi/Tl	PRE Bi/K	POST Bi/K	PRE Tl/K	POST Tl/K	PRE BiAir	POST BiAir
4-04-77	33.1	31.4	114.4	117.7	64.3	63.8	1.94	2.03	1.78	1.84	.514	.492	66.2	58.1
4-05-77	31.4	30.7	109.2	112.3	65.1	66.2	2.11	2.17	1.67	1.70	.482	.464	60.1	57.2
4-06-77	30.5	31.3	117.8	116.9	67.3	64.9	2.21	2.07	1.75	1.80	.453	.482	59.3	61.8
4-12-77	29.2	30.1	85.0	96.4	80.2	77.3	2.91	3.20	1.06	1.25	.360	.390	35.7	26.7

TABLE A3-1.PRE-FLIGHT AND POST FLIGHT BASELINE DATA SUMMARY.

F. EXPLANATORY NOTES

The data reduction and interpretation schedule was drastically delayed over plan. This occurred primarily from two causes. In June, 1977, a helicopter flying a radiometric survey under a joint venture arrangement between Geodata International and High Life Helicopters, crashed. In order to meet the contractural commitments to the Department of Energy, it was necessary to assemble and check out a new airborne system on an extremely short time schedule. This could only be accomplished at the expense of delay in other projects.

A second delay occurred when a stop on all data processing was ordered in early December, 1977. The stop order resulted from problems which appeared in the Lake Mead Dynamic Test Range results for the DC-3, N101OS, equipment. These problems were resolved but produced a delay of about six weeks in processing continuation.

REFERENCES

Bernard, H.A., LeBlanc, R.J. and Major, C.F. (1962). Recent and Pleistocene Geology of Southwest Texas in Geology of the Gulf Coast and Central Texas: Guidebook of Excursions; Houston Geological Society, Houston p. 175-254.

Brown, R.D., Jr., Eargle, D.H., and Moxham, R.M. (1961a), Preliminary Aeroradioactivity and Geologic Map of the Falls City NE Quadrangle, Karnes and Wilson Counties, Texas; USGS Geophysical Investigation Map GP-250, scale 1:31,680.

Brown,R.D., Jr., Eargle, D.H., and Moxham, R.M. (1961b), Preliminary Aeroradioactivity and Geologic Map of the Falls City NW Quadrangle, Atacosa, Karnes and Wilson Counties, Texas; USGS Geophysical Investigation Map GP-249, scale 1:31,680.

Bunder, C.M., and MacKallor, J.A., (1973). Geology of the Oxidized Uranium Or Ore Deposits of the Tordilla-Deweesville Area, Karnes County, Texas; a study of a district before mining; USGS Professional Paper 765.

Buol, S.W., Hole, F.D., and McCracken, R.J., (1973), Soil Genesis and Classification. The Iowa State University Press, Ames, Iowa, 1973,p.360.

Doering, J.A., (1967), Review of Quaternary Surface Formations of the Gulf Coast Region. American Association Petroleum Geologists, Bulletin, v. 40, p. 1816-1862.

Eardley, A.J., (1951), Tectonic Divisions of North America; American Association Petroleum Geologists, Bulletin, v. 35, p. 2229-2237.

Eargle, D.H., (1957), A Preliminary Report on the Stratigraphy of the Uranium Bearing Rocks of the Karnes County Area, Southcentral Texas; Bureau of Economic Geology, U of Texas Report, Invest. No. 30.

Eargle, D.H., (1959), Stratigraphy of the Jackson Group (Eocene) South-central Texas. American Association of Petroleum Geologists, Bulletin, v. 43, no. 11, p. 2623-2635.

Eargle, D.H., Brown, R.D., Jr., and Moxham, R.M. (1961), Preliminary Aeroradioactivity and Geologic map of the Falls City SW Quadrangle, Atacosa, Karnes and Live Oak Ctys., Texas; USGS Geophysical Invest. Map GP-252, scale 1:31,680.

Eargle, D.H., and Faust, R.T., (1962), Tertiary Stratigraphy and Uranium Mines of the Southeast Texas Coastal Plain; Houston to San Antonio, via Goliad. in Geology of the Gulf Coast and Central Texas and Guidebook of Excursions; Houston, p. 225-253.

REFERENCES (Continued)

Eargle, D.H., Hinds,G. W., and Weeks, A.D., (1971), Uranium Geology and Mines, South Texas; U of Texas at Austin, Bureau of Economic Geology Guidebook no. 12, p. 59.

Eargle, D.H. and Moxhom, R.M., (1961), Preliminary Aeroradioactivity and Geologic Map of the Falls City SE Quadrangle, Atacosa, Karnes and Live Oak Counties, Texas; USGS Geophysical Invest. Map GP-253, Scale 1:31,680.

Eargle, D.H., Trumbull, J.R.A., and Moxham, R.M. (1961a), Preliminary Aeroradioactivity and Geologic Map of the Floresville, SE Quadrangle, Karnes and Wilson Counties, Texas; USGS, Geophysical Invest. Map GP-248, Scale 1:31,680.

Eargle, D.H., Trumbull, J.R.A., and Moxham, R.M. (1961b), Preliminary Aeroradioactivity and Geologic Map of the Karnes City NW Quadrangle, Karnes County, Texas; USGS, Geophysical Invest. Map GP-251, Scale 1:31,680.

Eargle, D.H., Trumbull, J.R.A., and Moxham, R.M. (1961c), Preliminary Aeorradioactivity and Geologic Map of the Stockdale SE Quadrangle, Karnes, DeWitt and Wilson Ctys, Texas. USGS, Geophysical Invest. Map GP-248., Scale 1:31,680.

Eargle, D.H., and Weeks, A.D., (1961a), Possible Relation between Hydrogen Sulfide-bearing Hydrocarbons in Fault-line Oil Fields and Uranium Deposits in the Southeast Texas Coastal Plain; USGS Professional Paper 4240, p. D7-D9.

Eargle, D.H., and Weeks, A.D., (1961b), Uranium Bearing Clays and Tuffs of Southcentral Texas; in Folk, R.L. and others, Field Excursion Central Texas; Texas U, Bureau of Economic Geology. Guidebook no.3. p. 19-31.

Eargle, D.H., and Weeks, A.D., (1968), Factors in the Formation of Uranium Deposits, Coastal Plain of Texas; South Texas Geological Society, Bulletin, v. 9, no. 3, p. 12.

Fisher, W.L., and McGowen, J.H., (1967), Depositional Systems in the Wilcox Group of Texas and Their Relationship to the Occurrence of Oil and Gas; Gulf Coast Association of Geological Societies, v.17, p. 105-125.

Fisk, N.H. and McFarlan, E., Jr., (1955), Late Quaternary Deltaic Deposits of the Mississippi River; Geol. Soc. of Am., Paper 62, p. 279-320.

REFERENCES (Continued)

Geodata International, Inc., (1975), Gamma Radiation Spectral Survey of the Jackson/Goliad Formations in Texas; Geodata International, Inc., Dallas, Texas. Report prepared for the U.S. Atomic Energy Commission, Grand Junction, Colorado, p. 31.

Geologic Atlas of Texas Map Series 1:250,000, Bureau of Economic Geology. Houston Sheet, 1968.

Godfrey, C.L., McKee, G.S., Oakes, H., (1973), General Soil Map of Texas; Agricultural Experimental Station, Texas A&M U, in cooperation with the Soil Conservation Services, U.S. Dept. of Agriculture, 1973, scale 1:500,000.

Hardin, G.C., Jr., (1962), Notes on Cenozoic Sedimentation in the Gulf Coast Geosyncline, U.S.A.; in Geology of the Gulf Coast and Central Texas and Guidebook of Excursions; Houston Geological Society, Houston, p. 1-15.

Herrin, E., (1973), A Feasibility Study of Power Production from Overpressured Reservoirs; Final Technical Report to the Air Force Office of Scientific Research, Advanced Research Project Agency; Southern Methodist U., Dallas Geophysical Laboratory, unpublished.

Holcomb, C.W., (1964), Frio Fromation of Southern Texas; Gulf Coast Association of Geological Societies, Transactions, v. 14, p. 23-33.

Horne, J.D., (1964), A Stratigraphic Revision Within the Group in South Central Texas; Gulf Coast Assoc. of Geol. Soc., Transactions, v. 14, p. 277-283.

Jones, P.H., (1969), Hydrology of Neogene Deposits in the Northern Gulf of Mexico Basin; Louisiana Water Resources Research Institute, Bulletin GT-2, Louisiana State U., Baton Rouge, p. 106.

Kloh, M.L., and Pickens, W.R., (1970), Geology of the Felder Uranium Deposit, Live Oak County, Texas. Paper presented at the AIME annual meeting, Denver, Colo., Feb. 15-19, 1970, Soc. of Mining Eng. Preprint No. 70-1-38, N. Y., p. 19.

MacBride, E.F., Lindeman, W.L. and Freeman, P.S., (1968), Lithology and Petrology of the (Gueydan) Catahoula Formation in South Texas; U. of Texas, Bureau of Econ. Geol., Report of Invest. No. 63, p. 122.

REFERENCES (Continued)

MacKallor, J.A., Moxham, R.M., Tolozko, L. R., and Pokenoe, P., (1962), Radioactivity and Geologic Map of the Tordilla-Deweesville Area, Karnes County, Texas; USGS, Geophysical Invest. Map GP-199.

Meyerhoff, A.A., (1967), Future Hydrocarbon Provinces of the Gulf of Mexico-Caribbean Region; Gulf Coast Assoc. of Geol. Soc., Transactions, v. 17, p. 217-260.

Meyerhoff, A.A., (1968), Geology of Natural Gas in South Louisiana, in Natural Gases of North America (B.W. Beebe, ed.,) American Assoc. Petrol. Geol. Bulletin, v. 50, p. 376-581.

Moxham, R.M., and Eargle, D.H. (1962), Airborne Radioactivity and Geologic Map of Southeast Texas 1:250,000; USGS, Geophysical Invest. Map GP-198.

Murray, G.E., (1961), Geology of the Atlantic and Gulf Coastal Province of North America, Harper and Bros., N. Y., p. 692.

Murray, G.E., (1963), Geologic History and Framework of the Gulf Atlantic Geosyncline; American Assoc. of Petrol. Geol., Bulletin, v. 47, p. 364-365 (abstract).

Murray, G.E., (1968), Salt Structures of the Gulf of Mexico - A Review; American Assoc. of Petrol. Geol., Bulletin, v. 50, p. 439-478.

Ocamb, R.D., (1961), Growth Faults of South Louisiana; Gulf Coast Assoc. of Geol. Soc., Transactions, v. 11, p. 139-175.

Plummer, F.B., (1933), Cenozoic Systems in Texas. in The Geology of Texas, part 3: U. of Texas Bulletin, 3232, p. 517-818.

Rainwater, E.H., (1967), Resume of Jurassic to Recent Sedimentation History of The Gulf of Mexico Basin; Gulf Coast Assoc. of Geol. Soc., v. 17, p. 179-210.

Russell, R.J., (1940), Quaternary History of Louisiana; Geol. Soc. of Am., Bulletin, v. 51, p. 1199-1234.

Smith, F.E., (1962), Tertiary and Uppermost Cretaceous of the Brazos River Valley, Southeastern Texas; in Geology of the Gulf Coast and Central Texas and Guidebook of Excursions. Houston Geol. Soc., Houston, p. 132-174.

REFERENCES (Continued)

Southern Interstate Nuclear Board (1969), Uranium in the Southern United States; The Southern Interstate Nuclear Board, Atlanta, Georgia, Report prepared for the Division of Raw Materials, US AEC, July, 1969, p. 230.

Stapp, W.L., (1957), Notes on Pescadito Structure, Webb Cty, Texas; in Corpus Christi Geol. Soc. Annual Field Trip, April, 1954, p. 31-32; reprinted, Annual Field Trip, April, 1957, p. 18-19,.

Stinhauser, S.R., (1956), Uranium in the Gulf Coastal Plain of Texas; Mines Magazine, v. 46, no. 3, p. 73-76.

Tipsword, H.L., (1962), Tertiary Formations in Gulf Coast Petroleum and Development; in Geology of the Gulf Coast and Central Texas and Guidebook of Excursions; Houston Geological Soc., Houston, p.16-57.

Trowbridge, A.C., (1932), Tertiary and Quaternary Geology of the Lower Rio Grande Region of Texas; USGS, Bulletin no. 837, p. 260.

Weeks, A.D., and Eargle, D.H., (1963), Relation of the Diagenetic Alteration and Soil Forming Processes to the Uranium Deposits of the Southwest Coastal Plain; in Clays and Clay Minerals, 10th Conf., Pergamon Press, MacMillan Co., N. Y., p. 23-41.